REPORT DOCUMENTATION PAGE

Form Approved OMB No. 0704-0188

Public reporting burden for this collection of information is estimated to average 1 hour per response, including the time for reviewing instructions, searching existing data sources, gathering and maintaining the data needed, and completing and reviewing the collection of information. Send comments regarding this burden estimate or any other aspect of this collection of information, including suggestions for reducing the burden, to Department of Defense, Washington Headquarters Services, Directorate for Information Operations and Reports (0704-0188), 1215 Jefferson Davis Highway, Suite 1204, Arlington, VA 22202-4302. Respondents should be aware that notwithstanding any other provision of law, no person shall be subject to any penalty for failing to comply with a collection of information if it does not display a currently valid OMB control number.
PLEASE DO NOT RETURN YOUR FORM TO THE ABOVE ADDRESS.

1. REPORT DATE *(DD-MM-YYYY)*	2. REPORT TYPE	3. DATES COVERED *(From – To)*
20-05-2009	Final Report	1 December 2007 - 15-Dec-09

4. TITLE AND SUBTITLE

Design and Control of Wireless Mobile Adhoc and Sensor Networks

5a. CONTRACT NUMBER
FA8655-08-1-3020

5b. GRANT NUMBER

5c. PROGRAM ELEMENT NUMBER

6. AUTHOR(S)

Professor Leandros Tassiulas

5d. PROJECT NUMBER

5d. TASK NUMBER

5e. WORK UNIT NUMBER

7. PERFORMING ORGANIZATION NAME(S) AND ADDRESS(ES)

University of Thessaly
37 Glavani - 28th October Str, Deligiorgi Building, 5th floor
Volos 38221
Greece

8. PERFORMING ORGANIZATION REPORT NUMBER

N/A

9. SPONSORING/MONITORING AGENCY NAME(S) AND ADDRESS(ES)

EOARD
Unit 4515 BOX 14
APO AE 09421

10. SPONSOR/MONITOR'S ACRONYM(S)

11. SPONSOR/MONITOR'S REPORT NUMBER(S)
Grant 08-3020

12. DISTRIBUTION/AVAILABILITY STATEMENT

Approved for public release; distribution is unlimited.

13. SUPPLEMENTARY NOTES

14. ABSTRACT

In this project we investigated challenges of wireless networks design with focus on energy management on battery dependent devices and the impact of a new hidden terminal problem on the operational efficiency of wireless networks. The results summarized in this report have been presented in a number of papers published or submitted for publication. In the first part of this work we consider the optimal control of wireless networks operating with rechargeable batteries under general arrival, channel and recharge processes. The objective is to maximize total system utility while satisfying energy/power constraints. Starting from a downlink scenario, we propose a policy with decoupled admission control and power allocation decisions that achieves asymptotic optimality for sufficiently large battery capacity. Extensions to single-hop and multihop networks are also presented. Such policies are particularly suitable for satellite downlinks or sensor networks. In the second part of this work, we investigated performance unfairness (in terms of throughput and delay) on the Medium Access Control (MAC) mechanism of 802.11 standard in the presence of hidden terminals. To eliminate the impacts from the physical layer (PHY), we assume good channel. In this case, we may intuitively expect that all stations have equal success probabilities in their transmissions. This intuition is from the random access scheme of Carrier Sense Multiple Access with Collision Avoidance (CSMA/CA) which is employed by 802.11 MAC protocol. However, we will show that the intuition is not true due to hidden terminals. Instead, the following fact is revealed in this work: The success probability of a transmission is location-dependent. More specifically, the nodes far from the access point see more hidden terminals than those close to the access point, so they experience more collisions and thus smaller success probabilities. We build a model to analyze the throughput and collision probability for nodes at different locations, validate them via simulations and compare with the measurement results from experiments.

15. SUBJECT TERMS

EOARD, Distributed sensors, Complex Systems, Ad-hoc Networks

16. SECURITY CLASSIFICATION OF:			17. LIMITATION OF ABSTRACT	18, NUMBER OF PAGES	19a. NAME OF RESPONSIBLE PERSON
a. REPORT	b. ABSTRACT	c. THIS PAGE			JAMES LAWTON Ph. D.
UNCLAS	UNCLAS	UNCLAS	UL	43	19b. TELEPHONE NUMBER *(Include area code)* +44 (0)1895 616187

Adhoc wireless network control: energy efficiency and hidden terminal considerations

Abstract

In this project we investigated challenges of wireless networks design with focus on energy management on battery dependent devices and the impact of a new hidden terminal problem on the operational efficiency of wireless networks. The results summarized in this report have been presented in a number of papers published [1], [2] or submitted for publication [3], [4]. In the first part of this work we consider the optimal control of wireless networks operating with rechargeable batteries under general arrival, channel and recharge processes. The objective is to maximize total system utility while satisfying energy/power constraints. Starting from a downlink scenario, we propose a policy with decoupled admission control and power allocation decisions that achieves asymptotic optimality for sufficiently large battery capacity. Extensions to single-hop and multihop networks are also presented. Such policies are particularly suitable for satellite downlinks or sensor networks. In the second part of this work, we investigated performance unfairness (in terms of throughput and delay) on the Medium Access Control (MAC) mechanism of 802.11 standard in the presence of hidden terminals. To eliminate the impacts from the physical layer (PHY), we assume good channel. In this case, we may intuitively expect that all stations have equal success probabilities in their transmissions. This intuition is from the random access scheme of Carrier Sense Multiple Access with Collision Avoidance (CSMA/CA) which is employed by 802.11 MAC protocol. However, we will show that the intuition is not true due to hidden terminals. Instead, the following fact is revealed in this work: The success probability of a transmission is location-dependent. More specifically, the nodes far from the access point see more hidden terminals than those close to the access point, so they experience more collisions and thus smaller success probabilities. We build a model to analyze the throughput and collision probability for nodes at different locations, validate them via simulations and compare with the measurement results from experiments.

CONTENTS

I Introduction 3

II Asymptotically optimal control of wireless networks with rechargeable batteries 4
II-A System model and problem statement . . . 4
II-A1 Some intuitive remarks . . . 6
II-B Performance analysis . . . 6
II-B1 Virtual queues and policy specification . . . 7
II-B2 Some preliminary results . . . 8
II-B3 Stability and performance properties of DRABP . . . 9
II-B4 Performance bound of DRABP . . . 11
II-B5 Removal of the assumption $f_l'(0) < \infty$ . . . 12
II-C Extensions to single-hop and multihop networks . . . 13
II-C1 Multihop networks . . . 16

III The Hidden cost of hidden terminals 20
III-A Where is Hidden Terminal? . . . 20
III-B An Analytical Model for the Hidden Terminal Problem . . . 21
III-B1 System Model . . . 21
III-B2 Network Analysis . . . 22
III-C Throughput . . . 24
III-D Simulation . . . 25
III-D1 Simulation Settings . . . 25
III-D2 Performance of Saturated Networks . . . 25
III-D3 Simulation Results: Networks Without RTS/CTS . . . 27
III-E Impact on Real-Time Service . . . 27
III-F Experimental Measurements . . . 27
III-G Related Work . . . 28

IV Conclusion and Future Work 29

V Appendix 29
V-A Proof of Lemma 2 . . . 29
V-B Proof of Lemma 3 . . . 30
V-C Proof of Lemma 4 . . . 31
V-D Proof of Lemma 5 . . . 31
V-E Proof of Lemma 6 . . . 33
V-F Proof of Lemma 7 . . . 33
V-G Proof of Lemma 11 . . . 34
V-H Total Hidden Area S . . . 37
V-I Hidden Area $H(i,j)$ and Covered Area $E(i,j)$ . . . 38
V-J Derivation of Eq. 107 . . . 38

VI List Of Symbols, Abbreviations And Synonyms 40

References 41

LIST OF FIGURES

1 Queue connections in the downlink scenario with rechargeable battery. . . . 7
2 Illustration of the hidden terminal problem in ad hoc networks. For transmitter T, stations in in the shaded area are hidden terminals. . . . 21
3 Illustration of the hidden terminal problem in infrastructure mode 802.11 networks. Note that the hidden area in (a) is larger than that in (b) (where the source station is closer to the AP). . . . 22
4 t increases almost linearly with the distance to the AP. . . . 22
5 M evenly spaced concentric annuluses centered at the AP ($M = 4$ in this figure). . . . 23
6 Illustration of Hidden Area $H(i,j)$ and Covered Area $E(i,j)$. . . . 23
7 Aggregate Network Throughput: Model VS. Simulation. . . . 24
8 Per-node Throughput: Model VS. Simulation. . . . 26

9 Collision Probability and Packet Delay. 26
10 ns-2 simulation results for a saturated 16-node network with RTS/CTS turned on or off and various payload length. 26
11 ns-2 simulation results of VoIP service. 26
12 Topology: All stations are in a line, with access point in the middle. 28
13 Measured Per-node Throughput. 28
14 Measured Packet Loss Rate (PLR). 28
15 Schematic decomposition of $\mathcal{I}$ into $\mathcal{I}_j$. In the second case, it holds $\mathcal{I}_1 = \varnothing$. 35
16 Illustration of hidden area. The shaded region is the hidden area. 38
17 The 2D Markov chain to model 802.11 DCF. 39

LIST OF TABLES

I Parameters Used in Both Simulations and Model 25

I. Introduction

In the concept of that project we investigate the challenges of wireless networks design with focus on energy management on battery dependent devices and the impact of hidden terminals on their operational efficiency. This study provides ideas to explore and develop through that work. The report is organized in two parts. The fisrt one is affiliated with the energy managment on limited-energy devices and the latter with the operational cost of hidden terminals.

Efficient energy management is a crucial component of wireless network design, since it can lead to increased throughput and network lifetime. The latter concept, which has numerous application-dependent definitions, is meaningful for battery operated devices that do not have energy-harvesting capabilities (i. e. they cannot recharge themselves from ambient sources) and, hence, become inactive once they run out of energy. On the other hand, there exist applications where the wireless transmitters can replenish their batteries. Two common examples are solar-paneled satellites (where the recharge process depends on the satellite's exposure to sunlight during its orbit and can be determined *a priori* with high confidence) and sensor networks [5] (which harvest solar or wind energy so that the recharge process depends on atmospheric conditions and is better modeled as a stochastic process). Such rechargeable systems are usually regarded as having infinite lifetime,[1] so that long-term performance metrics become appropriate.

This document initially considers the control of a wireless downlink operating in discrete time under rechargeable batteries, and later generalizes the analysis to single-hop and multihop networks. The relevant literature has greatly expanded in recent years, with most works being based on a dynamic programming (DP) and/or Markov decision process (MDP) approach. Finite horizon control problems are studied in [7], for a single satellite downlink subject to stochastic power demands and rewards (although no packet dynamics are included), and [8], for a multihop network where the nodes have knowledge of the future short-term recharge process (an assumption we dispense with in this work). The model in [8] is inspired by the virtual circuit concept and, as such, performs resource allocation on a one-shot basis for each accepted service request (the latter is described by the source and destination nodes as well as the associated gained revenue). Specifically, a policy is developed that, for each accepted request, computes an appropriate energy-weighted shortest path from the source to the destination node of the request and *simultaneously* reduces the energy of all nodes lying on the selected path by the required cost (provided that the gained revenue is larger than the expended cost). Since the policy drops any requests that cannot be immediately served, queueing effects are ignored. Additionally, the link-based energy costs do not depend on channel variations.

In [9], a rechargeable group of cells under realistic battery fatigue is examined, where the objective is maximization of the energy delivered from the battery. Open and closed loop policies for finite and infinite horizon control also appear in [10]. Especially for sensor networks, [11] examines a scenario where the derived utility (namely, probability of event detection) depends only on the number of active sensors. The sensors are either recharging or transmitting (but not both) and, once completely drained, can only activate themselves when fully recharged. An upper bound for any feasible policy is derived and distributed threshold policies are proposed with a multiplicative guaranteed bound of 1/2 w. r. t. the optimal policy. In [12], the sensors are allowed to be activated even when partially recharged and an asymptotically optimal (w. r. t. battery capacity) policy is proposed for Poisson and exponential recharge/discharge processes, respectively. Although the last two works don't use DP (and hence scale well), the analytically derived bounds hold for a rather ideal setting. Finally, [13] focuses on the temporal correlations between the events sensed by a single sensor and studies, in terms of an MDP, the structure of the optimal policy under various observability conditions. Efficient suboptimal policies are also proposed and numerically evaluated for multiple node networks in [14]. References [11]–[14] focus exclusively on the sensing aspect of sensor networks rather than the network flow of information (i. e. what happens *once* an event is detected), which is the main focus of this document.

Our model is distinct from the aforementioned works and is directly influenced by the cross-layer stochastic optimization framework of [15], [16], which, in turn, was inspired by [17]. This framework was applied in [18], which proposed optimal adaptive backpressure policies (collectively referred to as ABP) for non-rechargeable power-constrained networks under long-term average constraints, and introduced the concept of virtual queues to handle the latter, while [19] addressed fairness issues in a similar setting. Unfortunately, the above methodology relies crucially on the fact that available controls depend only on current channel states and are independent of prior history, and this condition is violated in our model, as will become apparent later. Hence, this approach is not directly applicable. Our rechargeable model explicitly takes into account wireless channel variations and packet dynamics and aims in maximizing a suitably defined measure of user satisfaction, while imposing minimal assumptions on the arrival, recharge and channel processes (the basic assumption is that these processes are rate-convergent, as defined in [15]). Since the lifetime of rechargeable systems is practically infinite, the inclusion of packet dynamics forces us to study the stability properties of any policy under consideration. An adaptive stabilizing policy is proposed with guaranteed performance bounds that imply asymptotic optimality for sufficiently large battery capacities.

This report is structured as follows. Subsection II-A contains the system model and problem statement for a downlink scenario and also presents a connection with an infinite battery problem which offers important insight. Subsection II-B introduces the concept of virtual queues and proposes a policy for a rechargeable battery. Stability and performance analysis

[1] if we take into account battery fatigue (i. e. the fact that recharge capability deteriorates as the number of recharge cycles increases), the lifetime is, strictly speaking, finite. However, as shown in [6], proper design can lead to a lifetime of more than a year, for continuous operation (and even more for typical duty cycles), which can be considered as infinite for engineering purposes.

for this policy is carried out in detail. The gained experience is used in Subsection II-C to propose policies for single-hop and multihop networks, with the latter requiring a more complex analysis (performance bounds are provided in all cases)

As a predominant wireless local area network (WLAN) technology, IEEE 802.11 [20] has defined both contention-free point coordination function (PCF) and contention-based distributed coordination function (DCF) for medium access control (MAC). Nonetheless, only the DCF protocol, which is a random access scheme based on carrier sensing multiple access with collision avoidance (CSMA/CA), has been widely deployed in the field. The DCF protocol has further incorporated a ready-to-send/clear-to-send (RTS/CTS) handshake mechanism to mitigate the *hidden terminal problem*, which causes great performance degradation if left unattended [21].

Most research on the hidden terminal problem has been focused on the performance degradation to the overall network [22]-[23],[24]. This work, however, focuses on the level of the degradation imposed on *individual nodes*. We find that the level of performance degradation for a node is location-dependent. More specifically, it depends on the distance from the access point (AP). As we will see from the measurement results in section III-F, stations at different distances from the AP experience significantly different collisions probabilities and consequently achieve disparate throughput. Similar observations are made from our analysis and simulations (section III-D). In a 16-node WLAN, we observe that the throughput ratio between a node close to the AP and a node at the edge of the network ranges from *three times* to as much as *five times*. In order to establish a solid theoretical foundation, we propose an analytical model for WLANs in the presence of hidden terminals. To further demonstrate the performance unfairness in practice, we further report results from experiments carried out in real environments.

We will mainly focus on the scenario with RTS/CTS handshake in our analytical model, since the measurement results to be reported in section III-F corroborate that WiFi network performance in the presence of hidden nodes is much worse when RTS/CTS is turned off as compared to the case where RTS/CTS is switched on.

The rest of the second part will be organized as follows. Subsection III-G briefly summarizes the related work in the literature. Subsection III-A describes the hidden node problem and the resulting performance unfairness. Subection III-B builds an analytical model for a 802.11 WLAN. Subsection III-D validates the model with simulations. Subsection III-F presents the measurement results from our testbed. Finally, the Appendix provides the derivations of the hidden areas and Eq. 107.

II. Asymptotically optimal control of wireless networks with rechargeable batteries

A. System model and problem statement

As stated in the Introduction, the proposed policy applies to generic multihop networks under arbitrary rate-convergent arrival, channel state and (energy) recharge processes. However, in order to simplify the discussion and gain essential insight into the operation of the policy, we initially present the analysis for a downlink scenario with iid arrival, channel and recharge processes and, in a later section, describe the modifications needed for the general case. Non-iid processes can be handled by the T-slot analysis [16] of rate-convergent processes and are not covered here.

We consider a time-slotted system where slot t corresponds to the time interval $[t \quad t+1)$. There exists a single base node that transmits to L users (i. e. there exist L wireless downlinks[2]). The link channels are time-varying so that we denote with $\boldsymbol{S}(t)$ the channel state at slot t and assume it is iid distributed over a finite set $\mathcal{S}$, i. e. $\boldsymbol{S}(t) \in \mathcal{S}$ for all t. We also define $\pi_{\boldsymbol{s}} \triangleq \Pr(\boldsymbol{S}(t) = \boldsymbol{s})$, where, with no loss of generality, it holds $\pi_{\boldsymbol{s}} > 0 \ \forall \boldsymbol{s}$. Channel conditions remain constant for the duration of each slot but may change at slot boundaries. The base node has a distinct traffic stream for each downlink so that $A_l(t)$ stands for the number of exogenously generated bits during slot t that must be transmitted to (downlink) user l. These bits enter the transport layer and are stored, in a FIFO manner, in an external queue awaiting admission into the network layer and subsequent transmission. Admission control is necessary for the case of heavy traffic that exceeds the network capacity. When the bits are admitted into the network layer, they are first stored in an internal "network" queue, again in FIFO fashion, until transmission occurs. Let $V_l(t)$, $U_l(t)$ be, respectively, the number of bits stored at time t in the external/internal queues of the base node and destined for user l (through link l).[3] Denote with $R_{l,in}(t)$ the number of bits moved from the external to the internal queue (i. e. admitted into the network) of link l at time t, and define[4] $\boldsymbol{R}_{in}(t) \triangleq (R_{l,in}(t))_{l=1}^{L}$. Supply/demand constraints clearly require $R_{l,in}(t) \leq V_l(t) + A_l(t)$ for all l, t. It is further assumed that each exogenous arrival process $A_l(t)$ has a deterministic upper bound $\hat{A}_l$ (i. e. $A_l(t) \leq \hat{A}_l \quad \forall t$) and is iid distributed with expected value λ_l. We will write at times $\hat{\boldsymbol{A}} \triangleq (\hat{A}_l)_{l=1}^{L}$ and $\boldsymbol{\lambda} \triangleq (\lambda_l)_{l=1}^{L}$.

The base node is equipped with a rechargeable battery of maximal energy E_{max}. The battery level at time t is denoted as $E(t)$. The battery energy is depleted due to link transmissions but is also replenished due to a recharge process. Specifically, we denote with $B(t)$ the amount of replenished energy during slot t, where $B(t)$ is assumed bounded[5] (i. e. $B(t) \leq \hat{B} \ \forall t$) and iid distributed with an expected value of $\bar{B}$. At the beginning of each time slot t, the network controller chooses a power vector $\boldsymbol{P}(t) \triangleq (P_l(t))_{l=1}^{L}$, where $P_l(t)$ is the selected transmission power in link l during slot t. Available transmission power

[2] in the following, the terms user l and link l will be used interchangeably, since there exists a 1-1 correspondence between them.

[3] for economy of expression, we will refer to $U_l(t)$ as the internal queue of link l, and similarly for $V_l(t)$.

[4] we hereafter use bold face to denote vector quantities. The vector's dimension will be apparent from context.

[5] the deterministic bound assumptions on $A_l(t)$ and $B(t)$ can be replaced by the weaker conditions of finite second moments, which leads to slightly modified performance results (although the proposed policy is unaffected). We choose to stay with the former assumption in order not to obscure the discussion.

vectors may be channel-state dependent, i. e. $\boldsymbol{P}(t) \in \mathcal{P}_{\boldsymbol{S}}$ whenever $\boldsymbol{S}(t) = \boldsymbol{s}$, where $\mathcal{P}_{\boldsymbol{s}}$ is a finite set[6] for all $\boldsymbol{s} \in \mathcal{S}$. The only constraints imposed on $\mathcal{P}_{\boldsymbol{s}}$ are that for all $\boldsymbol{s} \in \mathcal{S}$ it holds $\mathbf{0} \in \mathcal{P}_{\boldsymbol{s}}$ and $\sum_{l=1}^{L} p_l \leq \hat{P} \quad \forall \boldsymbol{p} \in \mathcal{P}_{\boldsymbol{s}}$, where $\hat{P} \leq E_{max}$. The first constraint states that the system may always select to decline transmission while the second constraint models hardware limitations or standard regulations. The existence of the finite-energy battery further restricts the available power vectors for slot t by the natural condition $\sum_{l=1}^{L} p_l \leq E(t) \ \forall \boldsymbol{p} \in \mathcal{P}_{\boldsymbol{S}(t)}$.

To facilitate analysis, it is assumed that all values of the recharge process $B(t)$ as well as all members of $\mathcal{P}_{\boldsymbol{s}}$ are integer multiples of an arbitrary constant (i. e. they are quantized), so that $E(t)$ effectively takes values in a countable set. For a given state $\boldsymbol{S}(t)$ and selected power $\boldsymbol{P}(t)$, the transmission rate $\boldsymbol{\mu}(t) \triangleq (\mu_l(t))_{l=1}^{L}$ in slot t (i. e. the number of bits that can be transmitted in each link) is upped bounded, component-wise, by a vector function $\boldsymbol{c}\left(\boldsymbol{S}(t), \boldsymbol{P}(t)\right)$ that satisfies the following properties

- it holds $c_l\left(\boldsymbol{s}, \boldsymbol{p}\right) = 0$ for any $\boldsymbol{s}$, $\boldsymbol{p}$ such that $p_l = 0$. A consequence of the previous statement is the fact that $\boldsymbol{c}\left(\boldsymbol{s}, \mathbf{0}\right) = \mathbf{0}$.
- for any $\boldsymbol{s}, \boldsymbol{p}$, and for all l, it holds $c_l\left(\boldsymbol{s}, \boldsymbol{p}\right) \leq c_l\left(\boldsymbol{s}, \tilde{\boldsymbol{p}}\right)$ where $\tilde{p}_k = \delta_{lk} p_k$ and δ_{lk} is Kronecker's delta. The function $c_l\left(\boldsymbol{s}, \tilde{\boldsymbol{p}}\right)$ is non-decreasing, differentiable and concave w. r. t. p_l. Interpreting the first condition, it is equivalent to saying that the maximum rate of link l decreases (for a fixed p_l) as the other links are assigned non-zero power, which follows from interference properties. The second condition is also typical of most rate functions and appears often in literature.
- it holds $\frac{\partial c_l}{\partial p_l}\left(\boldsymbol{s}, \mathbf{0}\right) < \infty$ for all l and $\boldsymbol{s}$.

Since all sets encountered so far are finite, we define the bound[7] $\hat{c}_l \triangleq \max_{s \in \mathcal{S}, \boldsymbol{p} \in \mathcal{P}_{\boldsymbol{s}}} c_l(\boldsymbol{s}, \boldsymbol{p})$.

Under the previous assumptions and notation, the queues $\boldsymbol{V}(t) \triangleq (V_l(t))_{l=1}^{L}$, $\boldsymbol{U}(t) \triangleq (U_l(t))_{l=1}^{L}$ and the battery level $E(t)$ evolve as[8]

$$V_l(t+1) = V_l(t) + A_l(t) - R_{l,in}(t), \tag{1}$$

$$U_l(t+1) = \left[U_l(t) - \mu_l\left(\boldsymbol{S}(t), \boldsymbol{P}(t)\right)\right]^{+} + R_{l,in}(t), \tag{2}$$

$$E(t+1) = \min\left(E(t) - \sum_{l=1}^{L} P_l(t) + B(t), E_{max}\right), \tag{3}$$

where $[x]^{+} = \max(x, 0)$, subject to constraints

$$R_{l,in}(t) \leq V_l(t) + A_l(t) \quad \forall\, l,\, t, \tag{4}$$

$$\boldsymbol{P}(t) \in \mathcal{P}_{\boldsymbol{S}(t)}, \quad \sum_{l=1}^{L} P_l(t) \leq \min\left(E(t), \hat{P}\right) \quad \forall\, t, \tag{5}$$

$$0 \leq \mu_l\left(\boldsymbol{S}(t), \boldsymbol{P}(t)\right) \leq c_l\left(\boldsymbol{S}(t), \boldsymbol{P}(t)\right) \quad \forall\, l,\, t. \tag{6}$$

It can be argued that $\mu_l\left(\boldsymbol{S}(t), \boldsymbol{P}(t)\right)$ should be replaced by $c_l\left(\boldsymbol{S}(t), \boldsymbol{P}(t)\right)$ in (2) since, intuitively, there is no benefit in transmitting fewer bits than those allowed by the selected power (assuming there are sufficient bits to transmit in the first place). Although this argument is indeed correct, we elect to keep the current notation and reach the same conclusion through the policy specification itself rather than mere intuition.

Denote with $R_l(t)$ the number of bits *actually* transmitted in link l during slot t so that the corresponding time-average rate is

$$\bar{r}_l(t) \triangleq \frac{1}{t} \sum_{\tau=0}^{t-1} \mathbb{E}[R_l(\tau)]. \tag{7}$$

We also use the shorthand $\bar{\boldsymbol{r}}(t) \triangleq (\bar{r}_L(t))_{l=1}^{L}$ and write $\bar{\boldsymbol{r}}(t) = \frac{1}{t} \sum_{\tau=0}^{t-1} \mathbb{E}\left[\boldsymbol{R}(\tau)\right]$. Each user l derives a satisfaction $f_l\left(\bar{r}_l(t)\right)$ based on its current time-average rate $\bar{r}_l(t)$, where the utility function $f_l(\cdot)$ is assumed to be non-negative, increasing, differentiable and concave. We also impose the constraints $f_l(0) = 0$, $f_l'(0) < \infty$. The total system satisfaction $g\left(\bar{\boldsymbol{r}}(t)\right)$ at time t is $g\left(\bar{\boldsymbol{r}}(t)\right) \triangleq \sum_{l=1}^{L} f_l\left(\bar{r}_l(t)\right)$. We finally make the following natural

Assumption 1: At time $t = 0$, all bit queues are empty.

No assumption is made regarding the initial battery level; hence $E(0)$ can take any value in $[0 \quad E_{max}]$. Loosely speaking, a decision rule is a procedure for selecting the control variables $\boldsymbol{R}_{in}(t), \boldsymbol{P}(t)$ for a specific time slot t subject to all aforementioned constraints, while a policy is a sequence of decision rules for all time slots. We restrict attention to policies that stabilize the network according to the definition of [15]. Specifically, a network with a composite queue $\boldsymbol{U}(t)$ is stable iff $\limsup_{t \to \infty} \frac{1}{t} \sum_{\tau=0}^{t-1} \mathbb{E}[U_l(\tau)] < \infty \ \forall\, l$. Note that the notion of stability considers only the internal queue $\boldsymbol{U}(t)$ since the

[6]although in our case it holds $\mathcal{P}_{\boldsymbol{s}} = \mathcal{P} \ \forall\, \boldsymbol{s} \in \mathcal{S}$, since there is no reason for available power choices to depend on the channel state, there exist scenarios where the available powers depend on a properly defined state space (which may include more components than channel conditions only). These cases also fall under the considered model.

[7]unless otherwise noted, the accent $\hat{}$ will always denote an upper bound.

[8]unless otherwise noted, the indices $l, \boldsymbol{s}, \boldsymbol{p}$ will hereafter range, respectively, over the sets $\{1, \ldots, L\}, \mathcal{S}, \mathcal{P}_{\boldsymbol{s}}$ (e. g. we write $\forall\, \boldsymbol{s}$ instead of the formally correct $\forall\, \boldsymbol{s} \in \mathcal{S}$, etc).

external queue $\boldsymbol{V}(t)$ is, by definition, not part of the network layer (in fact, for heavy arrival traffic that exceeds network capacity, $\boldsymbol{V}(t)$ must grow without bound). Hence, we state our problem as follows

Problem 1: For the downlink scenario described by the queuing evolutions of (1)–(3) and the constraints of (4), (5), find a stabilizing policy that maximizes $\liminf_{t\to\infty} g\left(\bar{\boldsymbol{r}}(t)\right)$. *The optimization is performed over the set of all stabilizing policies, including those with perfect knowledge of future events. Denote the optimal objective value as* g_{re}^*.

Determination of the optimal policy in Problem 1 is very challenging, so we instead seek a policy with a system utility that is close to the optimal one. Since $\hat{P}, \hat{B}$ are considered to be system parameters, we can fix their values and restate the problem as

Problem 2: Under the same assumptions as in Problem 1, find a policy that for any $\epsilon > 0$ *achieves an objective value no less than* $g_{re}^* - \epsilon$, *provided that* $E_{max} > E^*(\epsilon)$ *for a sufficiently large* $E^*(\epsilon)$.

Since g_{re}^* clearly depends on E_{max}, a better notation would be $g_{re}^*(E_{max})$ but we elect to simplify notation and keep the dependence implicit. Problems 1, 2 are essentially sequential decision problem that can, in principle, be attacked with dynamic programming (DP) and/or Markov chain techniques. However, these techniques are impractical since they suffer from the dimensionality curse of DP and require extensive knowledge of system parameters, e. g. $\pi_{\boldsymbol{s}}$, $\boldsymbol{\lambda}$, which may not be available to the network controller. On the other hand, the Lyapunov drift framework of [16]–[19] assumes that at any state $\boldsymbol{s}$, one may always choose any of the available controls in $\mathcal{P}_{\boldsymbol{s}}$. However, this is not the case in our model, as evidenced from (5), which implies that when $E(t) < \hat{P}$ the available powers $\boldsymbol{P}(t)$ depend explicitly on the battery level $E(t)$. Hence, this approach is not directly applicable to our problem. Nevertheless, it suggests the existence of a modified policy that solves Problem 2 when $E_{max} \gg \hat{B}, \hat{P}$. The intuition behind the last statement is explained below.

1) Some intuitive remarks: Equations (3), (5) imply

$$\sum_{\tau=0}^{t-1}\sum_{l=1}^{L} P_l(\tau) \leq E_{max} + \sum_{\tau=0}^{t-1} B(\tau) \Rightarrow \limsup_{t\to\infty} \frac{1}{t}\sum_{\tau=0}^{t-1} \mathbb{E}\left[\sum_{l=1}^{L} P_l(\tau)\right] \leq \bar{B}, \tag{8}$$

where the first relation expresses conservation of energy and the second one follows from the first by taking expectations, dividing with t and taking a limsup as $t \to \infty$. Eq. (8) implies that *any* policy (stabilizing or not) acting on the rechargeable battery satisfies an average power constraint of $\bar{B}$, which in turn allows us to perform the following "thought experiment". Consider the same downlink problem as above and replace the rechargeable battery with an infinite capacity battery, which essentially removes (3) and the $E(t)$ constraint in (5). Denote with g_{avg}^* the maximum system utility achieved over all policies acting on the infinite battery with average power constraint $\bar{B}$ (we collectively refer to these as "average" policies). This scenario is treatable by the methodology in [18], which proposes an ABP-based adaptive policy whose performance can approach g_{avg}^* arbitrarily close. Since it clearly holds $g_{re} \leq g_{avg}^*$, Problem 2 is solved if we can find a policy (for the rechargeable battery) that performs better than $g_{avg}^* - \epsilon$.

At this point, and since the finite energy content of the battery affects decisions only when $E(t) < \hat{P}$, one might be tempted to directly apply the ABP average policy on the rechargeable battery (obviously, when ABP selects a power that exceeds the currently available energy, a best-effort action is taken). After all, assuming $E(0) = E_{max} \gg \hat{P}$ and applying the ABP average policy, it would take a very long time for the battery level to drop below $\hat{P}$, where ABP is non-optimal. Hence, it can be argued that such a policy is optimal "most of the time" and the asymptotic optimality is essentially "proved". The previous reasoning is wrong in an infinite horizon model in that it neglects what happens *after* the battery drops below $\hat{P}$. Specifically, if ABP results in the battery level oscillating around $\hat{P}$, or, worse, staying under $\hat{P}$ for extended intervals of time, then even though ABP is optimal for the time interval before the battery dropped below $\hat{P}$ for the first time, it becomes non-optimal for long intervals of time after that. If this occurs for many sample paths, it is not evident that the suggested policy performs close to optimal.

The previous paragraph effectively described a mechanism through which any policy acting on the rechargeable battery suffers a performance loss with respect to the ABP average policy. The crucial point is that it is not *a priori* known (and neither is it intuitively obvious) whether this loss can be made arbitrarily small. Another mechanism that leads to performance degradation is the loss of recharged energy due to the E_{max} cap. Specifically, for a slot t, it may hold $E(t) \geq E_{max} - \hat{B}$ and for a poor channel state the controller elects to transmit with low power (so that power is withheld for better channel states which can offer increased utility) and when the battery is recharged, the replenishment is too high so that some energy is lost due to the E_{max} cap. Obviously, if the controller knew in advance the exact amount of energy replenishment, it could elect to increase the selected transmitted power by the amount of overflow above E_{max}. This would have the effect that the battery energy would still be the same at the end of the time slot but now the user has received a higher satisfaction. Clearly, the ABP average policy is immune to this effect, since there is no battery to overflow in the first place.

The previous observations indicate that a policy closely resembling the ABP average policy when $E(t) \geq \hat{P}$ and under which $\Pr(E(t) < \hat{P})$ and $\Pr(E_{max} - \hat{B} < E(t) \leq E_{max})$ are small should perform nearly optimally. This is quantified next.

B. Performance analysis

1) Virtual queues and policy specification: We now focus on the rechargeable battery setting and, in the spirit of [15], introduce a virtual queue for each linear long-term constraint. Two such constraints exist in our model, the first one due to the finite arrivals, as modeled in (1), and the second one due to (8). Hence, we define virtual queues $\boldsymbol{Y}(t) \triangleq (Y_l(t))_{l=1}^{L}$ and $D(t)$ which evolve as

$$Y_l(t+1) = [Y_l(t) - R_{l,in}(t)]^+ + \gamma_l(t), \tag{9}$$

$$D(t+1) = [D(t) - (1-\delta)B(t)]^+ + \sum_{l=1}^{L} P_l(t), \tag{10}$$

for some $0 < \delta < 1$, where $\gamma_l(t)$ is an auxiliary process introduced for mathematical convenience. Since $\boldsymbol{R}_{in}(t), \boldsymbol{\gamma}(t)$ are determined by the policy, we can impose arbitrary bounds on them. Specifically, we require $R_{l,in}(t), \gamma_l(t) \leq \hat{A}_l \ \forall l$. The virtual queues are constructed in such a way that any policy that stabilizes them also satisfies the appropriate long-term constraints (this novel insight was introduced in [18]). Eq. (10) is different from the standard approach of [18], which would replace $(1-\delta)B(t)$ with $\bar{B}$, since the latter is the actual constraint to be satisfied. This modification is an essential ingredient of our approach and has important consequences, as will become apparent later. Fig. 1 represents the interconnections between the various physical and virtual queues, as defined by their evolutions in (1)–(3) and (9), (10). The dotted line in Fig. 1 is used

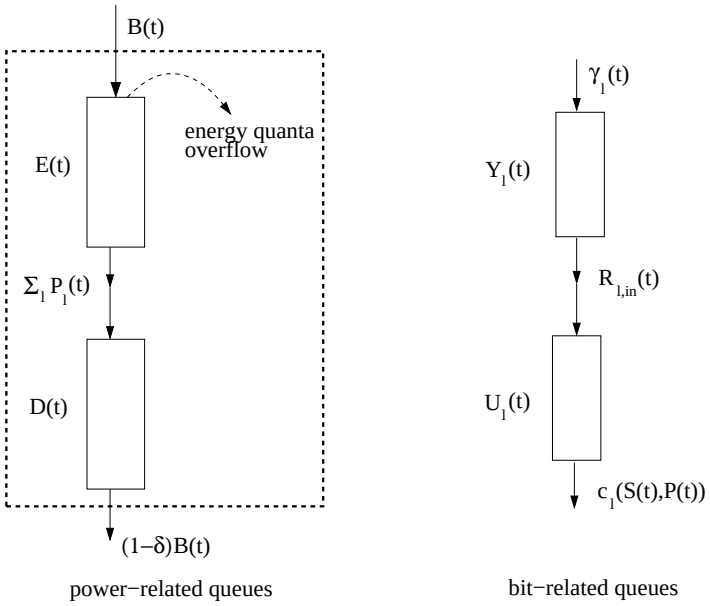

Fig. 1. Queue connections in the downlink scenario with rechargeable battery.

to examine the aggregate queue of $E(t)$, $D(t)$. Since the compound queue has an arrival rate of $B(t)$ and a service rate of at most $(1-\delta)B(t)$, it is unstable,[9] a fact that will be of crucial importance later. In foresight, it will be used to show that the queue $E(t)$ is sufficiently loaded most of the time so that $\Pr(E(t) < \hat{P})$ is small.

To assist the reader, the policy description is given first, followed by the stability and performance analysis in later sections. Specifically, we propose the following

Downlink rechargeable adaptive backpressure policy (DRABP)

1) at the beginning of slot t, observe queues $\boldsymbol{U}(t), \boldsymbol{Y}(t), \boldsymbol{V}(t)$ and select $\boldsymbol{R}_{in}(t)$ bits for admission into the network layer according to

$$\begin{aligned} \boldsymbol{R}_{in}(t) = \arg\max \quad & \sum_{l=1}^{L} \left(\eta Y_l(t) - U_l(t)\right) r_l \\ \text{s.t.} \quad & 0 \leq r_l \leq \min\left(V_l(t) + A_l(t), \hat{A}_l\right) \quad \forall l, \end{aligned} \tag{11}$$

where η is a tuning parameter used for balancing the congestion among the physical and virtual queues.

[9] in principle, the aggregate queue would still be unstable if we replaced $(1-\delta)B(t)$ with $(1-\delta)\bar{B}$ in (10), though the analysis would be more complicated. Also, $\bar{B}$ may not be known to the controller while $B(t)$ can be easily computed.

2) select $\boldsymbol{\gamma}(t)$ as the solution to the following problem

$$\begin{aligned}\boldsymbol{\gamma}(t) = \arg\max \quad & \sum_{l=1}^{L} \left[V f_l\left(\gamma_l\right) - \eta Y_l(t)\gamma_l\right] \\ \text{s.t.} \quad & 0 \leq \gamma_l \leq \hat{A}_l \quad \forall\, l,\end{aligned} \tag{12}$$

3) observe $\boldsymbol{S}(t)$ and select $\boldsymbol{P}(t)$ as the solution to the following problem

$$\begin{aligned}\boldsymbol{P}(t) = \arg\max \quad & \sum_{l=1}^{L} \left[U_l(t)\mu_l\left(\boldsymbol{S}(t), \boldsymbol{p}\right) - D(t)p_l\right] = \arg\max \quad \sum_{l=1}^{L} \left[U_l(t)c_l\left(\boldsymbol{S}(t), \boldsymbol{p}\right) - D(t)p_l\right] \\ \text{s.t.} \quad & \boldsymbol{p} \in \mathcal{P}_{\boldsymbol{S}(t)}, \quad \sum_{l=1}^{L} p_l \leq \min\left(E(t), \hat{P}\right), \\ & 0 \leq \mu_l\left(\boldsymbol{S}(t), \boldsymbol{p}\right) \leq c_l\left(\boldsymbol{S}(t), \boldsymbol{p}\right) \quad \forall\, l,\end{aligned} \tag{13}$$

4) update queues $\boldsymbol{V}(t), \boldsymbol{Y}(t), \boldsymbol{U}(t), E(t), D(t)$, in that order, according to the appropriate evolution equations.

The previous policy will occasionally be denoted as DRABP(δ, η, V) to emphasize its dependence on these two parameters. Its difference from the policy of [15] lies in the presence of the term $E(t)$ in the constraint of (13). As previously mentioned, this term causes the analysis of [15] to become inapplicable to our model so that a new approach required. The following observations can be made

- Eq. (11) accepts a bang-bang solution of the form

$$R_{l,in}(t) = \begin{cases} \min\left(V_l(t) + A_l(t), \hat{A}_l\right) & \text{if } U_l(t) < \eta Y_l(t), \\ 0 & \text{otherwise,} \end{cases} \tag{14}$$

- the concave maximization problem in (12) is separable and has a closed form solution if $(f_l')^{-1}(\gamma_l)$ is analytically known (the $^{-1}$ superscript denotes functional inverse).
- the problem in (13) is the most computationally expensive step of DRABP and, depending on the form of $c_l\left(\cdot,\cdot\right)$ (which in turn depends on network interference properties), may not be separable.

Note that DRABP requires no knowledge of system parameters (e. g. $\pi_{\boldsymbol{s}}$, $\boldsymbol{\lambda}$) and the intuitive rule of transmitting with peak rate for a giver power arose naturally through (13). It remains to examine the stability and performance properties of the above policy. The latter requires some additional notation and results to be introduced.

2) Some preliminary results: The following lemma, which is proved in [15], characterizes the optimal solution to the infinite battery with average power constraint and, as stated in Section II-A1, provides an upper bound for *any* rechargeable policy

Lemma 1: No downlink stabilizing policy acting on an infinite capacity battery under an average power constraint of $\bar{B}$ can achieve an objective value larger than

$$\begin{aligned} g_{avg}^{*} = \max \quad & \sum_{l=1}^{L} f_l(r_l) \\ \text{s.t.} \quad & \boldsymbol{r} \in \mathcal{R}, \\ & \boldsymbol{0} \leq \boldsymbol{r} \leq \boldsymbol{\lambda}, \end{aligned} \tag{15}$$

where

$$\mathcal{R} = \left\{ \boldsymbol{r} \in \mathbb{R}^L : \exists\, \pi_{\boldsymbol{p}}^{\boldsymbol{s}} \geq 0 \ \text{ s.t. } \ 0 \leq r_l \leq \sum_{\boldsymbol{s}\in\mathcal{S}} \sum_{\boldsymbol{p}\in\mathcal{P}_{\boldsymbol{s}}} c_l\left(\boldsymbol{s}, \boldsymbol{p}\right) \pi_{\boldsymbol{p}}^{\boldsymbol{s}} \pi_{\boldsymbol{s}} \ \ \forall\, l, \ \sum_{\boldsymbol{s}\in\mathcal{S}} \sum_{\boldsymbol{p}\in\mathcal{P}_{\boldsymbol{s}}} \sum_{l=1}^{L} p_l \pi_{\boldsymbol{p}}^{\boldsymbol{s}} \pi_{\boldsymbol{s}} \leq \bar{B}, \ \sum_{\boldsymbol{p}\in\mathcal{P}_{\boldsymbol{s}}} \pi_{\boldsymbol{p}}^{\boldsymbol{s}} = 1 \ \ \forall\, \boldsymbol{s} \right\}. \tag{16}$$

Clearly, the quantity $\pi_{\boldsymbol{p}}^{\boldsymbol{s}}$ in the definition of $\mathcal{R}$ is a discrete pdf on the set $\mathcal{P}_{\boldsymbol{s}}$. In [15], it is interpreted as the probability with which a randomized policy would select power $\boldsymbol{p}$ when the current channel state is $\boldsymbol{s}$.

The starting point for deriving a performance bound for any rechargeable policy is the following variation on a known result [15, Lemma 5.3 and Theorem 5.4]

Lemma 2: Consider a concave function $g(\cdot)$ and stochastic processes $Q(t), \boldsymbol{X}(t), \boldsymbol{Z}(t)$. If there exists a non-negative function $Ly\left(\boldsymbol{X}(t)\right)$ (referred to as a Lyapunov function) such that $\mathbb{E}[Ly\left(\boldsymbol{X}(0)\right)] < \infty$ and the following relation is satisfied for all t and some constants $C, V > 0$

$$\Delta\left(\boldsymbol{X}(t)\right) - V\mathbb{E}\left[g\left(\boldsymbol{Z}(t)\right)|\, \boldsymbol{X}(t)\right] \leq C - Vg^{*} + Q(t), \tag{17}$$

it then holds

$$\liminf_{t\to\infty} g\left(\bar{\boldsymbol{z}}(t)\right) \geq g^{*} - \frac{C + \bar{Q}}{V}, \tag{18}$$

where $\bar{\boldsymbol{z}}(t)$ *is the time-average of* $\boldsymbol{Z}(t)$, $\Delta\left(\boldsymbol{X}(t)\right) \triangleq \mathbb{E}\left[Ly\left(\boldsymbol{X}(t+1)\right) - Ly\left(\boldsymbol{X}(t)\right)|\boldsymbol{X}(t)\right]$ *and*

$$\bar{Q} \triangleq \limsup_{t\to\infty} \frac{1}{t} \sum_{j=0}^{t-1} \mathbb{E}[Q(j)]. \tag{19}$$

See Appendix V-A for the proof. A variant of Lemma 2 can also be used to prove stability of any policy that satisfies a modified version of (17); however, we will actually be able to prove a stronger result (namely deterministic queue bounds) by examining the policy specification itself, so this variant is omitted.

We also define, for $0 < \delta < 1$, the set

$$\mathcal{R}_\delta \triangleq \left\{ \boldsymbol{r} \in \mathbb{R}^L : \exists \pi_{\boldsymbol{p}}^{\boldsymbol{s}} \geq 0 \text{ s.t. } \sum_{\boldsymbol{s},\boldsymbol{p},l} p_l \pi_{\boldsymbol{p}}^{\boldsymbol{s}} \pi_{\boldsymbol{s}} \leq (1-\delta)\bar{B},\ \ 0 \leq r_l \leq \sum_{\boldsymbol{s},\boldsymbol{p}} c_l\left(\boldsymbol{s},\boldsymbol{p}\right) \pi_{\boldsymbol{p}}^{\boldsymbol{s}} \pi_{\boldsymbol{s}}\ \ \forall l,\ \ \sum_{\boldsymbol{p}} \pi_{\boldsymbol{p}}^{\boldsymbol{s}} = 1\ \ \forall \boldsymbol{s} \right\}, \tag{20}$$

as the set of rates that can be stabilized by a randomized policy subject to an average power constraint of $(1-\delta)\bar{B}$, and the optimization problem

$$\begin{aligned} g_\delta^* = \max \quad & \sum_{l=1}^{L} f_l(r_l) \\ \text{s.t.} \quad & \boldsymbol{0} \leq \boldsymbol{r} \leq \boldsymbol{\lambda}, \\ & \boldsymbol{r} \in \mathcal{R}_\delta. \end{aligned} \tag{21}$$

Since $\boldsymbol{0} \in \mathcal{P}_{\boldsymbol{s}}\ \forall\, \boldsymbol{s}$, it follows that $\mathcal{R}_\delta \neq \varnothing$. Also, $\mathcal{R}_\delta$ has the following properties

- it is convex and compact
- $\boldsymbol{r} \in \mathcal{R}_\delta$ implies $\boldsymbol{r}_1 \in \mathcal{R}_\delta\ \forall\, \boldsymbol{r}_1 \leq \boldsymbol{r}$.

These properties are proved in a straightforward manner in [15], which also provides the following continuity result

$$\lim_{\delta \downarrow 0} g_\delta^* = g_{avg}^* \tag{22}$$

3) Stability and performance properties of DRABP: The following result, proved in Appendix V-B, provides all necessary information for the stability properties of DRABP

Lemma 3: Under DRABP, queues $\boldsymbol{Y}(t), \boldsymbol{U}(t), D(t)$ *are deterministically bounded for all* t *as follows*

$$\begin{aligned} & Y_l(t) \leq \frac{V f_l'(0)}{\eta} + \hat{A}_l \triangleq \hat{Y}_l \quad \forall\, l, \\ & U_l(t) \leq \eta \hat{Y}_l + \hat{A}_l \triangleq \hat{U}_l \quad \forall\, l, \\ & D(t) \leq \max_{1\leq l\leq L} \left(\hat{U}_l \hat{C}_l\right) + \hat{P} \triangleq \hat{D}, \end{aligned} \tag{23}$$

where $\hat{C}_l \triangleq \max_{\boldsymbol{s}\in\mathcal{S}} \frac{\partial c_l}{\partial p_l}\left(\boldsymbol{s},\boldsymbol{0}\right)$.

Hence, we have actually proved a much stronger result (namely deterministic bounds) than stability for DRABP. In order to derive a performance bound via Lemma 2, we define the composite queue $\boldsymbol{X}(t) \triangleq \left(\boldsymbol{U}(t), \boldsymbol{Y}(t), D(t)\right)$ and the Lyapunov function

$$Ly\left(\boldsymbol{X}(t)\right) = \sum_{l=1}^{L} \left(U_l^2(t) + \eta Y_l^2(t)\right) + D^2(t) \tag{24}$$

From (2), (9), (10) and Lemma 4.3 of [15], it follows after a little algebra

$$U_l^2(t+1) \leq U_l^2(t) + \mu_l^2\left(\boldsymbol{S}(t), \boldsymbol{P}(t)\right) + R_{l,in}^2(t) - 2U_l(t)\left[\mu_l\left(\boldsymbol{S}(t), \boldsymbol{P}(t)\right) - R_{l,in}(t)\right], \tag{25}$$

$$Y_l^2(t+1) \leq Y_l^2(t) + R_{l,in}^2(t) + \gamma_l^2(t) - 2Y_l(t)\left[R_{l,in}(t) - \gamma_l(t)\right], \tag{26}$$

$$D^2(t+1) \leq D^2(t) + (1-\delta)^2 B^2(t) + \left(\sum_{l=1}^{L} P_l(t)\right)^2 - 2D(t)\left[(1-\delta)B(t) - \sum_{l=1}^{L} P_l(t)\right]. \tag{27}$$

Summing (25), (26) over l and using all the imposed bounds results in

$$\begin{aligned} \Delta\left(\boldsymbol{X}(t)\right) \leq & \sum_{l=1}^{L} \left(\hat{c}_l^2 + (2\eta+1)\hat{A}_l^2\right) + \hat{B}^2 + \hat{P}^2 - 2\,\mathbb{E}\left[\sum_{l=1}^{L} U_l(t)\left[\mu_l\left(\boldsymbol{S}(t), \boldsymbol{P}(t)\right) - R_{l,in}(t)\right] \middle| \boldsymbol{X}(t)\right] \\ & - 2\eta\,\mathbb{E}\left[\sum_{l=1}^{L} Y_l(t)\left[R_{l,in}(t) - \gamma_l(t)\right] \middle| \boldsymbol{X}(t)\right] - 2D(t)\,\mathbb{E}\left[(1-\delta)B(t) - \sum_{l=1}^{L} P_l(t) \middle| \boldsymbol{X}(t)\right]. \end{aligned} \tag{28}$$

Exploiting the iid nature of $B(t)$, which implies $\mathbb{E}\left[B(t)|\boldsymbol{X}(t)\right]=\bar{B}$, subtracting $2V\,\mathbb{E}\left[\sum_{l=1}^{L} f_l\left(\gamma_l(t)\right)\middle|\boldsymbol{X}(t)\right]$ from both sides and rearranging terms yields

$$\begin{aligned}\Delta\left(\boldsymbol{X}(t)\right)-2V\,\mathbb{E}\left[\sum_{l=1}^{L} f_l\left(\gamma_l(t)\right)\middle|\boldsymbol{X}(t)\right]&\leq \dot{C}-2\,\mathbb{E}\left[\sum_{l=1}^{L}\left[Vf_l\left(\gamma_l(t)\right)-\eta Y_l(t)\gamma_l(t)\right]\middle|\boldsymbol{X}(t)\right]\\&-2\,\mathbb{E}\left[\sum_{l=1}^{L}\left[U_l(t)\mu_l\left(\boldsymbol{S}(t),\boldsymbol{P}(t)\right)-D(t)P_l(t)\right]\middle|\boldsymbol{X}(t)\right]-2\,\mathbb{E}\left[\sum_{l=1}^{L}\left[\eta Y_l(t)-U_l(t)\right]R_{l,in}(t)\middle|\boldsymbol{X}(t)\right]\\&-2(1-\delta)\bar{B}D(t),\end{aligned}\tag{29}$$

where $\dot{C}\triangleq\hat{B}^2+\hat{P}^2+\sum_{l=1}^{L}\left(\hat{c}_l^2+(2\eta+1)\hat{A}_l^2\right)$. The last equation justifies, in retrospect, the specification of DRABP since each step of DRABP is chosen so as to minimize the overall Lyapunov drift in (29).

Our intention is to bring (29) into the form of (17). To this end, we need to bound each term in (29) in such a way that the policy actions (i. e. $\boldsymbol{P}(t)$, $\boldsymbol{R}_{in}(t)$) are removed due to cancellations. This procedure will occupy the entire current section. The following remarks will be useful. For a given $\boldsymbol{X}(t)$ (which implies that $\boldsymbol{U}(t), D(t)$ are known) and $\boldsymbol{S}(t)=\boldsymbol{s}$, the solution to the optimization in (13) is independent from $E(t)$ when $E(t)\geq\hat{P}$. We denote this solution as $\boldsymbol{p}_{\boldsymbol{s}}^{*}$ and use the notation $\boldsymbol{P}\left(\boldsymbol{s},e\right)$ for the solution to the same problem when $E(t)=e<\hat{P}$. Since the zero power vector is always an allowable selection, it follows from optimality of (13) (recall that $\boldsymbol{P}(t)$ is selected according to the DRABP policy)

$$\begin{aligned}&\sum_{l=1}^{L}\left[U_l(t)c_l\left(\boldsymbol{S}(t),\boldsymbol{P}(t)\right)-D(t)P_l(t)\right]\geq\sum_{l=1}^{l}U_l(t)c_l\left(\boldsymbol{S}(t),\boldsymbol{0}\right)=0\quad\forall\,t\\\Rightarrow&\sum_{l=1}^{L}\left[U_l(t)c_l\left(\boldsymbol{s},\boldsymbol{P}\left(\boldsymbol{s},e\right)\right)-D(t)P_l\left(\boldsymbol{s},e\right)\right]\geq 0\quad\forall\,\boldsymbol{s},\,e,\,t.\end{aligned}\tag{30}$$

Consider now the joint probability $q_{\boldsymbol{s},e}(t)\triangleq\Pr\left(\boldsymbol{S}(t)=\boldsymbol{s},\,E(t)=e|\,\boldsymbol{X}(t)\right)$, when DRABP is applied, and denote with $\mathcal{E}(t)$ the set of values that $E(t)$ can take under DRABP (it is easy to show inductively that $\mathcal{E}(t)$ is countable). It holds

$$\begin{aligned}&\mathbb{E}\left[\sum_{l=1}^{L}\left[U_l(t)c_l\left(\boldsymbol{S}(t),\boldsymbol{P}(t)\right)-D(t)P_l(t)\right]\middle|\boldsymbol{X}(t)\right]=\sum_{\boldsymbol{s}\in\mathcal{S}}\sum_{e\in\mathcal{E}(t)}\sum_{l=1}^{L}\left[U_l(t)c_l\left(\boldsymbol{s},\boldsymbol{P}(\boldsymbol{s},e)\right)-D(t)P_l\left(\boldsymbol{s},e\right)\right]q_{\boldsymbol{s},e}(t)\\&\geq\sum_{\boldsymbol{s}\in\mathcal{S}}\sum_{\substack{e\in\mathcal{E}(t)\\e\geq\hat{P}}}\sum_{l=1}^{L}\left[U_l(t)c_l\left(\boldsymbol{s},\boldsymbol{p}_{\boldsymbol{s}}^{*}\right)-D(t)p_{l,\boldsymbol{s}}^{*}\right]q_{\boldsymbol{s},e}(t)\\&=\sum_{\boldsymbol{s}\in\mathcal{S}}\sum_{e\in\mathcal{E}(t)}\sum_{l=1}^{L}\left[U_l(t)c_l\left(\boldsymbol{s},\boldsymbol{p}_{\boldsymbol{s}}^{*}\right)-D(t)p_{l,\boldsymbol{s}}^{*}\right]q_{\boldsymbol{s},e}(t)-\sum_{\boldsymbol{s}\in\mathcal{S}}\sum_{\substack{e\in\mathcal{E}(t)\\e<\hat{P}}}\sum_{l=1}^{L}\left[U_l(t)c_l\left(\boldsymbol{s},\boldsymbol{p}_{\boldsymbol{s}}^{*}\right)-D(t)p_{l,\boldsymbol{s}}^{*}\right]q_{\boldsymbol{s},e}(t)\\&=\sum_{\boldsymbol{s}\in\mathcal{S}}\sum_{l=1}^{L}\left[U_l(t)c_l\left(\boldsymbol{s},\boldsymbol{p}_{\boldsymbol{s}}^{*}\right)-D(t)p_{l,\boldsymbol{s}}^{*}\right]\pi_{\boldsymbol{s}}-\sum_{\boldsymbol{s}\in\mathcal{S}}\sum_{l=1}^{L}\left[U_l(t)c_l\left(\boldsymbol{s},\boldsymbol{p}_{\boldsymbol{s}}^{*}\right)\right)-D(t)p_{l,s}^{*}\right]\Pr\left(E(t)<\hat{P},\,\boldsymbol{S}(t)=\boldsymbol{s}\middle|\,\boldsymbol{X}(t)\right)\\&\geq\sum_{\boldsymbol{s}\in\mathcal{S}}\sum_{l=1}^{L}\left[U_l(t)c_l(\boldsymbol{s},\boldsymbol{p}_{\boldsymbol{s}}^{*})-D(t)p_{l,s}^{*}\right]\pi_{\boldsymbol{s}}-\sum_{l=1}^{L}\hat{c}_l\hat{U}_l\Pr\left(E(t)<\hat{P}\middle|\,\boldsymbol{X}(t)\right),\end{aligned}\tag{31}$$

where the first inequality is due to (30), the fourth line is due to the independence of $\boldsymbol{p}_{\boldsymbol{s}}^{*}$ from e (the value of $E(t)$) and the final line follows from the bounds on $\boldsymbol{U}(t)$ (due to Lemma 3) and $c_l\left(\boldsymbol{s},\boldsymbol{p}\right)$. We also used the iid property to write $\sum_{\boldsymbol{s}\in\mathcal{S}}q_{\boldsymbol{s},e}(t)=\Pr\left(\boldsymbol{S}(t)=\boldsymbol{s}|\,\boldsymbol{X}(t)\right)=\pi_{\boldsymbol{s}}$ in the transition from the third to the fourth line.

Pick any pdf $\pi_{\boldsymbol{p}}^{\boldsymbol{s}}$ acting on the set $\mathcal{P}_{\boldsymbol{s}}$. We have, from optimality of (13),

$$\sum_{l=1}^{L}\left[U_l(t)c_l\left(\boldsymbol{s},\boldsymbol{p}_{\boldsymbol{s}}^{*}\right)-D_l(t)p_{l,\boldsymbol{s}}^{*}\right]\geq\sum_{l=1}^{L}\left[U_l(t)c_l\left(\boldsymbol{s},\boldsymbol{p}\right)-D(t)p_l\right]\quad\forall\,t,\,\boldsymbol{s},\,\boldsymbol{p},\tag{32}$$

so that multiplying with $\pi_{\boldsymbol{p}}^{\boldsymbol{s}}\pi_{\boldsymbol{s}}$, summing over $\boldsymbol{s},\boldsymbol{p}$ and exploiting the pdf property $\sum_{\boldsymbol{p}\in\mathcal{P}_{\boldsymbol{s}}}\pi_{\boldsymbol{p}}^{\boldsymbol{s}}=1$ yields

$$\begin{aligned}&\sum_{\boldsymbol{s}\in\mathcal{S}}\sum_{\boldsymbol{p}\in\mathcal{P}_{\boldsymbol{s}}}\sum_{l=1}^{L}\left[U_l(t)c_l\left(\boldsymbol{s},\boldsymbol{p}_{\boldsymbol{s}}^{*}\right)-D(t)p_{l,\boldsymbol{s}}^{*}\right]\pi_{\boldsymbol{p}}^{\boldsymbol{s}}\pi_{\boldsymbol{s}}\geq\sum_{\boldsymbol{s}\in\mathcal{S}}\sum_{\boldsymbol{p}\in\mathcal{P}_{\boldsymbol{s}}}\sum_{l=1}^{L}\left[U_l(t)c_l\left(\boldsymbol{s},\boldsymbol{p}\right)-D(t)p_l\right]\pi_{\boldsymbol{p}}^{\boldsymbol{s}}\pi_{\boldsymbol{s}}\\\Rightarrow&\sum_{\boldsymbol{s}\in\mathcal{S}}\sum_{l=1}^{L}\left[U_l(t)c_l\left(\boldsymbol{s},\boldsymbol{p}_{\boldsymbol{s}}^{*}\right)-D(t)p_{l,\boldsymbol{s}}^{*}\right]\pi_{\boldsymbol{s}}\geq\sum_{\boldsymbol{s}\in\mathcal{S}}\sum_{\boldsymbol{p}\in\mathcal{P}_{\boldsymbol{s}}}\sum_{l=1}^{L}\left[U_l(t)c_l\left(\boldsymbol{s},\boldsymbol{p}\right)-D(t)p_l\right]\pi_{\boldsymbol{p}}^{\boldsymbol{s}}\pi_{\boldsymbol{s}}.\end{aligned}\tag{33}$$

Now pick any $\boldsymbol{r}$ such that $\mathbf{0} \leq \boldsymbol{r} \leq \boldsymbol{\lambda}$, whence it follows

$$A_l(t)\,\frac{r_l}{\lambda_l} \leq A_l(t) \leq \min\left(V_l(t)+A_l(t), \hat{A}_l\right) \quad \forall\, l,\, t. \tag{34}$$

Hence, $A_l(t) r_l/\lambda_l$ belongs to the constraint set of the optimization in (11), so that

$$\sum_{l=1}^{L} \left(\eta Y_l(t) - U_l(t)\right) R_{l,in}(t) \geq \sum_{l=1}^{L} \left(\eta Y_l(t) - U_l(t)\right) A_l(t)\,\frac{r_l}{\lambda_l} \quad \forall\, t, \tag{35}$$

where $R_{l,in}(t)$ is selected by the DRABP policy. The last expression contains the random variables $R_{l,in}(t), A_l(t)$ so that taking conditional expectations upon $\boldsymbol{X}(t)$ and using the iid nature of $A_l(t)$ provides

$$\mathbb{E}\left[\sum_{l=1}^{L} \left(\eta Y_l(t) - U_l(t)\right) R_{l,in}(t) \middle| \boldsymbol{X}(t)\right] \geq \sum_{l=1}^{L} \left(\eta Y_l(t) - U_l(t)\right) r_l \quad \forall\, \boldsymbol{r}:\ \mathbf{0} \leq \boldsymbol{r} \leq \boldsymbol{\lambda}, \tag{36}$$

since $\mathbb{E}[A_l(t)|\boldsymbol{X}(t)] = \lambda_l$. Also, the above $\boldsymbol{r}$ satisfies $0 \leq r_l \leq \hat{A}_l$, so that optimality of (12) implies

$$\sum_{l=1}^{L} \left[V f_l\left(\gamma_l(t)\right) - \eta Y_l(t)\gamma_l(t)\right] \geq \sum_{l=1}^{L} \left[V f_l(r_l) - \eta Y_l(t) r_l\right] \quad \forall\, \boldsymbol{r}:\ \mathbf{0} \leq \boldsymbol{r} \leq \boldsymbol{\lambda}, \tag{37}$$

where $\gamma_l(t)$, which is selected according to the DRABP policy, is a random variable. Clearly, a similar inequality is produced for the conditional expectation upon $\boldsymbol{X}(t)$ of the LHS of (37).

Inserting (37), (36), (33) in (29) produces

$$\begin{aligned}\Delta\left(\boldsymbol{X}(t)\right) - 2V\,\mathbb{E}\left[\sum_{l=1}^{L} f_l\left(\gamma_l(t)\right) \middle| \boldsymbol{X}(t)\right] &\leq \dot{C} - 2\sum_{l=1}^{L}\left(V f_l(r_l) - \eta Y_l(t) r_l\right) - 2\sum_{l=1}^{L}\left(\eta Y_l(t) - U_l(t)\right) r_l \\ - 2\sum_{\boldsymbol{s}\in\mathcal{S}}\sum_{\boldsymbol{p}\in\mathcal{P}_{\boldsymbol{S}}}\sum_{l=1}^{L}\left[U_l(t) c_l\left(\boldsymbol{s},\boldsymbol{p}\right) - D(t) p_l\right]\pi_{\boldsymbol{p}}^{\boldsymbol{s}}\pi_{\boldsymbol{s}} &+ 2\sum_{l=1}^{L}\hat{c}_l\hat{U}_l \Pr\left(E(t) < \hat{P}\middle|\boldsymbol{X}(t)\right) - 2(1-\delta)\bar{B}D(t).\end{aligned} \tag{38}$$

Equation (38) holds for any $\boldsymbol{r}$ with $\mathbf{0} \leq \boldsymbol{r} \leq \boldsymbol{\lambda}$ and any pdf $\pi_{\boldsymbol{p}}^{\boldsymbol{s}}$. Hence, we can pick $\boldsymbol{r}$ to be the maximizing argument of (21) (i. e. the vector achieving g_δ^*) and $\pi_{\boldsymbol{p}}^{\boldsymbol{s}}$ the pdf that corresponds to it according to (20). This creates some cancellations in (38) and, through the definition of $\mathcal{R}_\delta$, strengthens (38) to

$$\Delta\left(\boldsymbol{X}(t)\right) - 2V\,\mathbb{E}\left[\sum_{l=1}^{L} f_l\left(\gamma_l(t)\right) \middle| \boldsymbol{X}(t)\right] \leq \dot{C} - 2V g_\delta^* + 2\sum_{l=1}^{L}\hat{c}_l\hat{U}_l \Pr\left(E(t) < \hat{P}\middle|\boldsymbol{X}(t)\right) \quad \forall\, t. \tag{39}$$

A direct application of Lemma 2 now provides

$$\liminf_{t\to\infty} \sum_{l=1}^{L} f_l\left(\bar{\gamma}_l(t)\right) \geq g_\delta^* - \frac{\dot{C}}{2V} - \frac{\sum_{l=1}^{L}\hat{c}_l\hat{U}_l}{V}\limsup_{t\to\infty}\frac{1}{t}\sum_{j=0}^{t-1}\Pr\left(E(j) < \hat{P}\right), \tag{40}$$

since $\mathbb{E}[\Pr(E(t) < \hat{P}|\boldsymbol{X}(t))] = \Pr(E(t) < \hat{P})$.

4) Performance bound of DRABP: Eq. (40) is not very informative since our original intention was to provide a bound for the liminf of $\sum_{l=1}^{L} f_l\left(\bar{r}_l(t)\right)$ and not $\sum_{l=1}^{L} f_l\left(\bar{\gamma}_l(t)\right)$, which has no physical meaning. Additionally, we need to estimate the limsup appearing in (40). The first issue is handled through the following Lemma, which essentially exploits the stabilizing properties of DRABP. The result, whose proof is found in Appendix V-C, is initially stated in a general setting and then reduced to our model

*Lemma 4: Consider any compound queue $\boldsymbol{Z}(t)$ (with physical or virtual components) with an arrival process $\boldsymbol{A}_{in}(t)$ and a bounded service process $\boldsymbol{\mu}_{out}(t)$ that evolves as $\boldsymbol{Z}(t+1) = \left[\boldsymbol{Z}(t) - \boldsymbol{\mu}_{out}(t)\right]^+ + \boldsymbol{A}_{in}(t)$, with $\mathbb{E}[\boldsymbol{Z}(0)] < \infty$. Denote with $\tilde{\boldsymbol{\mu}}_{out}(t)$ the number of bits **actually** transmitted at slot t and define the long-term averages $\bar{\boldsymbol{a}}_{in}(t)$, $\bar{\boldsymbol{\mu}}_{out}(t)$, $\bar{\tilde{\boldsymbol{\mu}}}_{out}(t)$. Under any stabilizing policy, it holds*

$$\liminf_{t\to\infty} g\left(\bar{\boldsymbol{a}}_{in}(t)\right) = \liminf_{t\to\infty} g\left(\bar{\tilde{\boldsymbol{\mu}}}_{out}(t)\right) \leq \liminf_{t\to\infty} g\left(\bar{\boldsymbol{\mu}}_{out}(t)\right), \tag{41}$$

where g is any continuous and component-wise increasing function (i. e. $\boldsymbol{x} \leq \boldsymbol{y}$ implies $g(\boldsymbol{x}) \leq g(\boldsymbol{y})$).

Consider now the queues $\boldsymbol{Y}(t)$, $\boldsymbol{U}(t)$. These queues are stable (in fact, finite) under DRABP, so that applying the above Lemma w. r. t. the evolution equations (9), (2) and setting $g(\boldsymbol{x}) = \sum_{l=1}^{L} f_l(x_l)$ (this g clearly satisfies the conditions of the Lemma) results in

$$\liminf_{t\to\infty}\sum_{l=1}^{L} f_l\left(\bar{\gamma}_l(t)\right) = \liminf_{t\to\infty}\sum_{l=1}^{L} f_l\left(\bar{\tilde{r}}_{l,in}(t)\right) \leq \liminf_{t\to\infty}\sum_{l=1}^{L} f_l\left(\bar{r}_{l,in}(t)\right) = \liminf_{t\to\infty}\sum_{l=1}^{L} f_l\left(\bar{r}_l(t).\right) \tag{42}$$

The following statement, proved in Appendix V-D, provides an estimation of the limsup appearing in (40)

Lemma 5: Under DRABP, it holds

$$\limsup_{t\to\infty}\frac{1}{t}\sum_{j=0}^{t-1}\Pr\left(E(j)<\hat{P}\right)\leq\Pr\left(\sum_{k=0}^{\sigma-1}B(k)\leq\frac{\hat{P}+\hat{D}-E_{max}}{\delta}\right), \tag{43}$$

where $\sigma=\lceil E_{max}/\hat{P}-1\rceil$.

Combining Lemma 5 with (42), (40) yields the main result for the downlink case

Theorem 1: DRABP stabilizes the system and achieves a performance bound of

$$\liminf_{t\to\infty}\sum_{l=1}^{L}f_l\left(\bar{r}_l(t)\right)\geq g_\delta^*-\dot{C}_1-\dot{C}_2\Pr\left(\sum_{k=0}^{\sigma-1}B(k)\leq\frac{\hat{P}+\hat{D}-E_{max}}{\delta}\right), \tag{44}$$

where $\dot{C}_1=\dot{C}/(2V)$ *and* $\dot{C}_2=\sum_{l=1}^{L}(\hat{c}_l\hat{U}_l)/V$.

An examination of Lemma 3 reveals that $\hat{U}_l,\hat{D}=\Theta(V)$, $\dot{C}=\Theta(1)$ and $\dot{C}_1=O(1/V)$. Theorem 1 admits the following

Corollary 1: For given policy parameters $V,\eta>0$*, a selection of* E_{max} *such that* $E_{max}>\hat{P}+\hat{D}$ *implies the following performance bound for DRABP*

$$\liminf_{t\to\infty}\sum_{l=1}^{L}f_l\left(\bar{r}_l(t)\right)\geq g_\delta^*-\dot{C}_1. \tag{45}$$

Since $\dot{C}_1=O(1/V)$ and $g_\delta^*\to g_{avg}^*$ as $\delta\to 0$, the above RHS can approach g_{avg}^* arbitrarily close as $\delta\to 0$ and $V\to\infty$ (provided that it holds $E_{max}>\hat{P}+\hat{D}$), which implies the asymptotic optimality of DRABP.

Additionally, a slightly more complicated asymptotic result can be established for the regime $\hat{P}+\hat{D}-\delta\sigma\bar{B}<E_{max}\leq\hat{P}+\hat{D}$ (the regime $E_{max}>\hat{P}+\hat{D}$ is handled by Corollary 1) according to the following

Lemma 6: For given policy parameters V,η,δ and iid recharge process $B(t)$, a selection of E_{max} s.t. $\hat{P}+\hat{D}-\sigma\delta\bar{B}<E_{max}\leq\hat{P}+\hat{D}$ implies the following bound for DRABP

$$\Pr\left(\sum_{k=0}^{\sigma-1}B(k)\leq\frac{\hat{P}+\hat{D}-E_{max}}{\delta}\right)\leq\exp\left[\sigma\,\ell\left(\frac{\hat{P}+\hat{D}-E_{max}}{\sigma\delta}-\bar{B}\right)\right], \tag{46}$$

where

$$\ell(x)\triangleq\sup_{\theta}\left(\theta x+\theta\bar{B}-\ln\mathbb{E}\left[\mathrm{e}^{\theta B(t)}\right]\right). \tag{47}$$

Due to the iid property, any value for t can be used in the last expectation.

Proof: See Appendix V-E. ∎

The qualitative aspect of the above corollary could, in retrospect, be derived independently through the following

Lemma 7: The condition $E_{max}>\hat{P}+\hat{D}$ *implies* $E(t)+D(t)\geq E_{max}$ *for all* $t\geq\tilde{\tau}$ *(where* $\tilde{\tau}=\inf\{t:E(t)=E_{max}\}$ *is the first time the battery hits* E_{max}*) and therefore* $E(t)\geq\hat{P}$ *for all* $t\geq\tilde{\tau}$*.*

Since $\tilde{\tau}$ is finite w. p. 1 (due to the infinitely often overflow mentioned in Appendix V-D) and we are interested in the infinite-horizon average utility, we expect that what happens in the finite part up to $\tilde{\tau}$ will not contribute to the average. Since for $t\geq\tilde{\tau}$ the battery never falls below $\hat{P}$, one of the loss mechanisms mentioned in Section II-A1 is eliminated so that performance loss (relative to an average policy with value $(1-\delta)\bar{B}$) can only come from lost recharge. This implies a DRABP bound similar to (45), where the $\dot{C}_1$ term is now attributed to the remaining mechanism of lost recharge. Although it is not used in the subsequent parts, the interested reader will find a proof of Lemma 7 and the previous intuition in Appendix V-F.

5) Removal of the assumption $f_l'(0)<\infty$*:* The only reason for imposing the assumption $f_l'(0)<\infty$ in Section II-A is that it allowed us to easily provide deterministic bounds for all queues according to Lemma 3. On the other hand, any utility function of the form $f(x)=x^a$ with $0<a<1$ satisfies $f'(0)=\infty$, so that the previous analysis must be modified. This is described next.

Specifically, we still assume monotonicity and concavity for all $f_l(\cdot)$ as well as $f_l(0)=0$ (since any other condition is unnatural) and $f_l'(x)<\infty\ \forall\,x>0$. However, it may hold $f_l'(0)=\infty$ for some l. For a given $\beta>0$, we propose the following policy that is identical to DRABP except for the second step (selection of $\boldsymbol{\gamma}(t)$) which is replaced by

- For l such that $f_l'(0)<\infty$, select

$$\begin{aligned}\gamma_l^\beta(t)=\arg\max\quad&\left[Vf_l(\gamma_l)-\eta Y_l(t)\gamma_l\right]\\ \text{s.t.}\quad&0\leq\gamma_l\leq\hat{A}_l,\end{aligned} \tag{48}$$

  i. e. $\gamma_l^\beta(t)$ has the same value as $\gamma_l(t)$ in DRABP.

For l such that $f_l'(0)=\infty$, first solve the problem

$$\begin{aligned}\tilde{\gamma}_l^{\beta}(t) = \arg\max \quad & [Vf_l(\gamma_l) - \eta Y_l(t)\gamma_l] \\ \text{s.t.} \quad & \beta \le \gamma_l \le \hat{A}_l,\end{aligned} \tag{49}$$

and then select $\gamma_l^{\beta}(t)$ as[10]

$$\gamma_l^{\beta}(t) = \begin{cases} 0 & \text{if } Y_l(t) \ge \frac{Vf_l'(\beta)}{\eta}, \\ \tilde{\gamma}_l^{\beta}(t) & \text{otherwise.}\end{cases} \tag{50}$$

We denote the above policy as β-DRABP to emphasize its dependence on β. This policy is chosen so that it approximates DRABP as $\beta \to 0$ and (most importantly) guarantees bounded queues for $\boldsymbol{Y}(t), \boldsymbol{U}(t), \boldsymbol{D}(t)$. In fact, a repetition of the proof of Lemma 3 provides the following

Corollary 2: Application of β-DRABP results in the following bounds for all t

$$\begin{aligned} Y_l(t) &\le \hat{Y}_l \triangleq \begin{cases} \frac{Vf_l'(\beta)}{\eta} + \hat{A}_l & \textit{if } f_l'(0)=\infty, \\ \frac{Vf_l'(0)}{\eta} + \hat{A}_l & \textit{otherwise}, \end{cases} \\ U_l(t) &\le \eta \hat{Y}_l + \hat{A}_l \triangleq \hat{U}_l, \\ D(t) &\le \max_{1\le l\le L} \left(\hat{U}_l \hat{C}_l\right) + \hat{P} \triangleq \hat{D}, \end{aligned} \tag{51}$$

where $\hat{C}_l \triangleq \max_{\boldsymbol{s}\in\mathcal{S}} \frac{\partial c_l}{\partial p_l}(\boldsymbol{s}, \boldsymbol{0})$.

Denote with $\gamma_l(t)$ the solution to (12), so that $\gamma_l(t) = \gamma_l^{\beta}(t)$ if $f_l'(0) < \infty$. If $f_l'(0)=\infty$, it holds either $Y_l(t) < Vf_l'(\beta)/\eta$ or $Y_l(t) \ge Vf_l'(\beta)/\eta$. In the former case, concavity of f_l implies that the function $Vf_l(x) - \eta Y_l(t)x$ is non-decreasing in the interval $[0 \quad \beta]$, so that the argmax of (12) lies in the interval $[\beta \quad \hat{A}_l]$, and therefore $\gamma_l^{\beta}(t) = \gamma_l(t)$. In the latter case, the argmax of (12) lies in the interval $[0 \quad \beta]$ while $\gamma_l^{\beta}(t) = 0$. Hence, the following bound holds in all cases

$$\begin{aligned} &[Vf_l(\gamma_l(t)) - \eta Y_l(t)\gamma_l(t)] - \left[Vf_l\left(\gamma_l^{\beta}(t)\right) - \eta Y_l(t)\gamma_l^{\beta}(t)\right] \le \max_{0\le x\le\beta} [Vf_l(x) - \eta Y_l(t)x] \\ &\le \max_{0\le x\le\beta} Vf_l(x) = Vf_l(\beta), \end{aligned} \tag{52}$$

where we used the monotonicity of f_l. We define $\mathcal{F} = \{l : f_l'(0)=\infty\}$ so that the separability of (12) implies

$$\sum_{l=1}^{L} \left[Vf_l\left(\gamma_l^{\beta}(t)\right) - \eta Y_l(t)\gamma_l^{\beta}(t)\right] \ge \sum_{l=1}^{L} [Vf_l(\gamma_l) - \eta Y_l(t)\gamma_l] - V\sum_{l\in\mathcal{F}} f_l(\beta), \tag{53}$$

for all $\boldsymbol{\gamma}$ such that $0 \le \gamma_l \le \hat{A}_l$. Repeating the Lyapunov drift calculation of Section II-B3 for β-DRABP results in a form identical to (29) with the addition of the term $2V\sum_{l\in\mathcal{F}} f_l(\beta)$ to the RHS. Hence, the following extension to Theorem 1 is derived

Theorem 2: β-DRABP stabilizes the system, with the queue bounds of (51), and achieves a performance bound of

$$\liminf_{t\to\infty} \sum_{l=1}^{L} f_l(\bar{r}_l(t)) \ge g_{\delta}^* - \sum_{l\in\mathcal{F}} f_l(\beta) - \dot{C}_1 - \dot{C}_2 \Pr\left(\sum_{k=0}^{\sigma-1} B(k) \le \frac{\hat{P} + \hat{D} - E_{max}}{\delta}\right). \tag{54}$$

Since f_l is continuous and $f_l(0)=0$, the term $\sum_{l\in\mathcal{F}} f_l(\beta)$ can be made arbitrarily small by picking a small enough β (with a corresponding increase in queue bounds) so that asymptotic optimality is retained.

Hence, the assumption $f_l'(0) < \infty$ can be removed w. l. o. g. In the remaining sections, we keep this assumption to slightly simplify the expressions under the implicit understanding that a generalization similar to the above is possible.

C. Extensions to single-hop and multihop networks

A careful examination of the proofs of the various statements in Section II-B reveals that, apart from algebraic manipulations, the optimality of DRABP rests on the following crucial point: queues $\boldsymbol{Y}(t), \boldsymbol{U}(t), D(t)$ are deterministically bounded (in fact, the boundedness of each queue is used to prove the boundedness of the subsequent ones) and, by construction of $D(t)$, the battery overflows infinitely often. Hence, we expect a policy that has the previous properties, when applied to a general network, to achieve similar performance to DRABP. This is studied next.

[10] clearly, β is used as a superscript, rather than an exponent, in this context.

a) Single-hop networks: Consider a single-hop network consisting of N nodes, where each node n is allowed to transmit to any of its neighbors belonging to the set $\mathcal{O}_n$. The single-hop constraint implies that once a bit is transmitted, it also exits the network layer. Hence, in terms of the bit queues, a single-hop network is just an aggregate of N interacting downlinks, so that most of the notation of Sections II-A, II-B can be modified to fit the new model. Specifically, we denote with $E_n(t)$ the battery level of node n at time t, and with $A_{nl}(t)$ the exogenous arrival process at node n destined for node l (where $l \in \mathcal{O}_n$), while $B_n(t)$ is the amount of replenished energy of node n at time t. These processes are still assumed iid with mean values of λ_{nl}, $\bar{B}_n$ and upper bounded by $\hat{A}_{nl}, \hat{B}_n$, respectively. Similarly, $V_{nl}(t)$ denotes the external queue of node n where bits destined for node l are kept, $R_{nl,in}(t)$ the number of bits admitted at slot t into node n destined for node l etc. Denoting with $\bar{r}_{nl}(t)$ the average rate up to time t from node n to node l, the objective is to maximize $\liminf_{t\to\infty} \sum_{n,l} f_{nl}\left(\bar{r}_{nl}(t)\right)$, where f_{nl} are, per link, utility functions with the properties mentioned in Section II-A. The evolution equations are essentially the "vectorized", w. r. t. the nodes, versions of the downlink evolutions, i. e.

$$V_{nl}(t+1) = V_{nl}(t) + A_{nl}(t) - R_{nl,in}(t), \tag{55}$$

$$U_{nl}(t+1) = \left[U_{nl}(t) - \mu_{nl}\left(\boldsymbol{S}(t), \boldsymbol{P}(t)\right)\right]^+ + R_{nl,in}(t), \tag{56}$$

$$E_n(t+1) = \min\left(E_n(t) - \sum_{l\in\mathcal{O}_n} P_{nl}(t) + B_n(t), E_{max}\right), \tag{57}$$

$$Y_{nl}(t+1) = \left[Y_{nl}(t) - R_{nl,in}(t)\right]^+ + \gamma_{nl}(t), \tag{58}$$

$$D_n(t+1) = \left[D_n(t) - (1-\delta)B_n(t)\right]^+ + \sum_{l\in\mathcal{O}_n} P_{nl}(t), \tag{59}$$

subject to constraints

$$\begin{aligned} &R_{nl,in}(t) \le V_{nl}(t) + A_{nl}(t) \quad \forall\, n,\, l,\, t, \\ &\boldsymbol{P}(t) \in \mathcal{P}_{\boldsymbol{S}(t)}, \quad \sum_{l\in\mathcal{O}_n} P_{nl}(t) \le \min\left(E_n(t), \hat{P}\right) \quad \forall\, n,\, t. \end{aligned} \tag{60}$$

Each node is therefore equipped with a set of queues connected as shown in Fig. 1. We denote the composite queue $\boldsymbol{X}(t) \triangleq (\boldsymbol{U}(t), \boldsymbol{Y}(t), \boldsymbol{D}(t))$ and select a Lyapunov function (unless otherwise stated, the indices n, l will range over the sets $\{1,\dots,N\}$, $\mathcal{O}_n$, respectively)

$$Ly\left(\boldsymbol{X}(t)\right) = \sum_{n,l}\left(U_{nl}^2(t) + \eta Y_{nl}^2(t)\right) + \sum_n D_n^2(t) \tag{61}$$

The analogue of Lemma 1 becomes

Lemma 8: No stabilizing policy acting on a single-hop network with infinite batteries and an average power constraint of $\bar{\boldsymbol{B}}$ can achieve performance greater than

$$\begin{aligned} g_{avg}^* = \max \quad & \sum_{n=1}^{N}\sum_{l\in\mathcal{O}_n} f_{nl}(r_{nl}) \\ \text{s.t.} \quad & \boldsymbol{r} \in \mathcal{R}, \\ & \boldsymbol{0} \le \boldsymbol{r} \le \boldsymbol{\lambda}, \end{aligned} \tag{62}$$

where

$$\begin{aligned} \mathcal{R} = \Bigg\{ \boldsymbol{r} : \exists\, \pi_{\boldsymbol{p}}^{\boldsymbol{s}} \text{ s.t. } 0 \le r_{nl} \le \sum_{\boldsymbol{s}\in\mathcal{S}}\sum_{\boldsymbol{p}\in\mathcal{P}_{\boldsymbol{s}}} c_{nl}\left(\boldsymbol{s},\boldsymbol{p}\right)\pi_{\boldsymbol{p}}^{\boldsymbol{s}}\pi_{\boldsymbol{s}} \quad \forall\, n,l \\ \sum_{\boldsymbol{s}\in\mathcal{S}}\sum_{\boldsymbol{p}\in\mathcal{P}_{\boldsymbol{s}}}\sum_{l\in\mathcal{O}_n} p_{nl}\pi_{\boldsymbol{p}}^{\boldsymbol{s}}\pi_{\boldsymbol{s}} \le \bar{B}_n \quad \forall\, n, \quad \sum_{\boldsymbol{p}\in\mathcal{P}_{\boldsymbol{s}}} \pi_{\boldsymbol{p}}^{\boldsymbol{s}} = 1 \quad \forall\, \boldsymbol{s} \Bigg\}, \end{aligned} \tag{63}$$

with a similar definition for $\mathcal{R}_\delta$ (i. e. replace $\bar{B}_n$ with $(1-\delta)\bar{B}_n$ in (63)). It still holds $\lim_{\delta\downarrow 0} g_\delta^* = g_{avg}^*$, where g_δ^* is the solution to the optimization of (15), albeit with the new definition for $\mathcal{R}_\delta$.

The reader can repeat the steps of Section II-B and arrive at a result similar to Theorem 1. To avoid redundant repetition and assist the reader, we provide only the salient points of this procedure. Specifically, the Lyapunov drift under any policy

satisfies the following analogue of (29)

$$\begin{aligned}\Delta\left(\boldsymbol{X}(t)\right)-2V\,\mathbb{E}\left[\sum_{n,l}f_{nl}\left(\gamma_{nl}(t)\right)\middle|\boldsymbol{X}(t)\right]&\leq\dot{C}-2\,\mathbb{E}\left[\sum_{n,l}\left[Vf_{nl}\left(\gamma_{nl}(t)\right)-\eta Y_{nl}(t)\gamma_{nl}(t)\right]\middle|\boldsymbol{X}(t)\right]\\&-2\,\mathbb{E}\left[\sum_{n,l}\left[U_{nl}(t)\mu_{nl}\left(\boldsymbol{S}(t),\boldsymbol{P}(t)\right)-D_n(t)P_{nl}(t)\right]\middle|\boldsymbol{X}(t)\right]-2\,\mathbb{E}\left[\sum_{n,l}\left[\eta Y_{nl}(t)-U_{nl}(t)\right]R_{nl,in}(t)\middle|\boldsymbol{X}(t)\right]\\&-2(1-\delta)\sum_n\bar{B}_nD_n(t),\end{aligned}\tag{64}$$

where $\dot{C}\triangleq N\hat{P}^2+\sum_n\hat{B}_n^2+\sum_{n,l}\left((2\eta+1)\hat{A}_{nl}^2+\hat{c}_{nl}^2\right)$ is a policy independent parameter, with $\hat{c}_{nl}=\max_{\boldsymbol{s},\boldsymbol{p}}c_{nl}\left(\boldsymbol{s},\boldsymbol{p}\right)$. We now propose the following policy, which is again a "vectorized" version of DRABP.

Single-hop rechargeable adaptive backpressure policy (SRABP)

- at the beginning of slot t, observe $\boldsymbol{U}(t),\boldsymbol{Y}(t),\boldsymbol{V}(t)$ and admit $\boldsymbol{R}_{in}(t)$ bits into the network layer according to

$$\begin{aligned}\boldsymbol{R}_{in}(t)=\arg\max\quad&\sum_{n,l}\left(\eta Y_{nl}(t)-U_{nl}(t)\right)r_{nl}\\\text{s.t.}\quad&0\leq r_{nl}\leq\min\left(V_{nl}(t)+A_{nl}(t),\hat{A}_{nl}\right)\quad\forall\,n,l,\end{aligned}\tag{65}$$

- select $\boldsymbol{\gamma}(t)$ as the solution to the following problem

$$\begin{aligned}\boldsymbol{\gamma}(t)=\arg\max\quad&\sum_{n,l}\left[Vf_{nl}(\gamma_{nl})-\eta Y_{nl}(t)\gamma_{nl}\right]\\\text{s.t.}\quad&0\leq\gamma_{nl}\leq\hat{A}_{nl}\quad\forall\,n,l,\end{aligned}\tag{66}$$

- observe channel state $\boldsymbol{S}(t)$ and select transmission power $\boldsymbol{P}(t)$ according to

$$\begin{aligned}\boldsymbol{P}(t)=\arg\max\quad&\sum_{n,l}\left[U_{nl}(t)c_{nl}\left(\boldsymbol{S}(t),\boldsymbol{p}\right)-D_n(t)p_{nl}\right]\\\text{s.t.}\quad&\boldsymbol{p}\in\mathcal{P}_{\boldsymbol{S}(t)},\quad\sum_{l\in\mathcal{O}_n}p_{nl}\leq\min\left(E_n(t),\hat{P}\right)\quad\forall\,n,\end{aligned}\tag{67}$$

Applying the above policy results in queues $\boldsymbol{Y}(t)$, $\boldsymbol{U}(t)$, $\boldsymbol{D}(t)$ being deterministically bounded (essentially, the vectorized version of Lemma 3, proved in an identical manner as in Appendix V-B, provides bounds $\hat{Y}_{nl},\hat{U}_{nl},\hat{D}_n$). The finiteness of $D_n(t)$ implies, with an argument identical to the one in Appendix V-D, that each battery overflows infinitely often and hence

$$\Pr\left(E_n(t)<\hat{P},\tilde{\tau}_n\leq t\right)\leq\Pr\left(\sum_{k=0}^{\sigma-1}B_n(k)\leq\frac{\hat{P}+\hat{D}_n-E_{max}}{\delta}\right),\tag{68}$$

where $\tilde{\tau}_n=\inf\{t:E_n(t)=E_{max}\}$ is the first time the battery of node n hits E_{max}.

To derive the analogue of (31) under SRABP, we define $q_{\boldsymbol{s},\boldsymbol{e}}(t)\triangleq\Pr\left(\boldsymbol{S}(t)=\boldsymbol{s},\boldsymbol{E}(t)=\boldsymbol{e}|\boldsymbol{X}(t)\right)$ and denote with $\boldsymbol{P}\left(\boldsymbol{s},\boldsymbol{e}\right)$ the general solution to (67). For the special case of $\boldsymbol{E}(t)\geq\hat{\boldsymbol{P}}$ (i. e. when all batteries are above $\hat{P}$, so that the optimization of (67) is independent of $\boldsymbol{E}(t)$) we denote $\boldsymbol{P}\left(\boldsymbol{s},\boldsymbol{e}\right)=p^*_{\boldsymbol{s}}$, so that it holds

$$\begin{aligned}&\mathbb{E}\left[\sum_{n,l}\left[U_{nl}(t)c_{nl}\left(\boldsymbol{S}(t),\boldsymbol{P}(t)\right)-D_n(t)P_{nl}(t)\right]\middle|\boldsymbol{X}(t)\right]=\sum_{\boldsymbol{s}\in\mathcal{S}}\sum_{\boldsymbol{e}\in\mathcal{E}(t)}\sum_{n,l}\left[U_{nl}(t)c_{nl}\left(\boldsymbol{s},\boldsymbol{P}(\boldsymbol{s},\boldsymbol{e})\right)-D_n(t)P_{nl}\left(\boldsymbol{s},\boldsymbol{e}\right)\right]q_{\boldsymbol{s},\boldsymbol{e}}(t)\\&\geq\sum_{\boldsymbol{s}\in\mathcal{S}}\sum_{\substack{\boldsymbol{e}\in\mathcal{E}(t)\\\boldsymbol{e}\geq\hat{\boldsymbol{P}}}}\sum_{n,l}\left[U_{nl}(t)c_{nl}\left(\boldsymbol{s},\boldsymbol{p}^*_{\boldsymbol{s}}\right)-D_n(t)p^*_{nl,\boldsymbol{s}}\right]q_{\boldsymbol{s},\boldsymbol{e}}(t)\\&=\sum_{\boldsymbol{s}\in\mathcal{S}}\sum_{\boldsymbol{e}\in\mathcal{E}(t)}\sum_{n,l}\left[U_{nl}(t)c_{nl}\left(\boldsymbol{s},\boldsymbol{p}^*_{\boldsymbol{s}}\right)-D_n(t)p^*_{nl,\boldsymbol{s}}\right]q_{\boldsymbol{s},\boldsymbol{e}}(t)-\sum_{\boldsymbol{s}\in\mathcal{S}}\sum_{\substack{\boldsymbol{e}\in\mathcal{E}(t)\\\boldsymbol{e}\not\geq\hat{\boldsymbol{P}}}}\sum_{n,l}\left[U_{nl}(t)c_{nl}\left(\boldsymbol{s},\boldsymbol{p}^*_{\boldsymbol{s}}\right)-D_n(t)p^*_{nl,\boldsymbol{s}}\right]q_{\boldsymbol{s},\boldsymbol{e}}(t)\\&\geq\sum_{\boldsymbol{s}\in\mathcal{S}}\sum_{n,l}\left[U_{nl}(t)c_{nl}\left(\boldsymbol{s},\boldsymbol{p}^*_{\boldsymbol{s}}\right)-D_n(t)p^*_{nl,\boldsymbol{s}}\right]\pi_{\boldsymbol{s}}-\sum_{\boldsymbol{s}\in\mathcal{S}}\sum_{n,l}U_{nl}(t)c_{nl}\left(\boldsymbol{s},\boldsymbol{p}^*_{\boldsymbol{s}}\right)\Pr\left(\bigcup_{n=1}^N\{E_n(t)<\hat{P},\boldsymbol{S}(t)=\boldsymbol{s}\}\middle|\boldsymbol{X}(t)\right)\\&\geq\sum_{\boldsymbol{s}\in\mathcal{S}}\sum_{n,l}\left[U_{nl}(t)c_{nl}\left(\boldsymbol{s},\boldsymbol{p}^*_{\boldsymbol{s}}\right)-D_n(t)p^*_{nl,\boldsymbol{s}}\right]\pi_{\boldsymbol{s}}-\left(\sum_{n,l}\hat{c}_{nl}\hat{U}_{nl}\right)\Pr\left(\bigcup_{n=1}^N\{E_n(t)<\hat{P}\}\middle|\boldsymbol{X}(t)\right),\end{aligned}\tag{69}$$

where we used the fact that $\sum_{n,l}\left[U_{nl}(t)c_{nl}\left(\boldsymbol{s},\boldsymbol{P}\left(\boldsymbol{s},\boldsymbol{e}\right)\right)-D_n(t)P_{nl}\left(\boldsymbol{s},\boldsymbol{e}\right)\right]\geq 0\ \forall\,\boldsymbol{s},\,\boldsymbol{e}$ (since $\boldsymbol{p}=\boldsymbol{0}$ is always an allowable choice) in the second line and the queue bounds on the last one. Using the maximization properties of SRABP in (65)–(67) and repeating the arguments used in the derivation of (32)–(37) results in

$$\Delta\left(\boldsymbol{X}(t)\right)-2V\mathbb{E}\left[\sum_{n,l}f_{nl}\left(\gamma_{nl}(t)\right)\middle|\boldsymbol{X}(t)\right]\leq\dot{C}-2\sum_{n,l}\left[Vf_{nl}(r_{nl})-\eta Y_{nl}(t)r_{nl}\right]-2\sum_{n,l}\left[\eta Y_{nl}(t)-U_{nl}(t)\right]r_{nl}$$
$$-2\sum_{\boldsymbol{s},\boldsymbol{p}}\sum_{n,l}\left[U_{nl}(t)c_{nl}\left(\boldsymbol{s},\boldsymbol{p}\right)-D_n(t)p_{nl}\right]\pi_{\boldsymbol{p}}^{\boldsymbol{s}}\pi_{\boldsymbol{s}}+2\sum_{n,l}\hat{c}_{nl}\hat{U}_{nl}\Pr\left(\bigcup_{n=1}^{N}\{E_n(t)<\hat{P}\}\middle|\boldsymbol{X}(t)\right)-2(1-\delta)\sum_{n}\bar{B}_nD_n(t). \tag{70}$$

The last equation holds for any pdf $\pi_{\boldsymbol{p}}^{\boldsymbol{s}}$ and $\boldsymbol{r}$ s.t. $\boldsymbol{0}\leq\boldsymbol{r}\leq\boldsymbol{\lambda}$. Hence, we can pick $\boldsymbol{r}=\boldsymbol{r}^*$ to be the vector achieving g_δ^* and $\pi_{\boldsymbol{p}}^{\boldsymbol{s}}$ the corresponding pdf. It then follows from the definition of $\mathcal{R}_\delta$

$$\begin{aligned}&r_{nl}^*\leq\sum_{\boldsymbol{s}\in\mathcal{S}}\sum_{\boldsymbol{p}\in\mathcal{P}_{\boldsymbol{s}}}c_{nl}\left(\boldsymbol{s},\boldsymbol{p}\right)\pi_{\boldsymbol{p}}^{\boldsymbol{s}}\pi_{\boldsymbol{s}}\quad\forall\,n,\,l,\\&\sum_{\boldsymbol{s}\in\mathcal{S}}\sum_{\boldsymbol{p}\in\mathcal{P}_{\boldsymbol{s}}}\sum_{l\in\mathcal{O}_n}p_{nl}\pi_{\boldsymbol{p}}^{\boldsymbol{s}}\pi_{\boldsymbol{s}}\leq(1-\delta)\bar{B}_n\quad\forall\,n,\end{aligned} \tag{71}$$

so that the analogue of (39) is

$$\Delta\left(\boldsymbol{X}(t)\right)-2V\mathbb{E}\left[\sum_{n,l}f_{nl}\left(\gamma_{nl}(t)\right)\middle|\boldsymbol{X}(t)\right]\leq\dot{C}-2Vg_\delta^*+2\sum_{n,l}\hat{c}_{nl}\hat{U}_{nl}\Pr\left(\bigcup_{n=1}^{N}\{E_n(t)<\hat{P}\}\middle|\boldsymbol{X}(t)\right). \tag{72}$$

We now invoke Lemmas 2, 4 to get the following

Theorem 3: SRABP stabilizes any single-hop network and achieves a performance bound of

$$\liminf_{t\to\infty}\sum_{n,l}f_{nl}\left(\bar{r}_{nl}(t)\right)\geq g_\delta^*-\frac{\dot{C}}{2V}-\frac{\sum_{n,l}\hat{c}_{nl}\hat{U}_{nl}}{V}\limsup_{t\to\infty}\frac{1}{t}\sum_{j=0}^{t-1}\Pr\left(\bigcup_{n=1}^{N}\{E_n(j)<\hat{P}\}\right). \tag{73}$$

Using the union bound, standard properties of limsup and the fact that each queue individually overflows infinitely often (so that Lemma 5 is applicable) results in the following

Corollary 3: SRABP satisfies the following bound

$$\liminf_{t\to\infty}\sum_{n,l}f_{nl}\left(\bar{r}_{nl}(t)\right)\geq g_\delta^*-\frac{\dot{C}}{2V}-\frac{\sum_{n,l}\hat{c}_{nl}\hat{U}_{nl}}{V}\sum_{n=1}^{N}\Pr\left(\sum_{k=0}^{\sigma-1}B_n(k)\leq\frac{\hat{P}+\hat{D}_n-E_{max}}{\delta}\right). \tag{74}$$

Hence, selecting $E_{max}>\hat{P}+\max_n\hat{D}_n$ makes the probability appearing in the RHS of the last equation zero, so that SRABP is asymptotically optimal.

1) Multihop networks: The main difference between single-hop and multihop networks is that in the latter case intra-node traffic, in addition to exogenous arrivals, is explicitly allowed. This suggests that a vectorization of DRABP to a multihop setting will be more involved. In fact, new notation is required to capture the fact that a packet may need many hops to reach its destination. Specifically, we model a multihop network as a standard digraph $(\mathcal{N},\mathcal{L})$ (with $\mathcal{N}=\{1,\ldots,N\}$) and use the commodity concept of [15] to assume that each bit belongs to a packet with an associated commodity $c\in\mathcal{K}$ (which minimally defines the packet destination[11] but may contain additional information). Hence, we denote with $A_n^{(c)}(t)$ the number of commodity c bits exogenously generated at node n and slot t (we assume $A_n^{(c)}(t)$ to be iid with expectation $\lambda_n^{(c)}$ and an upper bound of $\hat{A}_n^{(c)}$) with similar interpretations for the internal/external queues $U_n^{(c)}(t)$, $V_n^{(c)}(t)$, respectively. We also denote with $R_{n,in}^{(c)}(t)$ the number of externally admitted commodity c bits at node n and slot t, while $\mu_{ab}^{(c)}(t)$ is the number of commodity c bits transmitted on link (a,b) during slot t. The total number of bits (for all commodities) transmitted over a link is upper bounded by a vector function $\boldsymbol{c}\left(\boldsymbol{S}(t),\boldsymbol{P}(t)\right)$ with the properties mentioned in Section II-A, so that it holds $\sum_c\mu_{ab}^{(c)}\left(\boldsymbol{S}(t),\boldsymbol{P}(t)\right)\leq c_{ab}\left(\boldsymbol{S}(t),\boldsymbol{P}(t)\right)$. We also define $\hat{c}_{ab}\triangleq\max_{\boldsymbol{s},\boldsymbol{p}}c_{ab}\left(\boldsymbol{s},\boldsymbol{p}\right)$. The objective is to maximize[12] $\liminf_{t\to\infty}\sum_{n,c}f_{nc}\left(\bar{r}_{n,in}^{(c)}\right)$, where $\bar{r}_{n,in}^{(c)}(t)\triangleq\frac{1}{t}\sum_{\tau=0}^{t-1}\mathbb{E}[R_{n,in}^{(c)}(\tau)]$ and $f_{nc}(\cdot)$ are typical utility functions.

[11] e. g., for sensor networks, different commodities may correspond to different data collection points (sinks).

[12] in the following, the indices n,c will range over the sets $\mathcal{N}$, $\mathcal{K}$, respectively, unless otherwise stated.

Motivated by the downlink and single-hop analysis, we introduce virtual queues $D_n(t)$ and $Y_n^{(c)}(t)$ to handle the average power and (finite) arrival constraints, respectively. Hence, the queues' evolution is as follows

$$V_n^{(c)}(t+1) = V_n^{(c)}(t) + A_n^{(c)}(t) - R_{n,in}^{(c)}(t), \tag{75}$$

$$U_n^{(c)}(t+1) \leq \left[U_n^{(c)}(t) - \sum_b \mu_{nb}^{(c)}\left(\boldsymbol{S}(t), \boldsymbol{P}(t)\right)\right]^+ + R_{n,in}^{(c)}(t) + \sum_a \mu_{an}^{(c)}\left(\boldsymbol{S}(t), \boldsymbol{P}(t)\right), \tag{76}$$

$$E_n(t+1) = \min\left(E_n(t) - \sum_b P_{nb}(t) + B_n(t), E_{max}\right), \tag{77}$$

$$Y_n^{(c)}(t+1) = \left[Y_n^{(c)}(t) - R_{n,in}^{(c)}(t)\right]^+ + \gamma_n^{(c)}(t), \tag{78}$$

$$D_n(t+1) = \left[D_n(t) - (1-\delta)B_n(t)\right]^+ + \sum_b P_{nb}(t), \tag{79}$$

subject to constraints

$$\begin{aligned} &R_{n,in}^{(c)}(t) \leq V_n^{(c)}(t) + A_n^{(c)}(t) \quad \forall\, n, c, t, \\ &\mu_{ab}^{(c)} \geq 0, \quad \mu_{ab}^{(c)}\left(\boldsymbol{S}(t), \boldsymbol{P}(t)\right) = 0 \quad \forall\, (a,b) \notin \mathcal{L}^{(c)}, t, \\ &\boldsymbol{P}(t) \in \mathcal{P}_{\boldsymbol{S}(t)}, \quad \sum_b P_{nb}(t) \leq \min\left(E_n(t), \hat{P}\right) \quad \forall\, n, t, \end{aligned} \tag{80}$$

where indices a, b range over the set of incoming and outgoing neighbors of node n, respectively. The second constraint in (80) models the fact that all commodity c bits may be required to be transmitted through links belonging to a specific set $\mathcal{L}^{(c)} \subseteq \mathcal{L}$ *only* (setting $\mathcal{L}^{(c)} = \mathcal{L}$ for all c effectively removes this constraint so that all commodities can be routed to all links). Finally, the reason for (76) being an inequality rather than an equality is that the actual amount of incoming traffic to node n may be less than $\sum_a \mu_{an}^{(c)}\left(\boldsymbol{S}(t), \boldsymbol{P}(t)\right)$ due to low queue occupancy of the neighbors.

In order to derive an analogue of Lemma 1, we first introduce the following

Definition 1: For given node set $\mathcal{N}$, commodity set $\mathcal{K}$ and link constraint sets $\mathcal{L}^{(c)}$, a (consistent) multi-commodity flow $\left\{f_{ab}^{(c)}\right\}$ is a vector that satisfies the following conditions for all $a, b \in \mathcal{N}$ and $c \in \mathcal{K}$

$$\begin{aligned} &f_{ab}^{(c)} \geq 0, \\ &(a,b) \notin \mathcal{L}^{(c)} \Rightarrow f_{ab}^{(c)} = 0, \\ &f_{aa}^{(c)} = f_{dest(c),b}^{(c)} = 0, \end{aligned} \tag{81}$$

where $dest(c)$ is the destination node for commodity c.

In the subsequent analysis, the term "flow" will exclusively refer to a consistent flow. Reference [15] provides the following

Lemma 9: No stabilizing policy acting on a multihop network with infinite capacity batteries and an average power constraint of $\bar{\boldsymbol{B}}$ can achieve performance greater than

$$\begin{aligned} g_{avg}^* = \max \quad & \sum_{n,c} f_{nc}\left(r_n^{(c)}\right) \\ \text{s.t.} \quad & \boldsymbol{r} \in \mathcal{R}, \\ & 0 \leq r_n^{(c)} \leq \lambda_n^{(c)} \quad \forall\, n, c, \end{aligned} \tag{82}$$

where

$$\begin{aligned} \mathcal{R} = \Bigg\{ \boldsymbol{r} = \left(r_n^{(c)}\right) : \exists\, \pi_{\boldsymbol{p}}^{\boldsymbol{s}},\ \text{flow } \{f_{ab}^{(c)}\} \text{ s.t.} \quad & r_n^{(c)} \leq \sum_b f_{nb}^{(c)} - \sum_a f_{an}^{(c)} \quad \forall\, n, c, \quad \sum_{\boldsymbol{p}} \pi_{\boldsymbol{p}}^{\boldsymbol{s}} = 1 \quad \forall\, \boldsymbol{s}, \\ & \sum_c f_{ab}^{(c)} \leq \sum_{\boldsymbol{s}} \sum_{\boldsymbol{p}} c_{ab}\left(\boldsymbol{s}, \boldsymbol{p}\right) \pi_{\boldsymbol{p}}^{\boldsymbol{s}} \pi_{\boldsymbol{s}} \quad \forall\, a, b, \quad \sum_{\boldsymbol{s}} \sum_{\boldsymbol{p}} \sum_b p_{nb} \pi_{\boldsymbol{p}}^{\boldsymbol{s}} \pi_{\boldsymbol{s}} \leq \bar{B}_n \quad \forall\, n \Bigg\}. \end{aligned} \tag{83}$$

In accordance with previous sections, we define the set $\mathcal{R}_\delta$ in a manner similar to $\mathcal{R}$ except that the average power constraint $\bar{\boldsymbol{B}}$ is replaced by $(1-\delta)\bar{\boldsymbol{B}}$. We also define the multihop analogue of (21) as

$$\begin{aligned} g_\delta^* = \max \quad & \sum_{n,c} f_{nc}\left(r_n^{(c)}\right) \\ \text{s.t.} \quad & \boldsymbol{r} \in \mathcal{R}_\delta, \\ & \boldsymbol{0} \leq \boldsymbol{r} \leq \boldsymbol{\lambda}, \end{aligned} \tag{84}$$

where $\boldsymbol{\lambda} \triangleq \left(\lambda_n^{(c)}\right)_{n,c}$. The continuity properties of (22) are still applicable as well. We denote the composite queue $\boldsymbol{X}(t) \triangleq (\boldsymbol{U}(t), \boldsymbol{Y}(t), \boldsymbol{D}(t))$ and select a Lyapunov function

$$Ly\left(\boldsymbol{X}(t)\right) = \sum_{n,c}\left[\left(U_n^{(c)}(t)\right)^2 + \eta\left(Y_n^{(c)}(t)\right)^2\right] + \sum_n D_n^2(t). \tag{85}$$

Squaring the evolution equations (76), (78), (79), performing some algebra and rearranging terms yields

$$\begin{aligned}\Delta\left(\boldsymbol{X}(t)\right) - 2V\mathbb{E}\left[\sum_{n,c} f_{nc}\left(\gamma_n^{(c)}(t)\right)\middle|\boldsymbol{X}(t)\right] &\leq \dot{C} - 2\mathbb{E}\left[\sum_{n,c}\left[Vf_{nc}\left(\gamma_n^{(c)}(t)\right) - \eta Y_n^{(c)}(t)\gamma_n^{(c)}(t)\right]\middle|\boldsymbol{X}(t)\right] \\ - 2\mathbb{E}\left[\sum_{a,b}\left[\sum_c\left(U_a^{(c)}(t) - U_b^{(c)}(t)\right)\mu_{ab}^{(c)}\left(\boldsymbol{S}(t), \boldsymbol{P}(t)\right) - D_a(t)P_{ab}(t)\right]\middle|\boldsymbol{X}(t)\right] \\ - 2\mathbb{E}\left[\sum_{n,c}\left[\eta Y_n^{(c)}(t) - U_n^{(c)}(t)\right]R_{n,in}^{(c)}(t)\middle|\boldsymbol{X}(t)\right] &- 2(1-\delta)\sum_n \bar{B}_n D_n(t).\end{aligned} \tag{86}$$

The rationale of minimizing overall Lyapunov drift suggests the following policy

Network rechargeable adaptive backpressure policy (NRABP)

- at the beginning of slot t, observe queues $\boldsymbol{U}(t)$, $\boldsymbol{Y}(t)$, $\boldsymbol{V}(t)$ and select $\boldsymbol{R}_{in}(t) = \left(R_{n,in}^{(c)}(t)\right)$ bits for admission according to

$$\begin{aligned}\boldsymbol{R}_{in}(t) = \arg\max \quad & \sum_{n,c}\left(\eta Y_n^{(c)}(t) - U_n^{(c)}(t)\right) r_n^{(c)} \\ \text{s.t.} \quad & 0 \leq r_n^{(c)} \leq \min\left(V_n^{(c)}(t) + A_n^{(c)}(t), \hat{A}_n^{(c)}\right) \quad \forall\, n, c,\end{aligned} \tag{87}$$

- select $\boldsymbol{\gamma}(t)$ according to

$$\begin{aligned}\boldsymbol{\gamma}(t) = \arg\max \quad & \sum_{n,c}\left[Vf_{nc}\left(\gamma_n^{(c)}\right) - \eta Y_n^{(c)}(t)\gamma_n^{(c)}\right] \\ \text{s.t.} \quad & 0 \leq \gamma_n^{(c)} \leq \hat{A}_n^{(c)} \quad \forall\, n, c,\end{aligned} \tag{88}$$

- observe $\boldsymbol{S}(t)$ and select $\boldsymbol{P}(t)$, $\mu_{ab}^{(c)}(t)$ so as to maximize

$$\begin{aligned}& \sum_{ab}\left[\sum_c W_{ab}^{(c)}(t)\mu_{ab}^{(c)} - D_a(t)p_{ab}\right] \\ \text{s.t.} \quad & \boldsymbol{p} \in \mathcal{P}_{\boldsymbol{S}(t)}, \quad \sum_b p_{nb} \leq \min\left(E_n(t), \hat{P}\right) \quad \forall\, n, \\ & \sum_c \mu_{ab}^{(c)} \leq c_{ab}\left(\boldsymbol{S}(t), \boldsymbol{P}(t)\right) \quad \forall\, a, b, \\ & \mu_{ab}^{(c)} = 0 \quad \forall\,(a,b) \notin \mathcal{L}^{(c)},\end{aligned} \tag{89}$$

  where $W_{ab}^{(c)}(t) \triangleq U_a^{(c)}(t) - U_b^{(c)}(t)$ will be referred to as the differential backlog between a, b.

The following observations can be made. The problems in (87), (88) are separable and can be solved distributively. It is also easy to show, using a greedy exchange argument, that the solution to (89) is equivalent to

$$\begin{aligned}\boldsymbol{P}(t) = \arg\max \quad & \sum_{ab}\left[\tilde{W}_{ab}(t)c_{ab}\left(\boldsymbol{S}(t), \boldsymbol{p}\right) - D_a(t)p_{ab}\right] \\ \text{s.t.} \quad & \boldsymbol{p} \in \mathcal{P}_{\boldsymbol{S}(t)}, \quad \sum_b p_{nb} \leq \min\left(E_n(t), \hat{P}\right) \quad \forall\, n,\end{aligned} \tag{90}$$

where

$$\tilde{W}_{ab}(t) = \max_{c:(a,b)\in\mathcal{L}^{(c)}}\left\{U_a^{(c)}(t) - U_b^{(c)}(t)\right\}, \tag{91}$$

so that, for each time slot, we need only select a single commodity $c_{ab}^*(t) = \arg\max_{c:(a,b)\in\mathcal{L}^{(c)}}\{U_a^{(c)}(t) - U_b^{(c)}(t)\}$ per link (obviously, different links may carry different commodities). A casual glance at (90) also reveals that the optimal solution has the property that $P_{ab}(t) = 0$ if $\tilde{W}_{ab}(t) \leq 0$. Hence, with no loss of optimality, we define

$$W_{ab}^*(t) = \left[\max_{c:(a,b)\in\mathcal{L}^{(c)}}\left\{U_a^{(c)}(t) - U_b^{(c)}(t)\right\}\right]^+, \tag{92}$$

and use this value instead of $\tilde{W}_{ab}(t)$ in the subsequent expressions. Hence, the following result is true

Lemma 10: Application of NRABP results in the following conditions being satisfied

- *for each $c \in \mathcal{K}$, there exists a sufficiently large $\hat{F}^{(c)}$ such that $R_{n,in}^{(c)}(t) = 0$ whenever $U_n^{(c)}(t) > \hat{F}^{(c)}$.*
- *for any link (a,b) such that $W_{ab}^{(c)}(t) \leq 0$ it holds $\mu_{ab}^{(c)}(t) = 0$. As a result, the implication $W_{ab}^*(t) = 0 \Rightarrow P_{ab}(t) = 0$ is true.*

Proof: The first condition follows from the bang-bang property of the solution to (87) and the fact that all queues $Y_n^{(c)}(t)$ are stable under NRABP (the latter is proved by a vectorization of the proof in Appendix V-B), while the second one has already been proved. ■

Under the previous observations, (86) becomes

$$\begin{aligned}
&\Delta\left(\boldsymbol{X}(t)\right) - 2V\mathbb{E}\left[\sum_{n,c} f_{nc}\left(\gamma_n^{(c)}(t)\right)\middle|\boldsymbol{X}(t)\right] \leq \dot{C} - 2\mathbb{E}\left[\sum_{n,c}\left[Vf_{nc}\left(\gamma_n^{(c)}(t)\right) - \eta Y_n^{(c)}(t)\gamma_n^{(c)}(t)\right]\middle|\boldsymbol{X}(t)\right] \\
&- 2\mathbb{E}\left[\sum_{a,b}\left[W_{a,b}^*(t)c_{ab}\left(\boldsymbol{S}(t),\boldsymbol{P}(t)\right) - D_a(t)p_{ab}\right]\middle|\boldsymbol{X}(t)\right] - 2\mathbb{E}\left[\sum_{n,c}\left[\eta Y_n^{(c)}(t) - U_n^{(c)}(t)\right]R_{n,in}^{(c)}(t)\middle|\boldsymbol{X}(t)\right] \\
&- 2(1-\delta)\sum_n \bar{B}_n D_n(t).
\end{aligned} \tag{93}$$

The main stability result, proved in Appendix V-G, is now stated

Lemma 11: NRABP stabilizes all queues according to the following bounds

$$\begin{aligned}
&Y_n^{(c)}(t) \leq \frac{Vf_{nc}'(0)}{\eta} + \hat{A}_n^{(c)} \triangleq \hat{Y}_n^{(c)}, \\
&U_n^{(c)}(t) \leq \hat{U}_n^{(c)}, \\
&D_n(t) \leq \hat{U}_n\hat{C}_n + \hat{P}_n \triangleq \hat{D}_n,
\end{aligned} \tag{94}$$

where $\hat{U}_n = \max_c \hat{U}_n^{(c)}$ and $\hat{C}_n = \max_{\boldsymbol{s}} \sum_b \frac{\partial c_{ab}}{\partial p_{ab}}(\boldsymbol{s},\boldsymbol{0})$.

As before, we denote with $q_{\boldsymbol{s},\boldsymbol{e}}(t) = \Pr\left(\boldsymbol{S}(t) = \boldsymbol{s}, \boldsymbol{E}(t) = \boldsymbol{e} \middle| \boldsymbol{X}(t)\right)$ the respective probability under NRABP and with $\boldsymbol{P}(\boldsymbol{s},\boldsymbol{e})$ the solution to (90) when $\boldsymbol{S}(t) = \boldsymbol{s}$ and $\boldsymbol{E}(t) = \boldsymbol{e}$ (when $\boldsymbol{e} \geq \hat{\boldsymbol{P}}$, the solution is independent of $\boldsymbol{e}$ and is denoted as $\boldsymbol{p}_{\boldsymbol{S}}^*$). The analogue of (31) is

$$\begin{aligned}
&\mathbb{E}\left[\sum_{a,b}\left[W_{ab}^*(t)c_{ab}\left(\boldsymbol{S}(t),\boldsymbol{P}(t)\right) - D_a(t)P_{ab}(t)\right]\middle|\boldsymbol{X}(t)\right] = \sum_{\boldsymbol{s}\in\mathcal{S}}\sum_{\boldsymbol{e}\in\mathcal{E}(t)}\sum_{a,b}\left[W_{ab}^*(t)c_{ab}\left(\boldsymbol{s},\boldsymbol{P}(\boldsymbol{s},\boldsymbol{e})\right) - D_a(t)P_{ab}\left(\boldsymbol{s},\boldsymbol{e}\right)\right]q_{\boldsymbol{s},\boldsymbol{e}}(t) \\
&\geq \sum_{\boldsymbol{s}\in\mathcal{S}}\sum_{\substack{\boldsymbol{e}\in\mathcal{E}(t)\\ \boldsymbol{e}\geq\hat{\boldsymbol{P}}}}\sum_{a,b}\left[W_{ab}^*(t)c_{ab}\left(\boldsymbol{s},\boldsymbol{p}_{\boldsymbol{s}}^*\right) - D_a(t)p_{ab,\boldsymbol{s}}^*\right]q_{\boldsymbol{s},\boldsymbol{e}}(t) \\
&\geq \sum_{\boldsymbol{s}\in\mathcal{S}}\sum_{\substack{\boldsymbol{e}\in\mathcal{E}(t)\\ \boldsymbol{e}\geq\hat{\boldsymbol{P}}}}\sum_{a,b}\left[W_{ab}^*(t)c_{ab}\left(\boldsymbol{s},\boldsymbol{p}_{\boldsymbol{s}}^*\right) - D_a(t)p_{ab,\boldsymbol{s}}^*\right]q_{\boldsymbol{s},\boldsymbol{e}}(t) - \sum_{\boldsymbol{s}\in\mathcal{S}}\sum_{\substack{\boldsymbol{e}\in\mathcal{E}(t)\\ \boldsymbol{e}\not\geq\hat{\boldsymbol{P}}}}\sum_{a,b}\left[W_{ab}^*(t)c_{ab}\left(\boldsymbol{s},\boldsymbol{p}_{\boldsymbol{s}}^*\right) - D_a(t)p_{ab,\boldsymbol{s}}^*\right]q_{\boldsymbol{s},\boldsymbol{e}}(t) \\
&\geq \sum_{\boldsymbol{s}\in\mathcal{S}}\sum_{a,b}\left[W_{ab}^*(t)c_{ab}\left(\boldsymbol{s},\boldsymbol{p}_{\boldsymbol{s}}^*\right) - D_a(t)p_{ab,\boldsymbol{s}}^*\right]\pi_{\boldsymbol{s}} - \left(\sum_{a,b}\hat{U}_a\hat{c}_{ab}\right)\Pr\left(\bigcup_{n=1}^N\{E_n(t) < \hat{P}\}\middle|\boldsymbol{X}(t)\right),
\end{aligned} \tag{95}$$

where the usual manipulations have been performed.[13]

We now follow a procedure similar to the one that produced (33), (36), (37). Specifically, the maximizing properties of NRABP yield for all $\boldsymbol{r}$ s.t. $0 \leq r_n^{(c)} \leq \lambda_n^{(c)}$

$$\mathbb{E}\left[\sum_{n,c}\left[Vf_{nc}\left(\gamma_n^{(c)}(t)\right) - \eta Y_n^{(c)}(t)\gamma_n^{(c)}(t)\right]\middle|\boldsymbol{X}(t)\right] \geq \sum_{n,c}\left[Vf_{nc}\left(r_n^{(c)}\right) - \eta Y_n^{(c)}(t)r_n^{(c)}\right], \tag{96}$$

$$\mathbb{E}\left[\sum_{n,c}\left(\eta Y_n^{(c)}(t) - U_n^{(c)}(t)\right)R_{n,in}^{(c)}(t)\middle|\boldsymbol{X}(t)\right] \geq \sum_{n,c}\left(\eta Y_n^{(c)}(t) - U_n^{(c)}(t)\right)r_n^{(c)}. \tag{97}$$

[13]specifically, the transition from the third to the fourth line of (95) relied on the fact that $W_{ab}^*(t) = U_a^{(c_{ab}^*(t))}(t) - U_b^{(c_{ab}^*(t))}(t) \leq \hat{U}_a$.

The solution to (89) when $E_n(t) \geq \hat{P}$ for all n also implies

$$\begin{aligned}\sum_{a,b}\left[W_{ab}^{*}(t)c_{ab}\left(\boldsymbol{s},\boldsymbol{p}_{\boldsymbol{s}}^{*}\right)-D_a(t)p_{ab,\boldsymbol{s}}^{*}\right] &\geq \sum_{a,b}\left[W_{ab}^{*}(t)c_{ab}\left(\boldsymbol{s},\boldsymbol{p}\right)-D_a(t)p_{ab}\right] \\ &\geq \sum_{a,b}\left[\sum_{c}W_{ab}^{(c)}(t)\mu_{ab}^{(c)}\left(\boldsymbol{s},\boldsymbol{p}\right)-D_a(t)p_{ab}\right] \quad \forall\,\boldsymbol{s}\in\mathcal{S},\,\forall\,\boldsymbol{p}\in\mathcal{P}_{\boldsymbol{s}},\end{aligned} \tag{98}$$

where the second inequality follows from the facts $W_{ab}^{*}(t) \geq W_{ab}^{(c)}(t)$ for all c and $\sum_c \mu_{ab}^{(c)}\left(\boldsymbol{s},\boldsymbol{p}\right) \leq c_{ab}\left(\boldsymbol{s},\boldsymbol{p}\right)$. Multiplying the last inequality by $\pi_{\boldsymbol{p}}^{\boldsymbol{s}}\pi_{\boldsymbol{s}}$ (where $\pi_{\boldsymbol{p}}^{\boldsymbol{s}}$ is an arbitrary pdf) and summing over $\boldsymbol{s},\boldsymbol{p}$ produces

$$\sum_{\boldsymbol{s}\in\mathcal{S}}\sum_{a,b}\left[W_{ab}^{*}(t)c_{ab}\left(\boldsymbol{s},\boldsymbol{p}_{\boldsymbol{s}}^{*}\right)-D_a(t)p_{ab,\boldsymbol{s}}^{*}\right]\pi_{\boldsymbol{s}} \geq \sum_{\boldsymbol{s}\in\mathcal{S}}\sum_{\boldsymbol{p}\in\mathcal{P}_{\boldsymbol{s}}}\sum_{a,b}\left[\sum_{c}W_{ab}^{(c)}(t)\mu_{ab}^{(c)}\left(\boldsymbol{s},\boldsymbol{p}\right)-D_a(t)p_{ab}\right]\pi_{\boldsymbol{p}}^{\boldsymbol{s}}\pi_{\boldsymbol{s}}. \tag{99}$$

We now insert (99), (97), (96), (95) into (93) and perform some algebra to get

$$\begin{aligned}&\Delta\left(\boldsymbol{X}(t)\right)-2V\mathbb{E}\left[\sum_{n,c}f_{nc}\left(\gamma_n^{(c)}(t)\right)\middle|\boldsymbol{X}(t)\right] \leq \dot{C}-2V\sum_{n,c}Vf_{nc}\left(r_n^{(c)}\right)+2\sum_{n,c}U_n^{(c)}(t)r_n^{(c)}-2(1-\delta)\sum_{n}\bar{B}_nD_n(t) \\ &-2\sum_{\boldsymbol{s}\in\mathcal{S}}\sum_{\boldsymbol{p}\in\mathcal{P}_{\boldsymbol{s}}}\sum_{a,b}\left[\sum_{c}W_{ab}^{(c)}(t)\mu_{ab}^{(c)}\left(\boldsymbol{s},\boldsymbol{p}\right)-D_a(t)p_{ab}\right]\pi_{\boldsymbol{p}}^{\boldsymbol{s}}\pi_{\boldsymbol{s}}+2\left(\sum_{a,b}\hat{U}_a\hat{c}_{ab}\right)\Pr\left(\bigcup_{n=1}^{N}\{E_n(t)<\hat{P}\}\middle|\boldsymbol{X}(t)\right).\end{aligned} \tag{100}$$

Expanding $W_{ab}^{(c)}(t)$ into $U_a^{(c)}(t)-U_b^{(c)}(t)$ and performing a change of indices so that all backlogs appear with index n in the above relation yields for all $\boldsymbol{r}$ with $\mathbf{0}\leq\boldsymbol{r}\leq\boldsymbol{\lambda}$

$$\begin{aligned}&\text{LHS of (100)} \leq \dot{C}-2V\sum_{n,c}f_{nc}\left(r_n^{(c)}\right)+2\sum_{n,c}U_n^{(c)}(t)\left[r_n^{(c)}-\sum_{\boldsymbol{s},\boldsymbol{p}}\sum_{b}\mu_{nb}^{(c)}\left(\boldsymbol{s},\boldsymbol{p}\right)\pi_{\boldsymbol{p}}^{\boldsymbol{s}}\pi_{\boldsymbol{s}}+\sum_{\boldsymbol{s},\boldsymbol{p}}\sum_{a}\mu_{ab}^{(c)}\left(\boldsymbol{s},\boldsymbol{p}\right)\pi_{\boldsymbol{p}}^{\boldsymbol{s}}\pi_{\boldsymbol{s}}\right] \\ &+2\sum_{n}D_n(t)\left[\sum_{\boldsymbol{s},\boldsymbol{p}}\sum_{b}p_{nb}\pi_{\boldsymbol{p}}^{\boldsymbol{s}}\pi_{\boldsymbol{s}}-(1-\delta)\bar{B}_n\right]+2\left(\sum_{a,b}\hat{U}_a\hat{c}_{ab}\right)\Pr\left(\bigcup_{n=1}^{N}\{E_n(t)<\hat{P}\}\middle|\boldsymbol{X}(t)\right).\end{aligned} \tag{101}$$

Selecting $\boldsymbol{r}$ as the solution to (84) and $\pi_{\boldsymbol{p}}^{\boldsymbol{s}}$ as the corresponding pdf in the definition of $\mathcal{R}_\delta$ creates many cancellations in (101) and finally produces

$$\text{LHS of (100)} \leq \dot{C}-2Vg_\delta^{*}+2\left(\sum_{a,b}\hat{U}_a\hat{c}_{ab}\right)\Pr\left(\bigcup_{n=1}^{N}\{E_n(t)<\hat{P}\}\middle|\boldsymbol{X}(t)\right). \tag{102}$$

As in previous sections, we invoke Lemmas 2, 5 (since each individual queue $E_n(t)$ overflows infinitely often) to get the final

Theorem 4: NRABP stabilizes any multihop network and achieves a performance bound of

$$\liminf_{t\to\infty}\sum_{n,c}f_{nc}\left(\bar{r}_n^{(c)}(t)\right) \geq g_\delta^{*}-\frac{\dot{C}}{2V}-\frac{1}{V}\left(\sum_{a,b}\hat{U}_a\hat{c}_{ab}\right)\sum_{n=1}^{N}\Pr\left(\sum_{k=0}^{\sigma-1}B_n(k)\leq\frac{\hat{P}+\hat{D}_n-E_{max}}{\delta}\right), \tag{103}$$

where $\sigma=\lceil E_{max}/\hat{P}-1\rceil$.

III. The Hidden cost of hidden terminals

A. Where is Hidden Terminal?

The hidden terminal problem is closely related with the Transmission Range (TX_Range), Carrier Sensing Range (CS_Range) and Interference Range (IF_Range) of stations in WLAN. The followings are the widely adopted definitions for these three ranges [25] [26]. The TX_Range is the range (with respect to the transmitting station) within which a transmitted frame can be successfully received. The CS_Range is the range (with respect to the transmitting station) within which the other stations detect a transmission. The IF_Range is the range within which stations in receive mode will be "interfered with" by a transmitter, and thus suffer a loss.

The measurement study by [25] shows the following relationship for 802.11b networks: TX_Range < IF_Range < CS_Range. In addition, it shows that CS_Range is about 1.5 times of the TX_Range. We have also measured the three ranges in 802.11g networks and got similar results [27]. From our measurements, CS_Range is between 1.2×TX_Range and 1.6×TX_Range, depending on the environment. Although the exact values of these two measurement results are different, their ratios between

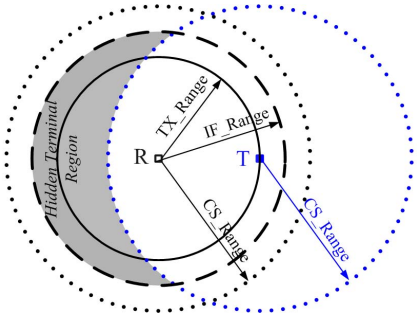

Fig. 2. Illustration of the hidden terminal problem in ad hoc networks. For transmitter T, stations in in the shaded area are hidden terminals.

CS_Range and TX_Range are within the same range (1.2, 1.6). The difference is mainly due to different wireless cards used for the measurements and different measuring environments.

As illustrated by Fig. 2, nodes within the interference range of a receiver and out of the carrier sensing range of the transmitter are usually called hidden terminals [26]. In a single-cell WLAN, all nodes are within the TX_Range of the AP, so hidden terminals are those within the TX_Range of the AP and out of the CS_Range of the transmitter, as illustrated by Fig. 3a. As we can see from Fig. 3a, to eliminate hidden nodes, CS_Range must be no less than 2×TX_Range to make sure that a node at the edge of a WLAN can sense all of the other nodes. However, both the measurement results from [25] and from us [27] show that CS_Range is less than 2×TX_Range for many existing 802.11 wireless cards. This is why hidden nodes exist in current 802.11 networks.

The performance degradation due to hidden terminals is best shown in the following example. In Figure 3a, a source station is trying to transmit to the access point (AP). It starts the transmission with a RTS/CTS handshake: The source station sends a RTS and the AP replies with a CTS. If the handshake is successful, all the nodes in the WLAN will be aware of the subsequent transmission and keep silent during the transmission period. Note that RTS signal cannot be sensed by the hidden nodes, who are beyond the CS_Range of the source station. So during the transmission of RTS, the hidden nodes may initiate their own transmissions if their backoff counters reach zero. In the 802.11 standard, the duration of RTS transmission is much longer than that of a backoff slot. For instance, With a typical setting of 802.11g [28], a RTS takes about 59 μs while a backoff slot duration is 9 μs. This implies that each hidden terminal has at least six chances to initiate their own transmissions during a RTS transmission, and collide with this RTS at the access point. The collisions waste channel time and thus degrade network performance. In this example, we assumed that RTS/CTS mechanism is active. If not, the hidden terminals will have more chances to initiate their own transmissions during the ongoing data packet transmission, which is much longer than the RTS transmission. Then the network performance will be degraded more severely.

Moreover, this performance degradation is not uniform for all nodes in a WLAN. Instead, it depends on the locations of the nodes. Assuming stations are randomly located in the network, Figure 3 shows that a station sees more hidden nodes when it is far away from the AP (Figure 3a), compared with the case when it is close to the AP (Figure 3b).

Various types of areas used in this paper are derived in the Appendix, which analytically shows the relationship between the total hidden area and the distance from the transmitter to the AP (Eq. 183). The relationship is plotted in Fig. 4, where the area is normalized by the whole network area and the distance is normalized with respect to TX_Range. As we can see, the hidden area grows almost linearly as the distance increases.

B. An Analytical Model for the Hidden Terminal Problem

1) System Model: We consider an 802.11 single-cell WLAN with only uplink traffic, wherein all transmissions are initiated by stations and destined to access point (AP). The RTS/CTS mechanism is assumed to be enabled. The AP is located at the center of the network and the other stations are randomly located within the AP's transmission range. Besides, we set

$$CS_Range = \eta \times TX_Range, \quad \eta \in (1, 2). \tag{104}$$

Note that this range of η well reflects the observations in independent WiFi measurements [25][27]. Other assumptions are listed below.

1) No capture effect, i.e., when two or more packets collide with each other, all of them will fail.
2) No channel errors.
3) All transmissions are at the same data rate.
4) All stations are always in backlog state.

As in [29], the conception of "time slot" is extended to refer to any continuous time period that a station observes. It is no longer only the backoff time slot in 802.11; instead, the duration of a time slot in our model can be one the followings:

- α: the duration of a successful transmission.

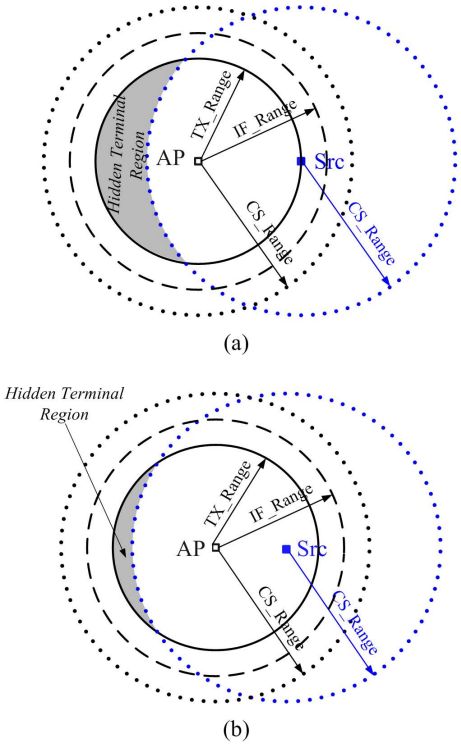

Fig. 3. Illustration of the hidden terminal problem in infrastructure mode 802.11 networks. Note that the hidden area in (a) is larger than that in (b) (where the source station is closer to the AP).

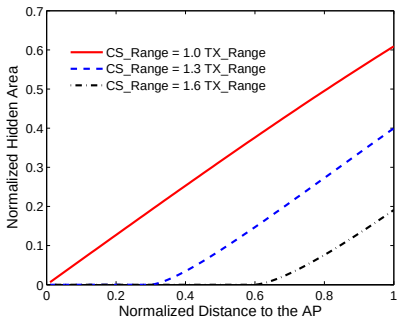

Fig. 4. t increases almost linearly with the distance to the AP.

- β: the duration of a collision period.
- δ: the duration of a backoff time slot.

2) Network Analysis: In [29], Bianchi models the 802.11 DCF with a two-dimensional Markov chain. For a given collision probability P_c, the model predicts the transmission probability τ:

$$\tau = \frac{2(1-2P_c)}{(1-2P_c)(W+1)+P_cW[1-(2P_c)^m]} \tag{105}$$

where W is the initial backoff window size and m is the maximum number of backoff stages. On the other hand, the network conditions for a transmitted packet to collide is that, in a time slot, at least one of the remaining stations transmits:

$$P_c = 1-(1-\tau)^{N-1} \tag{106}$$

where N is the number of nodes in the network. By solving these two equations numerically, Bianchi obtains τ and P_c, based on both of which he then computes the network throughput.

We will follow the same approach in our modeling. The main difference between Bianchi's analysis [29] and ours is that we consider hidden terminals. To capture the location-dependent nature of hidden terminal's impacts (as described in Section III-A), we slot the whole network area into M evenly spaced concentric annuluses centered at the AP, as shown in Fig. 5. Let r be the TX_Range of a station. Each annulus $A(i)$ ($i \geqslant 2$) is centered at AP and confined by two circles with radius

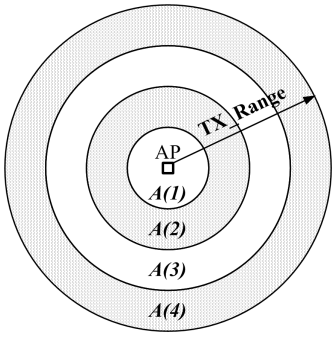

Fig. 5. M evenly spaced concentric annuluses centered at the AP ($M = 4$ in this figure).

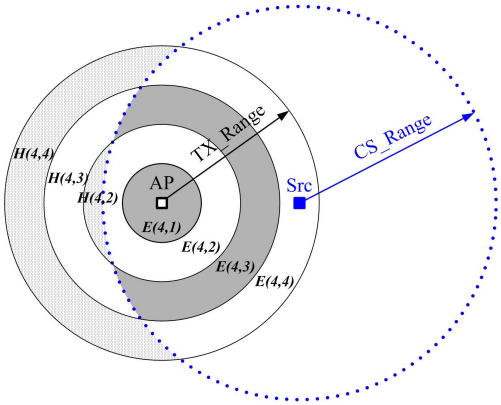

Fig. 6. Illustration of Hidden Area $H(i, j)$ and Covered Area $E(i, j)$.

$r(i-1)/M$ and ri/M respectively; while $A(1)$ is the interior of the innermost circle centered at AP and with radius r/M. As we can see from Fig. 5, stations in annulus $A(i)$ are at approximately the same distance $d(i)$ from the AP, so they observe approximately the same number of hidden nodes. Therefore, they experience approximately the same collision probability $P_c(i)$, which results in approximately the same transmission probability $\tau(i)$ (from Eq. 106). Of course, the larger M is, the better the approximations are. In fact, as we will show later, the approximations here are very accurate even when M is as small as 4.

As in [29], we adopt the key assumption that each station independently makes a transmission attempt at any time slot with a constant probability τ. However, there is a difference on the meaning of τ. In [29], τ is equal for all nodes, since the model assumes no hidden nodes. But in our model, τ depends on the distance between a node and the AP.

Following the same way that Bianchi derives Eq. 105 in [29], we obtain the relationship between $\tau(i)$ and $P_c(i)$ for a node in annulus $A(i)$ (A brief derivation is presented in the Appendix):

$$\tau(i) = \frac{2(1-2P_c(i))}{(1-2P_c(i))(W+1)+P_c(i)W[1-(2P_c(i))^m]} \quad (i = 1, 2, \ldots, M) \tag{107}$$

We now derive the network conditions for a transmitted packet to collide in the presence of hidden terminals. Let us first define the hidden area $H(i, j)$ and the covered area $E(i, j)$, with $i, j \in [1, M]$. For a source station (Src) located in annulus $A(i)$, $H(i, j)$ is defined as the part of annulus $A(j)$ that is out of the CS_Range of Src; while $E(i, j)$ is defined as the part of annulus $A(j)$ that is within the CS_Range of Src. Both of them are normalized with respect to the total area within the AP's TX_Range. Fig. 6 shows the $H(i, j)$ and $E(i, j)$ for a source station located in $A(4)$. Note that $H(4, 1)$ is zero in this example and not shown in the figure. The computations of the areas $H(i, j)$ and $E(i, j)$ can be found in Appendix.

We can then determine the expected number of nodes in hidden area $H(i, j)$ and covered area $E(i, j)$. Let the total number of stations in the network be N, then a station in annulus $A(i)$ sees an average $NH(i, j)$ hidden nodes and $NE(i, j)$ covered nodes in annulus $A(j)$.

Let us consider the conditions for a successful transmission. The transmission procedure is a RTS-CTS-DATA-ACK four-way handshake. Since Src senses the channel before the transmission of RTS, we are sure that all nodes within Src's CS_Range

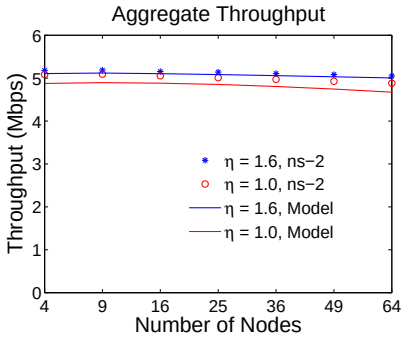

Fig. 7. Aggregate Network Throughput: Model VS. Simulation.

are idle in the time slot just before the RTS transmission. However, Src has no knowledge about the status of the hidden nodes. Denote ρ as the number of backoff time slots that a RTS transmission spans, that is,

$$t_{RTS} = \rho\delta \tag{108}$$

where t_{RTS} is RTS transmission time.

An obvious condition is that no nodes within Src's CS_Range initiates transmissions in the same time slot as Src does. Since Src's RTS signal cannot be sensed by its hidden nodes, another condition is that no hidden nodes transmit during the RTS transmission. Likewise, when Src initiates a transmission, a hidden node may already be transmitting a RTS, since Src cannot sense the RTS signal and is not aware of the transmission. So the third condition is that no hidden nodes transmits in the preceding t_{RTS} time. If all of the three conditions are satisfied, the RTS will be successfully received by the AP, which then replies with a CTS.

Irrespective of whether they have received the RTS or not, all the nodes in the source station's CS_Range will not transmit within a Distributed Interframe Space (DIFS) time. So they will not interfere with the CTS which is sent a Short Interframe Space (SIFS) time after the completion of the RTS, because a SIFS is shorter than DIFS. So only hidden nodes might interfere with the CTS. Therefore, the condition for the CTS to be successful is that no hidden node launches transmissions at the same time slot as the AP transmits a CTS. Since all nodes in the network are within the AP's TX_Range, they will find the channel busy during the CTS transmission and not transmit. Once the RTS/CTS handshake is successful, the transmission is guaranteed to be successful, since all stations will set their Network Allocation Vector (NAV), which keeps them silent during the transmission. Consequently, the conditional success probability $P_s(i)$ given that a node in annulus $A(i)$ initiates a transmission is

$$\begin{aligned} P_s(i) &= \prod_{j=1}^{M}[1-\tau(j)]^{NE(i,j)} \prod_{j=1}^{M}[1-\tau(j)]^{N(2\rho-1)H(i,j)} \\ &= \prod_{j=1}^{M}[1-\tau(j)]^{N[E(i,j)+(2\rho-1)H(i,j)]} \end{aligned} \tag{109}$$

Then the conditional collision probability $P_c(i)$ given that a node in annulus $A(i)$ initiates a transmissions is

$$\begin{aligned} P_c(i) &= 1-\prod_{j=1}^{M}[1-\tau(j)]^{N[E(i,j)+(2\rho-1)H(i,j)]} \\ &\quad (i=1,2,\ldots,M) \end{aligned} \tag{110}$$

With (107) and (110), we have $2M$ equations and $2M$ unknowns. Numerically solving the equations, we obtain $\tau(i)$ and $P_c(i)$ for i from 1 to M.

C. Throughput

Normalizing the area of annulus $A(i)$ with respect to the network area, we get

$$A(i) = [i^2-(i-1)^2]/M^2, \quad i=1,2,\ldots,M. \tag{111}$$

Since we assume that nodes are randomly located in the network, the expected number of stations located in annulus $A(i)$ is proportional to the normalized area of annulus $A(i)$:

$$N(i) = NA(i) = N[i^2-(i-1)^2]/M^2, \quad i=1,2,\ldots,M. \tag{112}$$

The probability that all stations are idle in a time slot is

$$P_{idle} = \prod_{i=1}^{M} [1-\tau(i)]^{N(i)}. \quad (113)$$

As the transmission probability $\tau(i)$ is very small and independent for each node, the probability that there is a successful transmission in a time slot can be approximately expressed as

$$P_{success} = \sum_{i=1}^{M} N(i)\tau(i)(1-P_c(i)) \quad (114)$$

The three different channel states in a time slot are: Successful Transmission, Collision and Idle. So the probability that there is a collision in a time slot is

$$P_{collision} = 1 - P_{success} - P_{idle} \quad (115)$$

Since most collisions occurs when a node launches RTS during the transmission of a RTS by another node, the collision period is just the overlapping of these two RTS's. So β approximates twice of t_{RTS}.

Let S be the expected aggregate throughput for the whole network, which can be computed in this way

$$S = P_{success}E[Payload]/T \quad (116)$$

where $E[Payload]$ is the expected payload length of a packet and T is mean duration of a time slot

$$T = P_{idle}\delta + P_{success}\alpha + P_{collision}\beta. \quad (117)$$

The per-node throughput for a node in annulus $A(i)$ is

$$S(i) = \tau(i)(1-P_c(i))E[Payload]/T \quad (118)$$

D. Simulation

To validate the model, we have run extensive simulations with the Network Simulator ns-2 v2.33 [30].

1) Simulation Settings: The system parameters for the simulations and for obtaining numerical solutions from the model have been set to values typical in 802.11g WLAN, as summarized in Table I. The capture effect has been turned off and the channel is free of errors. The AP is located at the center of the network, while the other stations are uniformly located within

TABLE I
PARAMETERS USED IN BOTH SIMULATIONS AND MODEL

Preamble Length	20 μs	Slot Time	9 μs
PLCP Header Length	4 μs	SIFS	10 μs
Max Propagation Delay	0.5 μs	DIFS	28 μs
W (CWMin)	31	m (CWMax)	1023

the TX_Range of of the AP. The AP does not initiate transmissions, while the other stations transmit UDP packets to the AP at 6 Mbps. From our previous experimental measurements for 802.11g WLAN, CS_Range is between 1.2 TX_Range and 1.6 TX_Range [27]. We also note that many existing papers assume CS_Range=TX_Range, which is not realistic. Taking the measurement results and the prevailing assumption into consideration, we decided to run simulations and obtain numerical values from the model with CS_Range set to 1.0 TX_Range, 1.3 TX_Range and 1.6 TX_Range respectively.

2) Performance of Saturated Networks: In this subsection, we present the results from both analysis and simulations for saturated networks. There are 16 uniformly-located nodes in the network. All nodes are at full load and the payload size has been fixed to 1500 bytes. The RTS/CST handshake has been turned on.

Fig. 7 compares the aggregate network throughput obtained from the analytical model and simulations. As shown in this figure, the model is very accurate, since the average difference between the model and simulation results is around 4%. Furthermore, this accuracy is observed for networks ranging from 4 nodes up to as many as 64 nodes. Besides, we note that the aggregate throughput does not change much with η.

Fig. 8 and Fig. 9 show the per-node throughput, collision probability and delay as a function of the distance from a node to the AP. The distance has been normalized with respect to the TX_Range. From Fig. 8, we can see that the per-node throughput from our model matches its counterpart from simulations well. In addition, as we can see from Fig. 8 and 9, both the analytical model and simulations reveal a significant unfairness in terms of both throughput and delay for nodes at different locations. For η=1.0, 1.3 and 1.6, the throughput for the closest node to the AP is eight, five, and three times as much as that for a node at the edge of TX_Range, respectively. The scenario $\eta = 1.0$, which is not realistic, is only for comparison with the literature. So in practice, the throughput ratio between the closest and the furthest node ranges from *three* to *five*. It is also clear that the

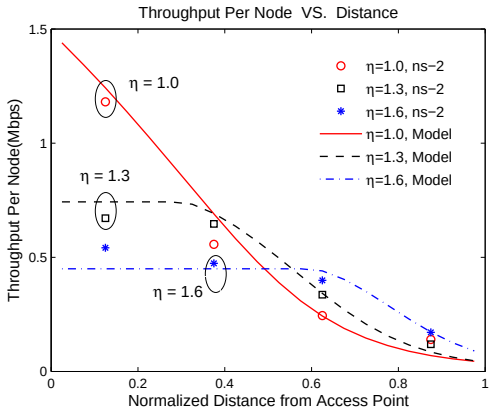

Fig. 8. Per-node Throughput: Model VS. Simulation.

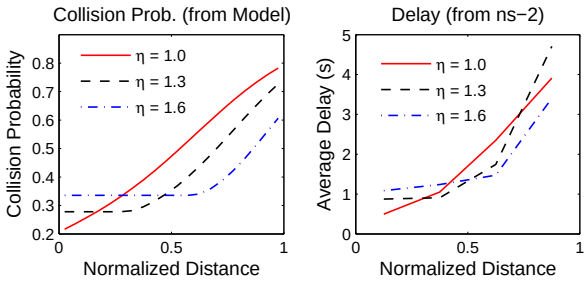

Fig. 9. Collision Probability and Packet Delay.

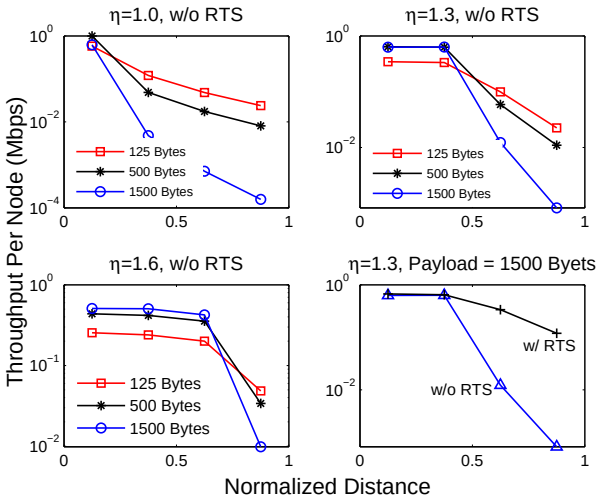

Fig. 10. ns-2 simulation results for a saturated 16-node network with RTS/CTS turned on or off and various payload length.

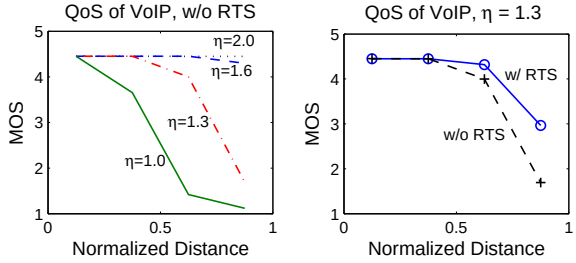

Fig. 11. ns-2 simulation results of VoIP service.

unfairness becomes less significant as η increases. Please note that we have assumed no channel errors in the model and set the simulator free of channel errors, therefore, this unfairness has nothing to do with the path loss which causes more packet loss for stations far from the AP than for stations close to the AP.

We have also run simulations with different network sizes (i.e., the number of nodes in the network), and obtained similar results as Fig. 8 and 9. Due to space limitation, the results are not shown in this paper.

3) Simulation Results: Networks Without RTS/CTS: All the previous sections are about networks with RTS/CTS handshake. We note that RTS/CTS mechanism is disabled in most deployed 802.11 WLANs. To investigate the hidden terminal problem in this case, we have run simulations with RTS/CTS disabled.

We have considered three scenarios with packet payload length set to 125, 500 and 1500 Bytes. The other simulation settings are exactly the same as those in section III-D2.

The per-node throughput are shown in Fig. 10. As we can see, with $\eta = 1.3$ and a 1500-Byte payload length, the throughput ratio between the closest node and the furthest node is 760 with RTS/CTS disabled and 5 with RTS/CTS enabled. This shows that the RTS/CTS mechanism does alleviate the performance unfairness due to hidden terminals, although it cannot completely solve the problem.

E. Impact on Real-Time Service

To evaluate the the impacts of the performance unfairness to real-time services, we have done simulations with Voice over IP (VoIP) services in ns-2. We have adopted the ns-2 VoIP framework established by [31] and [32].

The VoIP framework evaluates the Quality of Service (QoS) of VoIP sessions in terms of *Mean Opinion Score (MOS)* [33]. The higher the value of MOS, the better the QoS is. The quality of VoIP service is considered to be good if the MOS is above 4 [34].

In the simulations, each node initiates two VoIP sessions and talks to the AP. All the other settings are the same as those in section III-D2.

Fig. 11 shows the QoS of the VoIP services for nodes at different locations. As we can see, the QoS does not depend on location when there are no hidden nodes ($\eta = 2.0$); however, it greatly depends on location in the presence of hidden nodes ($\eta = 1.0, 1.3, 1.6$). Besides, the unfairness becomes less significant with a greater η. Note that when there are no hidden nodes ($\eta = 2.0$), the VoIP sessions for all nodes are with good quality (MOS$>$4). This indicates that the network is non-saturated. Therefore, hidden terminals cause significant performance unfairness not only under saturated load, but also under *non-saturated* load.

F. Experimental Measurements

We have set up a testbed to measure the throughput and packet loss rate in a WLAN with hidden nodes and single access point. houses and WiFi hot spots, which keeps the experiments free from external interference.

We have used five laptop computers (*A, B, C, D* and *E*) running Linux Fedora 5 (kernel: 2.6.16-prep). Each laptop is equipped with an Atheros 802.11g wireless card (chipset: Atheros AR5212) and uses the *MadWifi* driver [35] (version 0.9.4). To facilitate experimentation, the transmission power of each wireless card is fixed to 1 dBm (1.26 mW), which is greater than the minimum transmission power (1 mW) required by the 802.11 standard.

The topology of our experiments is shown and Fig. 12. All laptops are in a line, with laptop *C* in the middle. Laptop *C* acts as the AP and does not initiate transmissions; while the other laptops are at full load and transmit UDP packets to *C* with a fixed payload length of 1470 Bytes.

We first measure the TX_Range with a method which is similar as the one used by [25] and [36]. In our measurements, TX_Range is defined as the largest transmission distance when the packet loss rate is maintained below 10%. Let r denote TX_Range, then CS_Range is between $1.2r$ and $1.6r$ [27]. As observed from the topology in Fig. 12, nodes B and D which are close to the access point see one hidden node, while nodes A and E which are far away from the access point see two hidden nodes. For example, E is $1.6r$ away from B, so B sees E as a hidden node; both nodes D and E are more than $1.6r$ away from A, so A sees both of them as hidden nodes.

With RTS/CTS handshake turning on or off and the data rate for all nodes setting to 6Mbps or 36Mbps, we made measurements for four scenarios. The measured throughput and packet loss rate for each node are presented in Fig. 13 and Fig. 14, respectively.[14] These two figures tell us three things. Firstly, the performance of close stations (node B and node D) are much better than that of far stations (node A and node E), in terms of both throughput and packet loss rate. This is contrary to the case without hidden nodes, where all nodes enjoy equal chance to access the channel and the throughput for all nodes are almost the same, even if they transmit at different data rates [37].

Secondly, in both the 6Mbps and 36Mbps scenarios, enabling RTS/CTS significantly enhances the performance. This contradicts with the ad-hoc case, where RTS/CTS handshake is not effective in dealing with the hidden node problem [26].

[14] As in [25], we also experienced a high variability in channel conditions thus making a comparison between the *exact* values of the results difficult sometimes.

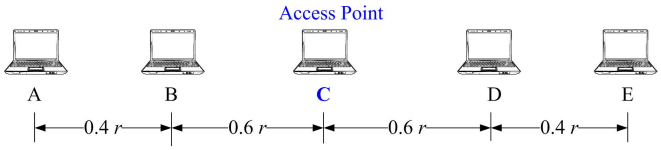

Fig. 12. Topology: All stations are in a line, with access point in the middle.

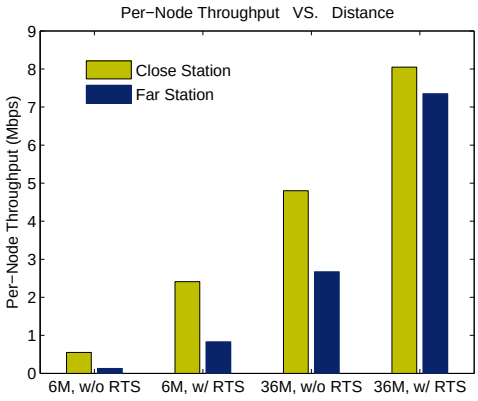

Fig. 13. Measured Per-node Throughput.

This is because for a given distance between the transmitter and receiver, there are more hidden nodes in ad hoc networks than in single-cell WLANs, which can be seen clearly by comparing Fig. 2 with Fig. 3a.

Thirdly, comparing the Packet Loss Rate (PLR) in scenarios “6Mbps without RTS” and “36Mbps without RTS”, we find that the PLR’s for close and far stations in the former scenario are about 20% greater than their counterparts in the latter scenario. This agrees with our analysis very well: since the transmission time of DATA packet at 6Mbps is much longer than that at 36Mbps, hidden nodes have more chances to initiate transmissions during the data packet transmission period, which gives rise to more collisions.

As we know, packet loss is mainly due to channel errors and collisions. As mentioned previously, we define TX_Range as the maximum transmission distance when the packet loss rate is maintained below 10%. Since all nodes are within the TX_Range of of the access point, the packet loss caused by channel errors is less than 10%. From Fig. 14 we can see that most measured PLR’s are far more than 10%, so collisions are the dominating contributor to packet losses.

G. Related Work

The existing research on evaluating the impacts of hidden terminals to the performance of 802.11 networks can be roughly categorized as follows. There are simulation-based studies [24] and analytical models [38]-[23]. A few papers also evaluate the impacts of hidden nodes with experiments [23][36]. Our work belongs to all the the three categories.

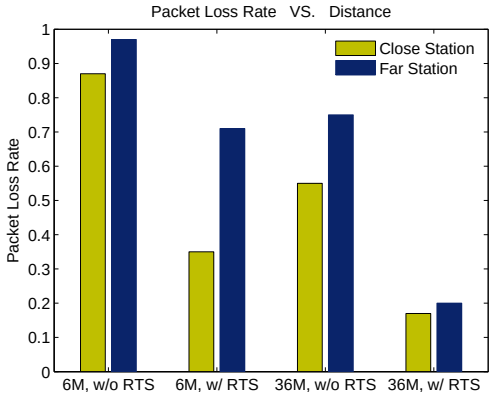

Fig. 14. Measured Packet Loss Rate (PLR).

Among the current analytical models, [38]-[39] are the closest to ours. These results can be classified into two groups, based on whether they utilize the relationship between the transmission distance and the number of hidden nodes, which is revealed in section III-A of this paper. In one group, the papers do not utilize this relationship. In both [38] and [40], Chhaya and Gupta build an analytical model for 802.11 WLAN in the presence of hidden nodes and capture effects. The model reveals the unfairness that the nodes far away from the access point (AP) have a less success probability of transmission than those close to the AP. However, the result is based on the assumption that every pair of nodes are hidden from each other with a *constant* probability, which holds only for a few network topologies. Similarly, [22] evaluates the network performance by building a model assuming that the number of hidden nodes is *equal* for all transmissions. In the other group, the relationship between transmission distance and the number of hidden terminals is exploited. Both [41], a seminal work from 1984, and recent work [39] show the relationship for a special case where CS_Range is the same as TX_Range, though CS_Range is usually greater than TX_Range in practice. The focus of both papers is the analysis of the network performance.

Experimental studies of the hidden terminal problem has been very rare. Ng and Liew in [23] have measured the aggregate network throughput of a 6-node ad-hoc network with hidden nodes. It does not conclude the performance unfairness problem.

Our paper is distinct from the existing work on the hidden terminal problem in the following three ways. Firstly, none of them answer why hidden terminals cause the performance unfairness problem. Secondly, no effort has been put on experimental measurements to validate this performance unfairness problem. Finally, our model is one of the few models that focus on the performance for *individual nodes* rather than the overall network.

IV. Conclusion and Future Work

The first work presented an on-line adaptive policy for stabilization and optimal control of wireless networks operating under rechargeable batteries. Using a Lyapunov drift argument and modifying the framework of [15] in subtle but non-trivial ways, a performance bound was provided that ensures asymptotic optimality as $E_{max} \to \infty$ (or $E_{max}/\hat{P} \to \infty$, to be exact). The policy requires only current information and is particularly suitable for satellite or wireless networks, which typically operate under high $E_{max}/\hat{P}$ ratios.

Future work includes extensive numerical evaluation of the proposed policy, in order to develop practical rules for selecting the $E_{max}/\hat{P}$ ratio (i. e. how large should the ratio be so that the performance loss is negligible), since the theoretically derived bounds are rather loose. The basic intuition may also be applicable to finite (non-rechargeable) batteries so that a nearly optimal policy may be developed for the problem of lifetime maximization. This problem is expected to require a completely new formulation and tools, and is of a more speculative nature.

In the second part of this project, we studied performance unfairness in 802.11 networks due to hidden nodes. We build an analytical model and validated it with simulations. We also set up a testbed and made experimental measurements. From our analysis, simulation and measurements, we conclude that the performance of a node in a randomly distributed 802.11 WLAN depends on the distance from the node to the AP. More specifically, the nodes close to the AP get much better performance than those far from the AP. Although our work is based on 802.11 networks, we believe it also applies to most random-access radio networks.

As future work, we are planning to extend the analysis for ad hoc networks. We will also design a MAC layer scheme to mitigate the performance unfairness.

V. Appendix

A. Proof of Lemma 2

We will need the following result from analysis

Lemma V-A.1: For any functions $f_1(t), f_2(t), w(t)$ such that $f_1(t) + w(t) = f_2(t)$ and $\lim_{t\to\infty} w(t) = 0$, it holds

$$\liminf_{t\to\infty} f_1(t) = \liminf_{t\to\infty} f_2(t), \tag{119}$$

with a similar equality for limsup.

Proof: Since $w(t) \to 0$ as $t \to \infty$, it follows that $(-w(t)) \to 0$ as $t \to \infty$ and, hence, $\liminf_{t\to\infty} w(t) = 0$, $\liminf_{t\to\infty} (-w(t)) = 0$. Using standard properties of liminf, we have

$$\begin{aligned}
\liminf_{t\to\infty} f_1(t) &= \liminf_{t\to\infty} (f_2(t) + (-w(t))) \geq \liminf_{t\to\infty} f_2(t) + \liminf_{t\to\infty} (-w(t)) = \liminf_{t\to\infty} f_2(t), \\
\liminf_{t\to\infty} f_2(t) &= \liminf_{t\to\infty} (f_1(t) + w(t)) \geq \liminf_{t\to\infty} f_1(t) + \liminf_{t\to\infty} w(t) = \liminf_{t\to\infty} f_1(t),
\end{aligned} \tag{120}$$

which completes the proof. ■

Following the approach in [16], we now take an expectation of (17), which produces

$$\mathbb{E}\left[Ly\left(\boldsymbol{X}(k+1)\right) - Ly\left(\boldsymbol{X}(k)\right)\right] - V\mathbb{E}\left[g\left(\boldsymbol{Z}(k)\right)\right] \leq C - Vg^* + \mathbb{E}[Q(k)], \tag{121}$$

and sum the above telescoping series for $k = 0, \ldots, t-1$ to arrive at

$$\mathbb{E}\left[Ly\left(\boldsymbol{X}(t)\right)\right] - \mathbb{E}\left[Ly\left(\boldsymbol{X}(0)\right)\right] - V\sum_{k=0}^{t-1}\mathbb{E}\left[g\left(\boldsymbol{Z}(k)\right)\right] \leq (C - Vg^*)t + \sum_{k=0}^{t-1}\mathbb{E}[Q(k)]. \tag{122}$$

Since $Ly\left(\boldsymbol{X}(t)\right) \geq 0$, the above inequality can be strengthened to

$$\begin{aligned} (Vg^* - C)t &\leq \sum_{k=0}^{t-1}\mathbb{E}[Q(k)] + \mathbb{E}\left[Ly\left(\boldsymbol{X}(0)\right)\right] + V\sum_{k=0}^{t-1}\mathbb{E}\left[g\left(\boldsymbol{Z}(k)\right)\right] \\ \Rightarrow g^* - \frac{C}{V} - \frac{1}{Vt}\sum_{k=0}^{t-1}\mathbb{E}[Q(k)] &\leq \frac{1}{Vt}\mathbb{E}\left[Ly\left(\boldsymbol{X}(0)\right)\right] + \frac{1}{t}\sum_{k=0}^{t-1}\mathbb{E}\left[g\left(\boldsymbol{Z}(k)\right)\right]. \end{aligned} \tag{123}$$

It also holds

$$\frac{1}{t}\sum_{k=0}^{t-1}\mathbb{E}\left[g\left(\boldsymbol{Z}(k)\right)\right] \leq \frac{1}{t}\sum_{k=0}^{t-1}g\left(\mathbb{E}[\boldsymbol{Z}(k)]\right) \leq g\left(\frac{1}{t}\sum_{k=0}^{t-1}\mathbb{E}\left[\boldsymbol{Z}(k)\right]\right), \tag{124}$$

where the first inequality is due to Jensen's inequality and the second one follows from the concavity of g. The reader will recognize the argument of g in the last RHS as $\bar{\boldsymbol{z}}(t)$. Combining (123), (124) yields

$$g^* - \frac{C}{V} - \frac{1}{Vt}\sum_{k=0}^{t-1}\mathbb{E}[Q(k)] \leq \frac{1}{Vt}\mathbb{E}\left[Ly\left(\boldsymbol{X}(0)\right)\right] + g\left(\bar{\boldsymbol{z}}(t)\right). \tag{125}$$

We now take a liminf in the last relation, exploit the properties $\liminf \sum \geq \sum \liminf$ and $\liminf(-x_n) = -\limsup x_n$, and use Lemma V-A.1. Since $\mathbb{E}\left[Ly\left(\boldsymbol{X}(0)\right)\right]/(Vt) \to 0$ as $t \to \infty$, it finally holds

$$g^* - \frac{C}{V} - \frac{1}{V}\limsup_{t\to\infty}\frac{1}{t}\sum_{k=0}^{t-1}\mathbb{E}[Q(k)] \leq \liminf_{t\to\infty} g\left(\bar{\boldsymbol{z}}(t)\right). \tag{126}$$

□

B. Proof of Lemma 3

The deterministic bounds of (23) are proved as follows. Examine (12) and note that it is a separable concave maximization over a compact set. Separability allows us to maximize individually over l so we seek the maximum of $Vf_l(\gamma_l) - \eta Y_l(t)\gamma_l$. It clearly follows, by computing the first derivative $Vf_l'(\gamma_l) - \eta Y_l(t)$, that if it holds $Vf_l'(0) - \eta Y_l(t) \leq 0$, the function $Vf_l(\gamma_l) - \eta Y_l(t)\gamma_l$ is non-increasing (since concavity of f_l implies $f'(\gamma_l) \leq f_l'(0)$) and therefore the maximum is achieved at $\gamma_l = 0$.

The bound for $Y_l(t)$ is now proved by induction. The bound is trivially true for $t = 0$. Assume now that it holds for some t, i. e. $Y_l(t) \leq Vf_l'(0)/\eta + \hat{A}_l$ and distinguish cases. It holds either $Y_l(t) < Vf_l'(0)/\eta$ or $Vf_l'(0)/\eta \leq Y_l(t) \leq Vf_l'(0)/\eta + \hat{A}_l$. In the former case, (9) and the bound $\gamma_l(t) \leq \hat{A}_l$ immediately imply the bound for $Y_l(t+1)$, while in the latter case we exploit the fact that in this range of $Y_l(t)$ it holds $\gamma_l(t) = 0$ so that $Y_l(t+1) \leq Y(t)$ and the bound is again proved.

For the bound on $U_l(t)$, note that $U_l(t) > \eta\hat{Y}_l$ implies $U_l(t) > \eta Y_l(t)$, whence it follows, from separability of (11) and its "bang-bang" solution, that $R_{l,in}(t) = 0$. The bound is now proved by induction on t and distinction of cases, in a similar manner as in the previous paragraph. Finally, for the bound on $D(t)$, we exploit the assumptions for $c_l\left(\boldsymbol{s}, \boldsymbol{p}\right)$ in Section II-A and write for all t and $\boldsymbol{p} \in \mathcal{P}_{\boldsymbol{S}(t)}$

$$\begin{aligned} U_l(t)c_l\left(\boldsymbol{S}(t), \boldsymbol{p}\right) - D(t)p_l &\leq U_l(t)c_l\left(\boldsymbol{S}(t), (0, \ldots, p_l, \ldots, 0)\right) - D(t)p_l \quad \forall\, l \\ \Rightarrow \sum_{l=1}^{L}\left[U_l(t)c_l\left(\boldsymbol{S}(t), \boldsymbol{p}\right) - D(t)p_l\right] &\leq \sum_{l=1}^{L}\left[U_l(t)c_l\left(\boldsymbol{S}(t), (0, \ldots, p_l, \ldots, 0)\right) - D(t)p_l\right]. \end{aligned} \tag{127}$$

Consider the maximization of the last RHS in (127) over the set $\left\{\boldsymbol{p} \in \mathcal{P}_{\boldsymbol{S}(t)} :\ p_l \leq \min\left(E(t), \hat{P}\right)\ \ \forall\, l\right\}$, which is actually a superset of the constraint set of (13), and denote its solution as $\mathring{\boldsymbol{P}}(t)$. The new problem is separable and a repetition of the derivative argument of the previous paragraphs reveals that it holds $\mathring{P}_l(t) = 0$ when $U_l(t)\frac{\partial c_l}{\partial p_l}\left(\boldsymbol{S}(t), \boldsymbol{0}\right) < D(t)$. Hence, $D(t) > \max_{1\leq l\leq L}\left(\hat{U}_l\hat{C}_l\right)$ implies $\mathring{\boldsymbol{P}}(t) = 0$, which, combined with (127), yields

$$\sum_{l=1}^{L}\left[U_l(t)c_l\left(\boldsymbol{S}(t), \boldsymbol{p}\right) - D(t)p_l\right] \leq 0. \tag{128}$$

On the other hand, the last inequality becomes an equality when $\boldsymbol{p}=\mathbf{0}$. Hence, with respect to the original problem in (13), it holds $\boldsymbol{P}(t)=0$ whenever $D(t)>\max_{1\leq l\leq L}\left(\hat{U}_l\hat{C}_l\right)$. Using this statement in combination with (10), the bound for $D(t)$ is proved by induction on t, similarly to the previous bounds.

□

C. Proof of Lemma 4

It obviously holds $\tilde{\boldsymbol{\mu}}_{out}(t)\leq\boldsymbol{\mu}_{out}(t)$ for all t. This implies $\bar{\tilde{\boldsymbol{\mu}}}_{out}(t)\leq\bar{\boldsymbol{\mu}}_{out}(t)$, which combined with the monotonicity of g and the liminf operator immediately produces the second inequality of Lemma 4. Hence, it remains to prove the first equality. It is shown in [15] that for any stable queue $\boldsymbol{Z}(t)$ with $\mathbb{E}[\boldsymbol{Z}(0)]<\infty$ and a bounded service process $\boldsymbol{\mu}_{out}(t)$ (i. e. $\boldsymbol{\mu}_{out}(t)\leq C\mathbf{1}$ for a sufficiently large C) it holds $\lim_{t\to\infty}\mathbb{E}[\boldsymbol{Z}(t)]/t=\mathbf{0}$. It also holds

$$\boldsymbol{Z}(0)+\sum_{\tau=0}^{t-1}\boldsymbol{A}_{in}(\tau)=\boldsymbol{Z}(t)+\sum_{\tau=0}^{t-1}\tilde{\boldsymbol{\mu}}_{out}(\tau)\Rightarrow\frac{\mathbb{E}[\boldsymbol{Z}(0)-\boldsymbol{Z}(t)]}{t}+\bar{\boldsymbol{a}}_{in}(t)=\bar{\tilde{\boldsymbol{\mu}}}_{out}(t),\tag{129}$$

where the $\Rightarrow$ part follows from taking expectations and dividing by t. Since $\mathbb{E}[\boldsymbol{Z}(0)-\boldsymbol{Z}(t)]/t\to\mathbf{0}$, it follows that for all $\epsilon>0$ there exists some $T(\epsilon)$ such that for all $t>T(\epsilon)$ it holds

$$\begin{aligned}\bar{\boldsymbol{a}}_{in}(t)-\epsilon\mathbf{1}&\leq\bar{\tilde{\boldsymbol{\mu}}}_{out}(t),\\ \bar{\tilde{\boldsymbol{\mu}}}_{out}(t)-\epsilon\mathbf{1}&\leq\bar{\boldsymbol{a}}_{in}(t),\end{aligned}\tag{130}$$

If we pick $\epsilon<C$, (130) implies $\bar{\boldsymbol{a}}_{in}(t)\leq 2C$ for all $t>T(\epsilon)$. Consider now the function g with domain the L-dimensional cube of length $2C$, i. e. $g:\times_{l=1}^{L}[0\quad 2C]\mapsto\mathbb{R}$. Since the domain set is compact and g is continuous, the Heine-Cantor theorem asserts that g is uniformly continuous in its domain. Hence, for any $\epsilon_1>0$ there exists an ϵ (depending on ϵ_1 only and *not* $\boldsymbol{x}$) such that

$$|g(\boldsymbol{x})-g(\boldsymbol{x}-\epsilon\mathbf{1})|<\epsilon_1\Rightarrow g(\boldsymbol{x}-\epsilon\mathbf{1})>g(\boldsymbol{x})-\epsilon_1\quad\forall\,\boldsymbol{x}.\tag{131}$$

We now set $\boldsymbol{x}=\bar{\boldsymbol{a}}_{in}(t)$ and $\boldsymbol{x}=\bar{\tilde{\boldsymbol{\mu}}}_{out}(t)$ in (131) (these $\boldsymbol{x}$ obviously belong to the domain set of g for $t>T(\epsilon)$) so that the previous relation becomes

$$\begin{aligned}g(\bar{\boldsymbol{a}}_{in}(t)-\epsilon\mathbf{1})&\geq g(\bar{\boldsymbol{a}}_{in}(t))-\epsilon_1,\\ g(\bar{\tilde{\boldsymbol{\mu}}}_{out}(t)-\epsilon\mathbf{1})&\geq g(\bar{\tilde{\boldsymbol{\mu}}}_{out}(t))-\epsilon_1,\end{aligned}\tag{132}$$

for all $t>T(\epsilon)$. Combining the monotonicity of g with (130), (132), it follows that for a given $\epsilon_1>0$ there exist $\epsilon(\epsilon_1)$ and $T(\epsilon)$ such that for all $t>T(\epsilon)$ it holds

$$\begin{aligned}g(\bar{\boldsymbol{a}}_{in}(t))-\epsilon_1\leq g(\bar{\boldsymbol{a}}_{in}(t)-\epsilon\mathbf{1})\leq g(\bar{\tilde{\boldsymbol{\mu}}}_{out}(t)),\\ g(\bar{\tilde{\boldsymbol{\mu}}}_{out}(t))-\epsilon_1\leq g(\bar{\tilde{\boldsymbol{\mu}}}_{out}(t)-\epsilon\mathbf{1})\leq g(\bar{\boldsymbol{a}}_{in}(t)).\end{aligned}\tag{133}$$

Taking a liminf in the last equations produces

$$\begin{aligned}\liminf_{t\to\infty}g(\bar{\boldsymbol{a}}_{in}(t))-\epsilon_1\leq\liminf_{t\to\infty}g(\bar{\tilde{\boldsymbol{\mu}}}_{out}(t)),\\ \liminf_{t\to\infty}g(\bar{\tilde{\boldsymbol{\mu}}}_{out}(t))-\epsilon_1\leq\liminf_{t\to\infty}g(\bar{\boldsymbol{a}}_{in}(t)),\end{aligned}\tag{134}$$

and using the fact that ϵ_1 is arbitrary completes the proof.

□

D. Proof of Lemma 5

We assume w. l. o. g. that the lost recharge energy quanta of Fig. 1 enter a virtual queue $E_{over}(t)$ of zero service rate, so that $E_{over}(t)$ is a non-decreasing function of time. Viewing the queues $E(t)$, $D(t)$, $E_{over}(t)$ of Fig. 1 as a single compound queue, this compound is unstable since it has an instantaneous arrival rate of $B(t)$ and a corresponding service rate of at most $(1-\delta)B(t)$. However, queues $E(t)$, $D(t)$ are finite, the former by definition and the latter due to Lemma 3, which implies that $\lim_{t\to\infty}E_{over}(t)=\infty$ w. p. 1. Since $E_{over}(t)$ is increased *only* when $E(t)$ overflows, it follows that, under DRABP, the queue $E(t)$ overflows infinitely often so that

$$\Pr\left(\bigcap_{t=0}^{\infty}\bigcup_{j=t}^{\infty}\{E(j)=E_{max}\}\right)=1\Rightarrow\Pr\left(\bigcup_{t=0}^{\infty}\bigcap_{j=t}^{\infty}\{E(j)<E_{max}\}\right)=0.\tag{135}$$

The RHS of (135) also implies $\Pr\left(\cap_{j=t}^{\infty}\{E(j)<E_{max}\}\right)=0$ for all t. We define the random variable $\tilde{\tau}\triangleq\inf\{t:E(t)=E_{max}\}$ as the first time, under DRABP, the battery hits E_{max} (obviously, $\tilde{\tau}=0$ if $E(0)=E_{max}$). Clearly, $\tilde{\tau}$ is finite

w. p. 1 since $\Pr\left(\tilde{\tau}=\infty\right)=\Pr\left(\cap_{j=0}^{\infty}\{E(j)<E_{max}\}\right)=0$, due to the implication of (135). We also construct the decreasing event sequence $A_j=\{\tilde{\tau}>j\}$, so that it holds $\cap_{j=0}^{\infty}A_j=\{\tilde{\tau}=\infty\}$. From standard probability theory we know that $\Pr(A_j)\to\Pr(\tilde{\tau}=\infty)=0$ as $t\to\infty$.

We now exploit limsup properties to write

$$\begin{aligned}
&\limsup_{t\to\infty}\frac{1}{t}\sum_{j=0}^{t-1}\Pr\left(E(j)<\hat{P}\right)=\limsup_{t\to\infty}\frac{1}{t}\sum_{j=0}^{t-1}\left[\Pr\left(E(j)<\hat{P},\tilde{\tau}\leq j\right)+\Pr\left(E(j)<\hat{P},\tilde{\tau}>j\right)\right]\\
&\leq\limsup_{t\to\infty}\frac{1}{t}\sum_{j=0}^{t-1}\Pr\left(E(j)<\hat{P},\tilde{\tau}\leq j\right)+\limsup_{t\to\infty}\frac{1}{t}\sum_{j=0}^{t-1}\Pr\left(E(j)<\hat{P},\tilde{\tau}>j\right) \qquad (136)\\
&\leq\limsup_{t\to\infty}\frac{1}{t}\sum_{j=0}^{t-1}\Pr\left(E(j)<\hat{P},\tilde{\tau}\leq j\right)+\limsup_{t\to\infty}\frac{1}{t}\sum_{j=0}^{t-1}\Pr\left(\tilde{\tau}>j\right).
\end{aligned}$$

Since $\Pr(\tilde{\tau}>j)\to 0$ as $j\to\infty$, it follows that for any $\epsilon>0$ there exists a J such that $\Pr(\tilde{\tau}>j)<\epsilon$ for all $j>J$. Hence, for $t>J$ it holds

$$\frac{1}{t}\sum_{j=0}^{t-1}\Pr\left(\tilde{\tau}>j\right)=\frac{1}{t}\sum_{j=0}^{J}\Pr\left(\tilde{\tau}>j\right)+\frac{1}{t}\sum_{j=J+1}^{t-1}\Pr\left(\tilde{\tau}<j\right)\leq\frac{J+1}{t}+\frac{t-J-1}{t}\,\epsilon \qquad (137)$$

Taking a limsup in the last equation and exploiting the fact that ϵ is arbitrary yields $\limsup_{t\to\infty}(1/t)\sum_{j=0}^{t-1}\Pr(\tilde{\tau}>j)=0$, so that we only need to compute the left limsup in the last line of (136). We will now prove the following bound for all j

$$\Pr\left(E(j)<\hat{P},\tilde{\tau}\leq j\right)\overset{?}{\leq}\Pr\left(\sum_{k=\tau_j}^{j-1}B(k)\leq\frac{\hat{P}+\hat{D}-E_{max}}{\delta}\right)\overset{?}{\leq}\Pr\left(\sum_{k=0}^{\sigma-1}B(k)\leq\frac{\hat{P}+\hat{D}-E_{max}}{\delta}\right), \qquad (138)$$

where $\tau_j\triangleq\sup_{s\leq j}\{s:E(s)=E_{max}\}$ is the last time up to (and including) j when the battery hit E_{max}. This quantity is well defined for all j with $\tilde{\tau}\leq j$.

If $\tilde{\tau}=j$, then $\tau_j=j$, $E(j)=E_{max}$ and $\{E(j)<\hat{P},\tilde{\tau}\leq j\}=\varnothing$, so that (138) holds trivially. Consider now the event $\{E(j)<\hat{P},\tilde{\tau}<j\}$. It holds

$$\left\{E(j)<\hat{P},\tilde{\tau}<j\right\}\subseteq\left\{j-\tau_j\geq\left\lceil\frac{E_{max}-\hat{P}}{\hat{P}}\right\rceil\triangleq\sigma\right\}, \qquad (139)$$

since the fastest way the battery can drop from E_{max} (its value at τ_j) to $E(j)$ is by transmitting with peak power and receiving zero recharge for all intermediate slots. Examining the combined queue $E(t)$, $D(t)$ in the interval $[\tau_j\quad j]$ yields

$$E(j)+D(j)-E(\tau_j)-D(\tau_j)\geq\delta\sum_{k=\tau_j}^{j-1}B(k)\Rightarrow E(j)+\hat{D}-E_{max}\geq\delta\sum_{k=\tau_j}^{j-1}B(k), \qquad (140)$$

where the last RHS is inferred by the boundedness of $D(t)$. Note that (140) holds for any j such that $E(j)<E_{max}$ and $\tilde{\tau}<j$. Hence, the following inclusion is true

$$\{E(j)<\hat{P},\tilde{\tau}<j\}\subseteq\left\{\hat{P}+\hat{D}-E_{max}\geq\delta\sum_{k=\tau_j}^{j-1}B(k)\right\}, \qquad (141)$$

and, due to (139), it also holds

$$\left\{\hat{P}+\hat{D}-E_{max}\geq\delta\sum_{k=\tau_j}^{j-1}B(k)\right\}\subseteq\left\{\hat{P}+\hat{D}-E_{max}\geq\delta\sum_{k=\tau_j}^{\tau_j+\sigma-1}B(k)\right\}. \qquad (142)$$

Combining (141), (142), taking probabilities in the resulting inclusion and using the stationarity of $B(t)$ produces (138). Since the RHS of (138) is independent of j (and therefore invariant under a convex combination), the proof is complete.

□

E. Proof of Lemma 6

It is easy to show through simple algebra that

$$\Pr\left(\sum_{k=0}^{\sigma-1} B(k) \leq \frac{\hat{P}+\hat{D}-E_{max}}{\delta}\right) = \Pr\left(\frac{1}{\sigma}\sum_{k=0}^{\sigma-1}[B(k)-\bar{B}] \leq \frac{\hat{P}+\hat{D}-E_{max}}{\sigma\delta} - \bar{B}\right). \tag{143}$$

In the selected regime for E_{max}, it holds $(\hat{P}+\hat{D}-E_{max})/(\sigma\delta) - \bar{B} < 0$ so that we can apply Chernoff's bound [42] in the form we state below

Lemma V-E.1: For a sequence $x_1, x_2, \ldots$ of iid random variables, it holds for all n and $a < \mathbb{E}[x_1]$

$$\Pr\left(x_1 + x_2 + \ldots + x_n \leq na\right) \leq \exp\left(-n\ell(a)\right), \tag{144}$$

where $\ell(a) \triangleq \sup_\theta \left(\theta a - \ln \mathbb{E}[\mathrm{e}^{\theta x_1}]\right)$. The following properties hold for $\ell(\cdot)$

- $\ell(a) \geq 0 \quad \forall\, a$.
- $a = 0 \Leftrightarrow \ell(a) = 0$.
- $\ell(a)$ *is a convex function of* a.

Constructing the iid random variables $x_k = B(k) - \bar{B}$ (with $\mathbb{E}[x_k] = 0$) and substituting σ for n in the above lemma immediately produces the desired result.

□

F. Proof of Lemma 7

We assume that $E_{max} > \hat{P} + \hat{D}$ and prove Lemma 7 by standard induction starting from $t = \tilde{\tau}$. The hypothesis is trivially true for $t = \tilde{\tau}$, since it holds, by definition, $E(\tilde{\tau}) = E_{max}$ and therefore $E(\tilde{\tau}) + D(\tilde{\tau}) \geq E_{max}$. We now assume that for some t it holds $E(t) + D(t) \geq E_{max}$, and distinguish cases for $E(t+1)$

- if $E(t+1) = E_{max}$, it follows immediately that $E(t+1) + D(t+1) \geq E_{max}$.
- if $E(t+1) < E_{max}$, we use (3), (10) to write

$$\begin{aligned} E(t+1) &= E(t) - \sum_{l=1}^{L} P_l(t) + B(t), \\ D(t+1) &\geq D(t) - (1-\delta)B(t) + \sum_{l=1}^{L} P_l(t), \end{aligned} \tag{145}$$

and add the previous relations by parts to derive

$$E(t+1) + D(t+1) \geq E(t) + D(t) + \delta B(t) \geq E(t) + D(t) \geq E_{max}, \tag{146}$$

where the last inequality follows from the inductive hypothesis for t.

Hence, the hypothesis is also true for $t+1$ and Lemma 7 is proved.

As mentioned in Section II-B4, the fact that the battery will eventually hit E_{max} in finite time and never fall below $\hat{P}$ afterwards suggests that the finite portion of time before the first hit does not affect the infinite horizon utility. A rigorous proof of this requires the following intermediate facts

Lemma V-F.1: Let $\mathring{\tau}$ a random variable taking values in $\mathbb{N}$ with $\mathbb{E}[\mathring{\tau}] < \infty$ and a stochastic process $Z(t)$ such that $0 \leq Z(t) \leq \hat{Z}$ a.s., where $\hat{Z}$ is an arbitrary constant. It then holds

$$\frac{1}{t}\sum_{k=0}^{t-1}\mathbb{E}[Z(k)] - \hat{Z}\,\frac{\mathbb{E}[\mathring{\tau}]}{t} \leq \frac{1}{t}\sum_{k=0}^{t-1}\mathbb{E}[Z(\mathring{\tau}+k)] \leq \frac{1}{t}\sum_{k=0}^{t-1}\mathbb{E}[Z(k)] + \hat{Z}\,\frac{\mathbb{E}[\mathring{\tau}]}{t} \quad \forall\, t > 0. \tag{147}$$

Proof: It holds

$$\sum_{k=0}^{t-1} Z\left(\mathring{\tau}+k\right) = \sum_{k=\mathring{\tau}}^{\mathring{\tau}+t-1} Z(k) = \sum_{k=0}^{t-1} Z(k) + \sum_{k=t}^{t+\mathring{\tau}-1} Z(k) - \sum_{k=0}^{\mathring{\tau}-1} Z(k) \quad \forall\, t, \tag{148}$$

so that

$$\sum_{k=0}^{t-1} Z\left(\mathring{\tau}+k\right) \geq \sum_{k=0}^{t-1} Z(k) - \sum_{k=0}^{\mathring{\tau}-1} Z(k) \geq \sum_{k=0}^{t-1} Z(k) - \sum_{k=0}^{\mathring{\tau}-1} \hat{Z} = \sum_{k=0}^{t-1} Z(k) - \hat{Z}\mathring{\tau}, \tag{149}$$

and

$$\sum_{k=0}^{t-1} Z\left(\mathring{\tau}+k\right) \leq \sum_{k=0}^{t-1} Z(k) + \sum_{k=t}^{t+\mathring{\tau}-1} Z(k) \leq \sum_{k=0}^{t-1} Z(k) + \sum_{k=t}^{t+\mathring{\tau}-1} \hat{Z} = \sum_{k=0}^{t-1} Z(k) + \hat{Z}\mathring{\tau}. \tag{150}$$

Taking expectations in the last two equations and dividing by t completes the proof. ■

Combining Lemmas V-A.1, V-F.1 produces the following

Corollary 4: For any random variable $\mathring{\tau}$ taking values in $\mathbb{N}$ with $\mathbb{E}[\mathring{\tau}] < \infty$ and stochastic process $Z(t)$ such that $0 \leq Z(t) \leq \hat{Z}$ a.s., it holds

$$\liminf_{t\to\infty} \frac{1}{t} \sum_{k=0}^{t-1} \mathbb{E}[Z(\mathring{\tau}+k)] = \liminf_{t\to\infty} \frac{1}{t} \sum_{k=0}^{t-1} \mathbb{E}[Z(k)]. \tag{151}$$

The following result is the key to proving our intuitive claim

Lemma V-F.2: Let $\tilde{\tau} = \inf\{t : E(t) = E_{max}\}$ be the first time the battery hits E_{max} under DRABP. It then holds $\mathbb{E}[\tilde{\tau}] < \infty$.

Proof: We use the well-known identity for discrete random variables

$$\mathbb{E}[\tilde{\tau}] = \sum_{j=0}^{\infty} \Pr(\tilde{\tau} > j), \tag{152}$$

and examine the joint queues $U(t)$, $D(t)$ in the interval $[0 \quad j]$. Since the battery has never overflowed up to time j, it holds

$$E(j) + D(j) - E(0) - D(0) \geq \delta \sum_{k=0}^{j-1} B(k) \Rightarrow E_{max} + \hat{D} \geq \delta \sum_{k=0}^{j-1} B(k), \tag{153}$$

so that the following inclusion is true

$$\{\tilde{\tau} > j\} \subseteq \left\{ E_{max} + \hat{D} \geq \delta \sum_{k=0}^{j-1} B(k) \right\}. \tag{154}$$

Taking probabilities in the last inclusion and performing some algebra similar to Appendix V-E yields

$$\Pr(\tilde{\tau} > j) \leq \Pr\left(\frac{E_{max} + \hat{D}}{j\delta} - \bar{B} \geq \frac{1}{j} \sum_{k=0}^{j-1} [B(k) - \bar{B}] \right). \tag{155}$$

Hence for $j > j^*$, where $j^* = 1 + \lceil (E_{max} + \hat{D})/(\delta \bar{B}) \rceil$, the LHS of the inequality in the second probability becomes negative so that we can apply Lemma V-E.1 and exploit the monotonicity of $\ell(\cdot)$ to get

$$\Pr(\tilde{\tau} > j) \leq \Pr\left(\frac{E_{max} + \hat{D}}{j\delta} - \bar{B} \geq \frac{1}{j} \sum_{k=0}^{j-1} B(k) \right) \leq \exp(-j\ell(a^*)) \quad \forall\, j > j^*, \tag{156}$$

where $a^* = (E_{max} + \hat{D})/(j^*\delta) - \bar{B} < 0$. Having provided an exponentially small tail bound, it easily follows from a standard procedure that $\mathbb{E}[\tilde{\tau}] < \infty$.

Combining Corollary 4 with Lemma V-F.2 finally proves the original claim. ■

□

G. Proof of Lemma 11

The boundedness of $Y_n^{(c)}(t)$ has already been established in the proof of Lemma 10. Also, if $U_n^{(c)}(t)$ is finitely bounded for all n, c, then repeating the procedure of Appendix V-B for $D_n(t)$ provides the bound of (94). Hence, it remains to prove the bound for $U_n^{(c)}(t)$. Although it follows from (87) that $R_{n,in}^{(c)}(t) = 0$ whenever $U_n^{(c)}(t) > \eta \hat{Y}_n^{(c)}$, the boundedness of $U_n^{(c)}(t)$ cannot be proved solely through the argument of Appendix V-B due to the additional term $\sum_a \mu_{an}^{(c)}(\boldsymbol{S}(t), \boldsymbol{P}(t))$ of intra-node incoming traffic. Hence, a new approach is required.

To prove the desired result, we can equivalently prove the following

Lemma V-G.1: For any policy whose application satisfies the conditions of Lemma 10 (clearly, NRABP is such a policy), there exists a finite sequence $a_1^{(c)}, a_2^{(c)}, \ldots, a_N^{(c)}$ such that it holds for all t, c

$$\max_{\substack{\mathcal{I}\subseteq\{1,\ldots,N\} \\ |\mathcal{I}|=k}} \sum_{i\in\mathcal{I}} U_i^{(c)}(t) \leq k\hat{F}^{(c)} + a_k^{(c)}, \tag{157}$$

where $\hat{F}^{(c)} \triangleq \eta \max_{1\leq n\leq N} \hat{Y}_n^{(c)}$ and $|\mathcal{I}|$ denotes the cardinality of $\mathcal{I}$.

Note that the maximum is taken over all sets of given cardinality. The above statement, if true, implies that $\sum_{i=1}^{N} U_i^{(c)}(t) \leq N\hat{F}^{(c)} + a_N^{(c)}$, which in turn implies the desired boundedness. Lemma V-G.1 will be proved by induction, and the following facts will be used in the process

Remark 1: Consider any policy that places an explicit upper bound on the exogenously admitted traffic $R_{n,in}^{(c)}(t)$ for all nodes n and commodities c (clearly, NRABP is such a policy). Then, there exists a sufficiently large $\mathring{C}$ such that, under this policy, it holds for all sets $\mathcal{I} \subseteq \{1,\ldots,N\}$

$$\sum_{i\in\mathcal{I}} U_i^{(c)}(t+1) \leq \sum_{i\in\mathcal{I}} U_i^{(c)}(t) + \mathring{C} \quad \forall\, c \in \mathcal{K}, \tag{158}$$

where $\mathcal{K}$ is the commodity set.

Remark 2: Consider any index set $\mathcal{I} \subseteq \{1,\ldots,N\}$. This set can be uniquely partitioned as $\mathcal{I} = \biguplus_{j=1}^{l} \mathcal{I}_j$ where

$$\mathcal{I}_1 \triangleq \begin{cases} \varnothing & \text{if } 1 \notin \mathcal{I}, \\ \{1,2,\ldots,i_{e_1}\} & \text{if } \{1,2,\ldots,i_{e_1}\} \subseteq \mathcal{I} \wedge i_{e_1}+1 \notin \mathcal{I}, \end{cases} \tag{159}$$

and the remaining sets are defined recursively through

$$\mathcal{I}_j \triangleq \left\{ i_{f_j}, i_{f_j}+1, \ldots, i_{e_j} \right\} \tag{160}$$

where i_{e_j} and i_{f_j} are uniquely defined by the following conditions

- $f_j \geq e_{j-1}+2$ (if $\mathcal{I}_1 = \varnothing$, we define $e_1 = 0$).
- $\left\{ i_{e_{j-1}}+1, \ldots, i_{f_j}-1 \right\} \subseteq \mathcal{I}^c$, where ^{c} denotes set complement.

Furthermore, for such a decomposition we can define the set

$$\mathcal{G} \triangleq \begin{cases} \varnothing & \text{if } l = 1, \\ \{i_{e_1}+1, \ldots, i_{f_2}-1\} & \text{otherwise}, \end{cases} \tag{161}$$

Remark 1 is true due to the fact that link rates are finitely bounded,[15] while Remark 2 is a notational description of the obvious fact that any index set can be uniquely decomposed into non-overlapping blocks of consecutive indices starting from low numbered indices, as shown in Fig. 15 (black nodes belong to $\mathcal{I}$ while white ones don't; two different examples are given depending on whether $1 \in \mathcal{I}$). The set $\mathcal{G}$ is essentially the set of indices located between the first and second blocks.

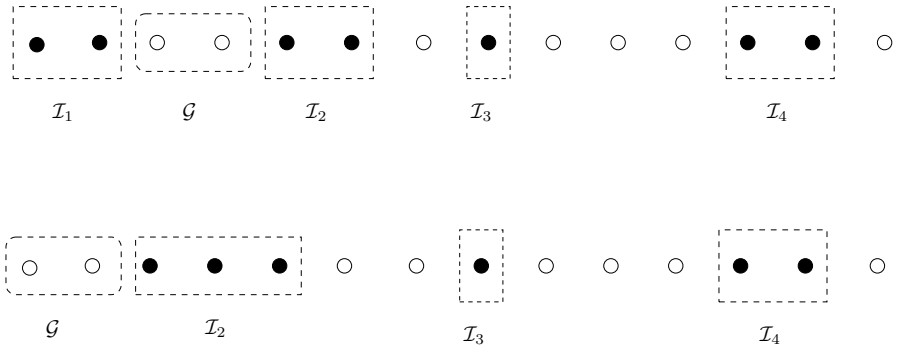

Fig. 15. Schematic decomposition of $\mathcal{I}$ into $\mathcal{I}_j$. In the second case, it holds $\mathcal{I}_1 = \varnothing$.

The following result will also be used

Lemma V-G.2: Let a non-increasing finite sequence $x_1 \geq x_2 \geq \ldots \geq x_N$ such that it holds $\sum_{i=1}^{n} x_i \leq n\hat{H} + a_n$ for all $n = 1,\ldots,N$. For consistency, define $a_0 = 0$. Then, for any index subset $\mathcal{I} \subseteq \{1,\ldots,N\}$ consisting of k elements it holds

$$\sum_{i\in\mathcal{I}} x_i \leq k\hat{H} + \frac{n_2-k}{n_2-n_1}\, a_{n_1} + \frac{k-n_1}{n_2-n_1}\, a_{n_2}, \tag{162}$$

where $k = |\mathcal{I}|$, $n_1 = |\mathcal{I}_1|$, $m = |G|$, $n_2 = m+k$ and $\mathcal{I}_1$, $\mathcal{G}$ are defined in Remark 2. The above inequality is meaningful when $n_2 > n_1$.

Proof: We explicitly use the notation of Remark 2 and distinguish cases as follows

- $1 \notin \mathcal{I}$. Then, by definition it holds $\mathcal{I}_1 = \varnothing$, $n_1 = 0$ and the desired inequality becomes

$$\sum_{i\in\mathcal{I}} x_i \overset{?}{\leq} k\hat{H} + \frac{m}{m+k}\, a_0 + \frac{k}{m+k}\, a_{m+k} \Leftrightarrow \sum_{i\in\mathcal{I}} x_i \overset{?}{\leq} k\hat{H} + \frac{k}{m+k}\, a_{m+k}. \tag{163}$$

[15] in fact, it is easy to show that (158) is true for any $\mathring{C} \geq \max_{\mathcal{I}\subseteq\{1,\ldots,N\}} \max_c \sum_{i\in\mathcal{I}} \left(\hat{A}_i^{(c)} + \sum_a \hat{c}_{ai} \right)$.

If $l=1$ so that $m=0$, we have to prove $\sum_{i\in\mathcal{I}} x_i \leq k\hat{H}+a_k$, which is true by assumption. For $l>1$, since $\mathcal{I}_1=\varnothing$ and x_n is a non-increasing sequence, the arithmetic means of non-overlapping index sets satisfies a similar inequality, i. e.

$$\frac{1}{m}\sum_{i\in\mathcal{G}} x_i \geq \frac{1}{k}\sum_{i\in\mathcal{I}} x_i \Rightarrow \sum_{i\in\mathcal{G}} x_i \geq \frac{m}{k}\sum_{i\in\mathcal{I}} x_i. \tag{164}$$

The monotonicity of x_i also implies

$$\sum_{i\in\mathcal{G}} x_i + \sum_{i\in\mathcal{I}} x_i \leq \sum_{i=1}^{m+k} x_i \leq (m+k)\hat{H}+a_{m+k}, \tag{165}$$

where the second inequality holds by assumption. Combining the last two equations yields

$$\Big(\frac{m}{k}+1\Big)\sum_{i\in\mathcal{I}} x_i \leq (m+k)\hat{H}+a_{m+k} \Rightarrow \sum_{i\in\mathcal{I}} x_i \leq k\hat{H}+\frac{k}{m+k}\,a_{m+k}, \tag{166}$$

so that (162) is proved.

- $1\in\mathcal{I}$, so that $\mathcal{I}_1\neq\varnothing$. The case $l=1$ is immediately eliminated since it implies $m=0$ and $n_2=n_1=k$. Hence, we assume $l>1$ so that the arithmetic means inequality is still applicable

$$\frac{1}{m}\sum_{i\in\mathcal{G}} x_i \geq \frac{1}{k-n_1}\sum_{i\in\mathcal{I}_2\uplus\ldots\uplus\mathcal{I}_l} x_i \Rightarrow \sum_{i\in\mathcal{G}} x_i \geq \frac{m}{k-n_1}\sum_{i\in\mathcal{I}_2\uplus\ldots\uplus\mathcal{I}_l} x_i, \tag{167}$$

and since it holds

$$\sum_{i\in\mathcal{I}} x_i + \sum_{i\in\mathcal{G}} x_i \leq (m+k)\hat{H}+a_{m+k}, \tag{168}$$

combining the last two equations yields

$$\begin{aligned}&\sum_{i\in\mathcal{I}} x_i + \frac{m}{k-n_1}\sum_{i\in\mathcal{I}_2\uplus\ldots\uplus\mathcal{I}_l} x_i \leq (m+k)\hat{H}+a_{m+k} \Leftrightarrow \sum_{i\in\mathcal{I}} x_i + \frac{m}{k-n_1}\left(\sum_{i\in\mathcal{I}} x_i - \sum_{i\in\mathcal{I}_1} x_i\right) \leq (m+k)\hat{H}+a_{m+k}\\ \Leftrightarrow &\left(1+\frac{m}{k-n_1}\right)\sum_{i\in\mathcal{I}} x_i \leq (m+k)\hat{H}+\frac{m}{k-n_1}\sum_{i\in\mathcal{I}_1} x_i + a_{m+k}.\end{aligned} \tag{169}$$

Using the fact that $\sum_{i\in\mathcal{I}_1} x_i \leq n_1\hat{H}+a_{n_1}$ and performing simple algebra in the last equation results in (162). ∎

We are now in position to prove Lemma V-G.1 inductively, so that we are essentially looking for a sequence $a_1^{(c)},\ldots,a_N^{(c)}$ that satisfies (157). Clearly, the proof is essentially complete if we find such a sequence for a specific c. Hence, in the remainder of the proof, we drop the c dependence on all quantities (i. e. we write $U_i(t), a_k$ etc. instead of $U_i^{(c)}(t), a_k^{(c)}$). Eq. (157) is trivially true for $t=0$, since all queues are initially empty, provided that $a_k^{(c)}\geq 0$. We assume that (157) holds for t and we examine what happens at $t+1$.

Pick any set $\mathcal{I}\subseteq\{1,\ldots,N\}$ and decompose it as $\mathcal{I}=\hat{\mathcal{I}}\cup\tilde{\mathcal{I}}$, where $\hat{\mathcal{I}}=\{i\in\mathcal{I}: U_i(t)>\hat{F}\}$ and $\tilde{\mathcal{I}}=\{i\in\mathcal{I}: U_i(t)\leq\hat{F}\}$. We also assume, w. l. o. g, that $U_1(t)\geq U_2(t)\geq\ldots\geq U_N(t)$ and distinguish cases:

- it holds $\tilde{\mathcal{I}}\neq\varnothing$. Using Remark 1, the definition of $\tilde{\mathcal{I}}$ and the inductive hypothesis on $\hat{\mathcal{S}}$ yields

$$\begin{aligned}&\sum_{i\in\mathcal{I}} U_i^{(c)}(t+1) \leq \sum_{i\in\mathcal{I}} U_i^{(c)}(t) + \mathring{C} = \sum_{i\in\hat{\mathcal{I}}} U_i^{(c)}(t) + \sum_{i\in\tilde{\mathcal{I}}} U_i^{(c)}(t) + \mathring{C}\\ &\leq |\hat{\mathcal{I}}|\hat{F}^{(c)} + a_{|\hat{\mathcal{I}}|} + |\tilde{\mathcal{I}}|\hat{F}^{(c)} + \mathring{C} \leq |\mathcal{I}|\hat{F}^{(c)} + a_{|\hat{\mathcal{I}}|} + \mathring{C} \overset{?}{\leq} |\mathcal{I}|\hat{F}^{(c)} + a_{|\mathcal{I}|}.\end{aligned} \tag{170}$$

  Since $\tilde{\mathcal{I}}\neq\varnothing$, the hypothesis is true for $t+1$ provided it holds $a_{k+1}\geq a_k+\mathring{C}$ for all $k=1,\ldots,N-1$.
- it holds $\tilde{\mathcal{I}}=\varnothing$ and the decomposition of $\hat{\mathcal{I}}$ according to Remark 2 consists of a single block (i. e. $l=1$ and $\mathcal{I}=\hat{\mathcal{I}}=\hat{\mathcal{I}}_1$). Since $\hat{\mathcal{I}}_1$ contains consecutive indices, it contains the $k=n_1$ largest backlog indices. Additionally, the policy, by construction, allows bit transfers only from higher backlog nodes to lower backlog. Hence any incoming traffic to a node of $\hat{\mathcal{I}}$ must originate from another node in $\hat{\mathcal{I}}$, which implies

$$\sum_{i\in\mathcal{I}} U_i(t+1) = \sum_{i\in\hat{\mathcal{I}}} U_i(t+1) \leq \sum_{i\in\hat{\mathcal{I}}} U_i(t) \leq |\hat{\mathcal{I}}|\hat{F}+a_{|\hat{\mathcal{I}}|} = |\mathcal{I}|\hat{F}+a_{|\mathcal{I}|}, \tag{171}$$

  where the last inequality holds due to the inductive hypothesis for t.

- it holds $\tilde{\mathcal{I}} = \varnothing$ and the decomposition of $\hat{\mathcal{I}}$ consists of two blocks or more (i. e. $l \geq 2$). Using Remark 1 and Lemma V-G.2 yields

$$\sum_{i\in\mathcal{I}} U_i(t+1) \leq \sum_{i\in\hat{\mathcal{I}}} U_i(t) + \mathring{C} \leq k\hat{F} + \frac{n_2-k}{n_2-n_1}\, a_{n_1} + \frac{k-n_1}{n_2-n_1}\, a_{n_2} + \mathring{C} \overset{?}{\leq} k\hat{F} + a_k, \tag{172}$$

  where $k = |\hat{\mathcal{I}}|$ and n_1, n_2 are defined in Remark 2. Hence, the inductive hypothesis is true for $t+1$ if it holds

$$a_k \geq \max_{\substack{n_1,n_2 \\ 0\leq n_1<k<n_2\leq N}} \left[\frac{n_2-k}{n_2-n_1}\, a_{n_1} + \frac{k-n_1}{n_2-n_1}\, a_{n_2}\right] + \mathring{C}. \tag{173}$$

Gathering the previous conditions, Lemma V-G.1 is proved if there exists a sequence $a_1, \ldots, a_N$ that satisfies the following conditions

$$\begin{aligned} &a_k \geq 0 \quad \forall\, k = 0, \ldots, N, \\ &a_{k+1} \geq a_k + \mathring{C} \quad \forall\, k = 0, \ldots, N-1, \\ &a_k \geq \max_{\substack{n_1,n_2 \\ 0\leq n_1<k<n_2\leq N}} \left[\frac{n_2-k}{n_2-n_1}\, a_{n_1} + \frac{k-n_1}{n_2-n_1}\, a_{n_2}\right] + \mathring{C} \quad \forall\, k = 1, \ldots, N-1, \end{aligned} \tag{174}$$

where we define $a_0 = 0$. Since the coefficients of a_{n_1}, a_{n_2} form a convex combination, a sequence satisfying (174) can be easily constructed as follows. Pick any strictly increasing and strictly concave sequence $b_0, \ldots, b_N$ with $b_0 = 0$ so that it holds[16]

$$b_k > \max_{\substack{n_1,n_2 \\ 0\leq n_1<k<n_2\leq N}} \left[\frac{n_2-k}{n_2-n_1}\, a_{n_1} + \frac{k-n_1}{n_2-n_1}\, a_{n_2}\right], \tag{175}$$

and define

$$\begin{aligned} c_1 &\triangleq \min_{0\leq k\leq N-1} \left[b_{k+1} - b_k\right], \\ c_2 &\triangleq \min_{1\leq k\leq N-1} \left[b_k - \max_{\substack{n_1,n_2 \\ 0\leq n_1<k<n_2\leq N}} \left[\frac{n_2-k}{n_2-n_1}\, b_{n_1} + \frac{k-n_1}{n_2-n_1}\, b_{n_2}\right]\right], \end{aligned} \tag{176}$$

The strict monotonicity and concavity imply that $c_1, c_2 > 0$. It now follows, after some simple algebra, that the sequence

$$a_k = b_k\, \frac{\mathring{C}}{\min(c_1, c_2)}, \tag{177}$$

satisfies (174), so that the hypothesis is true for $t+1$ and the induction is complete.

□

H. Total Hidden Area S

We first compute the total hidden area S for transmission from station O_2 to station O_1, as illustrated by Fig. 16. The distance between station O_2 and O_1 is d. The CS_Range and TX_Range are R and r respectively. In Fig. 16, the grey area S_{ABD} is the hidden area that we will compute.

From cosine theorem, we get θ and φ:

$$\theta = \arccos[(r^2 + d^2 - R^2)/(2rd)] \tag{178}$$

$$\varphi = \arccos[(d^2 + R^2 - r^2)/(2dR)] \tag{179}$$

Then we easily get the following areas

$$S_{AO_1B} = r^2(\pi - \theta)/2 \tag{180}$$

$$S_{AO_1O_2} = dr\sin\theta/2 \tag{181}$$

$$S_{AO_2C} = R^2\varphi/2 \tag{182}$$

Since $S_{ABD} = 2(S_{AO_1B} + S_{AO_1O_2} - S_{AO_2C})$, we have

$$S_{ABD} = \begin{cases} r^2(\pi-\theta) + dr\sin\theta - R^2\varphi & \text{if } r > R - d \\ 0 & \text{otherwise} \end{cases} \tag{183}$$

After the normalization procedure described later in this section, the relationship is plotted in Fig. 4. When $R = r$, the equation is reduced to the one established in [41] and [39].

[16] an example of such a sequence is $b_k = 1 - \mathrm{e}^{-k}$.

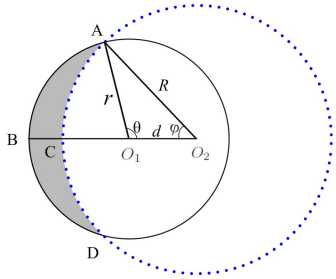

Fig. 16. Illustration of hidden area. The shaded region is the hidden area.

I. Hidden Area $H(i,j)$ and Covered Area $E(i,j)$

As shown in Fig. 6, $H(i,j)$ and $E(i,j)$ are the observed hidden and covered area in annulus $A(j)$ by a source station in annulus $A(i)$, respectively. When M is large, the distance d from a source station in annulus $A(i)$ to the AP approximates the distance from the middle of annulus $A(i)$ to the AP:

$$d = r(i - 1/2)/M \tag{184}$$

In Fig. 6, the hidden area $H(i,j)$ can be considered as the difference between total hidden area $S(i,j)$ and $S(i,j-1)$, where $S(i,j)$ is the total hidden area observed by a node in annulus $A(i)$ when the TX_Range of the AP is rj/M (i.e., the AP covers as far as annulus $A(j)$).[17] In (183), by replacing TX_Range r with rj/M and inserting the distance d from (184), we get

$$S(i,j) = \begin{cases} \frac{r^2}{M^2}[j^2(\pi-\theta) + j(i-\frac{1}{2})\sin\theta] - R^2\varphi \\ \qquad\qquad\qquad\qquad j = M-i+1,\ldots,M \\ 0 \qquad \text{otherwise} \end{cases} \tag{185}$$

Then we get the desired the hidden area

$$H(i,j) = S(i,j) - S(i,j-1) \tag{186}$$

Now let us discuss the covered area $E(i,j)$. Each annulus $A(j)$ is composed of $E(i,j)$ and $H(i,j)$. So $E(i,j)$ is:

$$E(i,j) = A(j) - H(i,j) \tag{187}$$

where $H(i,j)$ is expressed in (186) and the area $A(j)$ is

$$A(j) = \pi r^2[j^2 - (j-1)^2]/M^2 \tag{188}$$

For ease of mathematical manipulation, we normalize the above obtained areas with respect to the transmission area of a node, which is πr^2.

J. Derivation of Eq. 107

We consider a station located in annulus $A(i)$ (Fig. 5) of a saturated network with N nodes. Define $n \in (0,m)$ as the backoff stage. The maximum backoff window size at stage n is $W_n = 2^n W$. Let k be the stochastic process representing the reading of the backoff counter for a given station. Then we get a discrete two-dimensional Markov chain (n,k) (Fig. 17) to model the 802.11 DCF. It is the same as that in [29].

As in [29], the collision probability $P_c(i)$ is assumed to be independent of the state n of the station. From Fig. 17 we obtain the transition probabilities of the Markov chain:

$$\begin{cases} P\{n,k|n,k+1\} = 1, & k \in (0, W_n - 2), \\ & n \in (0,m); \\ P\{0,k|n,0\} = (1-P_c(i))/W_0, & k \in (0, W_0 - 1), \\ & n \in (0,m); \\ P\{n,k|n-1,0\} = P_c(i)/W_n, & k \in (0, W_n - 1), \\ & n \in (1,m); \\ P\{m,k|m,0\} = P_c(i)/W_m, & k \in (0, W_m - 1). \end{cases}$$

[17] This is only for the convenience of mathematical manipulation. The transmission ranges for all stations (including AP) are r, as stated before.

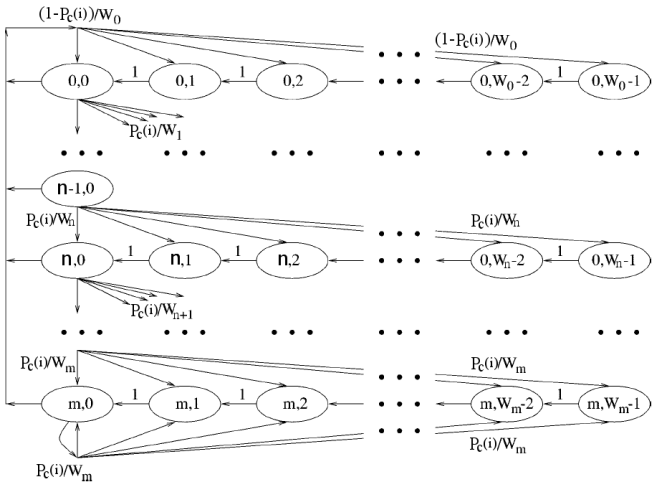

Fig. 17. The 2D Markov chain to model 802.11 DCF.

Denote $b_{n,k}$ as the probability of state (n,k) in steady state. From the above transition probabilities, we get the following relations:

$$\begin{cases} b_{n,0} = P_c(i)^n b_{0,0}, & n \in (0, m-1); \\ b_{m,0} = \frac{P_c(i)^m}{1-P_c(i)} b_{0,0}, & \\ b_{n,k} = \frac{W_n - k}{W_n} b_{n,0}, & k \in (0, W_n - 1). \end{cases}$$

With these three relations, each state probability $b_{n,k}$ can be expressed with $b_{0,0}$. Substitute $b_{n,k}$ into the normalization condition

$$\sum_{n=0}^{m} \sum_{k=0}^{W_n - 1} b_{n,k} = 1 \tag{189}$$

we get the value of $b_{0,0}$:

$$b_{0,0} = \frac{2[1-2P_c(i)][1-P_c(i)]}{[1-2P_c(i)](W+1) + P_c(i)W[1-(2P_c(i))^m]}. \tag{190}$$

As a transmission occurs only when the backoff counter is zero, the transmission probability $\tau(i)$ is the summation of the probabilities for the states with $k = 0$:

$$\tau(i) = \sum_{n=0}^{m} b_{n,0} \tag{191}$$

which leads to Eq. 107.

VI. List Of Symbols, Abbreviations And Synonyms

Notation	Definition
DRABP	Downlink Rechargeable Adaptive Back-Pressure policy
NRABP	Network Rechargeable Adaptive Back-Pressure policy
$\stackrel{\Delta}{=}$	equal by denition
$\boldsymbol{S}(t)$	vector of channel states for slot t
$\boldsymbol{P}(t)$	transmission power vector for slot t selected by the network control policy
$\mathcal{P}_{\boldsymbol{s}}$	set of power vectors where $\boldsymbol{P}(t)$ must belong when it holds $\boldsymbol{S}(t) = \boldsymbol{s}$
$\mathcal{K}$	set of commodities
$A_l(t)$	amount of exogenously generated bits during slot t intended for user l
$A_n^{(c)}(t)$	amount of commodity c bits exogenously generated at node n during slot t
$V_l(t),\ U_l(t)$	amount of bits stored at time t in the transport/network layer, respectively, queue of user l
$V_n^c(t),\ U_n^c(t)$	amount of commodity c bits stored at time t in the transport/network layer, respectively, queue of node n
$E_n(t)$	battery level of node n at time t (in a downlink scenario, we just write $E(t)$)
$B_n(t)$	amount of replenished energy during slot t due to battery recharge at node n (in a downlink scenario, we just write $B(t)$)
$R_{l,in}(t)$	number of bits (intended for user l) admitted into the network layer at slot t
$R_{n,in}^{(c)}(t)$	number of commodity c bits admitted into the network layer at node n and slot t
$\bar{x}$	time average of quantity x (depending on context, may also denote expected value)
$\hat{x}$	deterministic upper bound imposed on quantity x
$R_l(t)$	number of bits actually transmitted on link l during slot t
$\bar{r}_l(t)$	time average of $R_l(0)\ \ldots\ R_l(t-1)$
$\bar{r}_n^{(c)}(t)$	time average of $R_n^{(c)}(0)\ \ldots\ R_n^{(c)}(t-1)$
$\mathbb{E}[x]$	expectation of quantity x
$Y_l(t)$	amount of bits stored at time t in virtual bit queue of user l (downlink scenario only)
$D_n(t)$	amount of bits stored at time t in virtual power queue of node n (in a downlink scenario, we just write $D(t)$)
$Y_n^{(c)}(t)$	amount of commodity c bits stored at time t in virtual bit queue of node n
TX_Range	Transmission Range
CS_Range	Carrier Sensing Range
IF_Range	Interference Range
α	duration of a successful transmission
β	duration of a collision period
δ	duration of a backoff time slot
W	initial backoff eindow size
P_c	collision probability
τ	transmission probability
$A(i)$	annulus i
t_{RTS}	RTS transmission time
$P_s(i)$	conditional success probability given that a node in annulus $A(i)$ initiates a transmission
$P_c(i)$	conditional collision probability given that a node in annulus $A(i)$ initiates a transmission
P_{idle}	probability that all stations are idle at a time slot
$N(i)$	expected number of stations located at annulus $A(i)$
$P_{success}$	probability that is a successful transmission in a time slot
$P_{collision}$	probability that is a collision in time slot
S	expected aggregate throughput for all network
T	mean duration of a time slot
$S(i)$	per node throughput in annulus A(i)

REFERENCES

[1] M. Gatzianas, L. Georgiadis, and L. Tassiulas, "Asymptotically optimal policies for wireless networks with rechargeable batteries," proceedings of IWCMC, Crete, 2008.

[2] ——, "Control of wireless networks with rechargeable batteries," to appear in Transactions on Wireless Communications, 2009.

[3] J. Lin, F. Liu, T. Korakis, Z. Tao, E. Erkip, and S. Panwar, "Performance unfairness due to hidden terminals," submitted to Globecom 2009.

[4] F. Liu, J. Lin, Z. Tao, T. Korakis, E. Erkip, and S. Panwar, "The hidden cost of hidden terminals," submitted to Globecom 2009.

[5] I. Akyildiz, W. Su, Y. Sankarasubramaniam, and E. Cayirici, "Wireless sensor networks: a survey," *Computer Networks*, vol. 38, no. 4, pp. 393–422, March 2002.

[6] X. Jiang, J. Polastre, and D. Culler, "Perpetual environmentally powered sensor networks," in *4th International Symposium on Information Processing in Sensor Networks (IPSN)*, 2005, pp. 463–468.

[7] A. Fu, E. Modiano, and J. Tsitsiklis, "Optimal energy allocation and admission control for communication satellites," *IEEE/ACM Trans. Netw.*, vol. 11, no. 3, p. 488, June 2003.

[8] L. Lin, N. Shroff, and R. Srikant, "Asymptotically optimal power-aware routing for multihop wireless networks with renewable energy sources," in *Proc. IEEE INFOCOM*, 2005.

[9] M. Adamou and S. Sarkar, "A framework for optimal battery management for wireless nodes," in *Proc. IEEE INFOCOM*, 2002.

[10] V. Borkar, A. Kherani, and B. Prabhu, "Closed and open loop optimal control of buffer and energy of a wireless device," in *3rd Intl. Symposium on Modeling and Optimization in Mobile Ad Hoc and Wireless Networks (WiOpt)*, 2005.

[11] K. Kar, A. Krishnamurthy, and N. Jaggi, "Dynamic node activation in networks of rechargeable sensors," *IEEE/ACM Trans. Netw.*, vol. 14, no. 1, pp. 15–26, February 2006.

[12] N. Jaggi, A. Krishnamurthy, and K. Kar, "Utility maximizing node activation policies in networks of partially rechargeable sensors," in *39th Annual Conference on Information Sciences and Systems (CISS)*, 2005.

[13] N. Jaggi, K. Kar, and A. Krishnamurthy, "Rechargeable sensor activation under temporally correlated events," in *5th Intl. Symposium on Modeling and Optimization in Mobile Ad Hoc and Wireless Networks (WiOpt)*, 2007.

[14] N. Jaggi, "Node activation policies for energy-efficient coverage in rechargeable sensor networks," Ph.D. dissertation, Rensselaer Polytechnic Institue, 2007.

[15] L. Georgiadis, M. J. Neely, and L. Tassiulas, "Resource allocation and cross-layer control in wireless networks," *Foundations and Trends in Networking*, vol. 1, no. 1, 2006.

[16] M. J. Neely, "Dynamic power allocation and routing for satellite and wireless networks with time varying channels," Ph.D. dissertation, MIT, 2003.

[17] L. Tassiulas and A. Ephremides, "Stability properties of constrained queueing systems and scheduling policies for maximum throughput in multihop radio networks," *IEEE Trans. Autom. Control*, vol. 37, no. 12, pp. 1936–1949, December 1992.

[18] M. J. Neely, "Energy optimal control for time varying wireless networks," *IEEE Trans. Inf. Theory*, vol. 52, no. 7, pp. 2915–2934, July 2006.

[19] M. Neely, E. Modiano, and C. Li, "Fairness and optimal stochastic control for heterogeneous networks," *IEEE/ACM Trans. Netw.*, vol. 16, no. 2, pp. 396–409, April 2008.

[20] *Part II: Wireless LAN Medium Access Control (MAC) and Physical Layer (PHY) Specifications*. ANSI/IEEE Std 802.11, 1999.

[21] S. Khurana, A. Kahol, and A. Jayasumana, "Effect of hidden terminals on the performance of ieee 802.11 mac protocol."

[22] F. Hung, S. Pai, and I. Marsic, "Performance modeling and analysis of the ieee 802.11 distribution coordination function in presence of hidden stations," *MILCOM*, 2006.

[23] P. C. Ng and S. C. Liew, "Throughput analysis of ieee802.11 multi-hop ad hoc networks," *IEEE/ACM Trans. on Networking*, 2007.

[24] Z. Hadzi-Velkov and L. Gavrilovska, "Effect of hidden terminals on the performance of ieee 802.11 mac protocol."

[25] G. Anastasi, E. Borgia, M. Conti, and E. Gregori, "Wi-fi in ad hoc mode: a measurement study."

[26] K. Xu, M. Gerla, and S. Bae, "Effectiveness of rts/cts handshake in ieee 802.11 based adhoc networks."

[27] J. Lin and F. Liu, "Measurement of tx_range, if_range and cs_range in 802.11," Tech. Rep.

[28] *Part II: wireless LAN medium access control (MAC) and physical layer (PHY) specifications*. IEEE, 2003.

[29] G. Bianchi, "Performance analysis of the ieee 802.11 distributed coordination function," *IEEE JNL on Selected Areas in Communications*.

[30] T. N. S. ns 2, "http://www.isi.edu/nsnam/ns/."

[31] A. Bacioccola, C. Cicconetti, and G. Stea, "User-level performance evaluation of voip using ns-2."

[32] C. Cicconetti, E. Mingozzi, and G. Stea, "An integrated framework for enabling effective data collection and statistical analysis with ns2."

[33] R. G. Cole and J. H. Rosenbluth, "Voice over ip performance monitoring."

[34] P. Calyam, M. Sridharan, W. Mandrawa, and P. Schopis, "Performance measurement and analysis of h.323 traffic."

[35] madwifi.org Trac, "http://madwifi.org/."

[36] P. C. Ng, S. C. Lie, K. C. Sha, and W. T. To, "Experimental study of hidden-node problem in ieee 802.11 wireless networks."

[37] M. Heusse, F. Rousseau, G. Berger-Sabbatel, and A. Duda, "Performance anomaly of 802.11b."

[38] H. S. Chhaya and S. Gupta, "Throughput and fairness properties of asynchronous data transfer methods in the ieee 802.11 mac protocol."

[39] Y. Wang, N. Yan, and T. Li, "Throughput analysis of ieee 802.11 in multi-hop ad hoc networks."

[40] H. S. Chhaya and S. Gupta, "Performance of asynchronous data transfer methods of ieee 802.11 mac protocol," *IEEE Personal Communications*, 1996.

[41] H. Takagi and L. Kleinrock, "Optimal transmission ranges for randomly distributed packet radio terminals."

[42] A. Shwartz and A. Weiss, *Large deviations for performance analysis: queues, communications, and computing*. Chapman & Hall, 1995.